Article:

Aad, G. orcid.org/0000-0002-6665-4934, Aakvaag, E. orcid.org/0000-0001-7616-1554, Abbott, B. orcid.org/0000-0002-5888-2734 et al. (2919 more authors) (2024) Search for R-parity violating supersymmetric decays of the top squark to a b-jet and a lepton in s =13 TeV pp collisions with the ATLAS detector. Physical Review D, 110. 092004. ISSN 2470-0010

https://doi.org/10.1103/physrevd.110.092004

Search for R-parity violating supersymmetric decays of the top squark to a b-jet and a lepton in $\sqrt{s} = 13$ TeV pp collisions with the ATLAS detector

G. Aad *et al.*[*]
(ATLAS Collaboration)

(Received 28 June 2024; accepted 20 September 2024; published 12 November 2024)

A search is presented for direct pair production of the stop, the supersymmetric partner of the top quark, in a decay through an R-parity violating coupling to a charged lepton and a b-quark. The dataset corresponds to an integrated luminosity of 140 fb^{-1} of proton-proton collisions at a center-of-mass energy of $\sqrt{s} = 13$ TeV collected between 2015 and 2018 by the ATLAS detector at the LHC. The final state has two charged leptons (electrons or muons) and two b-jets. The results of the search are interpreted in the context of a Minimal Supersymmetric Standard Model with an additional $B - L$ gauge symmetry that is spontaneously broken. No significant excess is observed over the Standard Model background, and exclusion limits on stop pair production are set at 95% confidence level. The corresponding lower limits on the stop mass for 100% branching ratios to a b-quark and an electron, muon, or tau-lepton are 1.9 TeV, 1.8 TeV and 800 GeV, respectively, extending the reach of previous LHC searches.

DOI: 10.1103/PhysRevD.110.092004

I. INTRODUCTION

The extension of the Standard Model (SM) of particle physics with supersymmetry (SUSY) [1–9] leads to processes that violate both baryon number (B) and lepton number (L). This in turn may lead to rapid proton decay and lepton-number-violating processes, such as decays of $\mu \to e\gamma$, in conflict with experimental bounds. A conventional assumption to prevent these processes is to impose conservation of a multiplicative quantum number R-parity [10–14], defined as $R = (-1)^{3(B-L)+2s}$, where s is the spin of the particle. R has a value of $+1$ for SM particles and -1 for SUSY particles. R-parity conservation requires SUSY particles to be produced in pairs and the lightest supersymmetric particle (LSP) to be stable. The LSP cannot carry electric charge or color charge without coming into conflict with astrophysical data [15,16]. At the LHC, the conventional experimental signature for SUSY particles includes significant missing transverse momentum due to the noninteraction of the LSP with the detector.

An alternative approach is an R-parity violating (RPV) model which adds a local symmetry $U(1)_{B-L}$ to the $SU(3)_C \times SU(2)_L \times U(1)_Y$ SM and includes three generations of right-handed neutrino supermultiplets. The minimal supersymmetric extension then only needs a vacuum expectation value (VEV) for a right-handed sneutrino in order to spontaneously break the $B - L$ symmetry. The size of the RPV coupling is directly related to the right-handed sneutrino VEV, and therefore to the neutrino sector. The size of the coupling is kept small by the small values of the neutrino mass [17–30]. This minimal $B - L$ model, with a scalar top squark (stop or $\tilde{t}$) decaying into a quark and a lepton, violates lepton number but not baryon number. This model is consistent with proton stability and the bounds on lepton number violation [31]. The most noticeable effect of this small coupling related to the neutrino mass is that the LSP can now decay via RPV processes, and can carry color and electric charge. This leads to unique signatures [28,32–35] that are disallowed in conventional models with R-parity conservation.

A novel possibility with RPV is that the LSP could be a stop, where the large mass of the top quark acts to make the stop significantly lighter than the other squarks due to renormalization group effects [36–38]. Although, according to theory predictions based on this model, a stop LSP is much less likely than an electroweak gaugino LSP even when taking naturalness considerations into account; it is interesting nonetheless to perform a search for the stop in the LHC data. The stop pair production rate via the strong interaction is higher than the pair production rate of electroweak gauginos in the experimentally accessible mass ranges [34,35]. The total width of the stop is expected to be negligible relative to experimental resolution according to this model. Theory predicts stop pair production

[*]Full author list given at the end of the article.

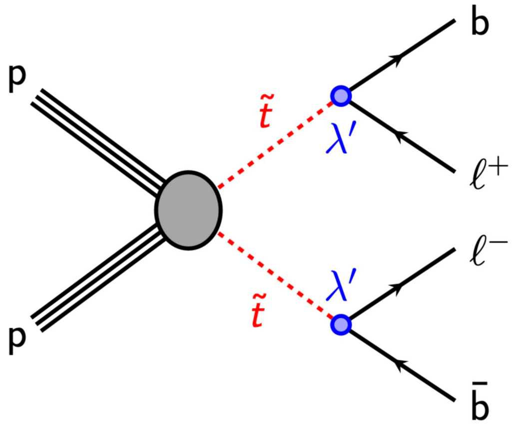

FIG. 1. Diagram for stop pair production, with each stop decaying into a charged lepton and a b-quark.

cross sections from 610 to 0.015 fb for 500 GeV to 2 TeV mass stops [39].

This paper presents a search for direct stop pair production, with the decay of each stop via an RPV interaction to a charged lepton and a b-quark (see Fig. 1), based on 140 fb^{-1} of proton-proton collisions at $\sqrt{s} = 13$ TeV recorded with the ATLAS detector. Previous related results include the RPV stop search with a partial Run 2 dataset with an integrated luminosity of 36.1 fb^{-1} [40], the RPV chargino/neutralino search with a trilepton resonance [41] and the search for top squarks in final states with two top quarks and several light-flavored jets [42]. Leptoquark results and RPV long-lived searches also include similar final states to this analysis [43–49]. In contrast to R-parity conserving searches for the stop, there is no significant missing transverse momentum. The stop decay branching ratios to eb, μb, and τb depend on the neutrino mass hierarchy [50,51]. The experimental signature comprises two oppositely charged leptons, which do not have to be the same flavor, and two b-jets. For this analysis, only events with electron or muon signatures are selected, and final states are split by flavor into ee, $e\mu$, and $\mu\mu$ channels. Sensitivity for a stop decaying to a b-jet and τ-lepton (through leptonic τ decay) is obtained through investigation of these electron and muon channels. A loose requirement of one or more identified b-jets is used to maximize signal selection efficiency for high values of the stop mass. There are two permutations of the leptons and jets to form lepton-jet pairs; the permutation with the smallest mass asymmetry is chosen to reconstruct the stop decays correctly with high efficiency and the value of the asymmetry is required to be small to reject background. The invariant mass of each lepton-jet resonance is required to be above the top quark mass to further reduce background from top quark pair and single top quark production. This analysis extends the reach of previous searches by performing a fit to the distribution of the mass of the leading lepton-jet pair.

The ATLAS detector is described in Sec. II, with the dataset collected during Run 2 of the LHC and the corresponding Monte Carlo simulation samples presented in Sec. III. The identification and reconstruction of jets and leptons is presented in Sec. IV, and the discriminating variables used to construct the signal regions are described in Sec. V. The method of background estimation is described in Sec. VI, and the systematic uncertainties are detailed in Sec. VII. Results are presented in Sec. VIII.

II. ATLAS DETECTOR

The ATLAS detector [52] at the LHC covers nearly the entire solid angle around the collision point.[1] It consists of an inner tracking detector surrounded by a thin superconducting solenoid, electromagnetic and hadron calorimeters, and a muon spectrometer incorporating three large superconducting air-core toroidal magnets.

The inner-detector system (ID) is immersed in a 2 T axial magnetic field and provides charged-particle tracking in the range $|\eta| < 2.5$. The high-granularity silicon pixel detector covers the vertex region and typically provides four measurements per track, the first hit normally being in the insertable B-layer installed before Run 2 [53,54]. It is followed by the silicon microstrip tracker, which usually provides eight measurements per track. These silicon detectors are complemented by the transition radiation tracker (TRT), which enables radially extended track reconstruction up to $|\eta| = 2.0$. The TRT also provides electron identification information based on the fraction of hits (typically 30 in total) above a higher energy-deposit threshold corresponding to transition radiation.

The calorimeter system covers the pseudorapidity range $|\eta| < 4.9$. Within the region $|\eta| < 3.2$, electromagnetic calorimetry is provided by barrel and end cap high-granularity lead/liquid-argon (LAr) calorimeters, with an additional thin LAr presampler covering $|\eta| < 1.8$ to correct for energy loss in material upstream of the calorimeters. Hadron calorimetry is provided by the steel/scintillator-tile calorimeter, segmented into three barrel structures within $|\eta| < 1.7$, and two copper/LAr hadron end cap calorimeters. The solid angle coverage is completed with forward copper/LAr and tungsten/LAr calorimeter modules optimized for electromagnetic and hadronic energy measurements respectively.

[1]ATLAS uses a right-handed coordinate system with its origin at the nominal interaction point (IP) in the centre of the detector and the z-axis along the beam pipe. The x-axis points from the IP to the center of the LHC ring, and the y-axis points upward. Polar coordinates (r, ϕ) are used in the transverse plane, ϕ being the azimuthal angle around the z-axis. The pseudorapidity is defined in terms of the polar angle θ as $\eta = -\ln\tan(\theta/2)$, and is equal to the rapidity $y = \frac{1}{2}\ln(\frac{E+p_z c}{E-p_z c})$ in the relativistic limit. Angular distance is measured in units of $\Delta R \equiv \sqrt{(\Delta y)^2 + (\Delta\phi)^2}$.

TABLE I. MC simulation details by physics process.

Process	Event generator	PS and hadronization	UE tune	PDF	Cross section order
$t\bar{t}$	POWHEG BOX v2	PYTHIA 8	A14	NNPDF3.0NLO	NNLO + NNLL [60–63]
single top (Wt)	POWHEG BOX v2	PYTHIA 8	A14	NNPDF3.0NLO	NNLO+NNLL [60–62,64]
W/Z + jets	SHERPA 2.2.1	SHERPA 2.2.1	Default	NNPDF3	LO + NLO [65–67]
Diboson, triboson	SHERPA 2.2.2	SHERPA 2.2.2	Default	NNPDF3	LO + NLO [66,68,69]
$t\bar{t} + V$	MADGRAPH5_AMC@NLO 2.3.3	PYTHIA 8	A14	NNPDF3	NLO [70]
$\tilde{t}\bar{\tilde{t}}$ signal	MADGRAPH5_AMC@NLO 2.6.2	PYTHIA 8	A14	CTEQ6L1	NLO + NLL [71–73]

The muon spectrometer (MS) comprises separate trigger and high-precision tracking chambers measuring the deflection of muons in a magnetic field generated by the superconducting air-core toroidal magnets. The field integral of the toroids ranges between 2.0 and 6.0 Tm across most of the detector. Three layers of precision chambers, each consisting of layers of monitored drift tubes, cover the region $|\eta| < 2.7$, complemented by cathode-strip chambers in the forward region, where the background is highest. The muon trigger system covers the range $|\eta| < 2.4$ with resistive-plate chambers in the barrel, and thin-gap chambers in the end cap regions.

Events are selected by the first-level trigger system implemented in custom hardware, followed by selections made by algorithms implemented in software in the high-level trigger [55]. The first-level trigger accepts events from the 40 MHz bunch crossings at a rate below 100 kHz, which the high-level trigger further reduces in order to record complete events to disk at about 1 kHz.

A software suite [56] is used in data simulation, in the reconstruction and analysis of real and simulated data, in detector operations, and in the trigger and data acquisition systems of the experiment.

III. DATA AND SIMULATED EVENT SAMPLES

This analysis is performed using data from the LHC pp collisions with center-of-mass energy of $\sqrt{s} = 13$ TeV, collected during 2015–2018 with the ATLAS detector. The total integrated luminosity of this dataset is 140 fb^{-1}. The uncertainty of the combined 2015–2018 integrated luminosity is 0.83% [57], obtained by the LUCID-2 detector [58] for the primary luminosity measurements, complemented by measurements using the inner detector and calorimeters. Due to the high instantaneous luminosity and large total inelastic pp cross section, there are on average 33.7 simultaneous ("pileup") collisions in each bunch crossing. Data events must satisfy quality requirements to be included in the analysis [59].

Monte Carlo (MC) simulation is used to predict the backgrounds from SM processes, estimate the detector response and efficiency to reconstruct the signal process and the associated systematic uncertainties. The largest sources of SM background are top quark pair production ($t\bar{t}$), single top quark production (single top), and Z + jets production, and their yields are estimated through data-driven methods described in Sec. VI. Smaller backgrounds originate from W + jets, $t\bar{t} + V(V = W, Z)$, and triboson and diboson (vector boson) production and are estimated directly from MC simulation. Details of the MC simulation are given below and are summarized in Table I.

The production of $t\bar{t}$ events was modeled using the POWHEG BOX v2 [60–62] generator at next-to-leading order (NLO) in QCD with the NNPDF3.0NLO [65] set of parton distribution functions (PDF) and the h_{damp} parameter[2] set to 1.5 times the mass of the top quark, which is about 172.5 GeV [74]. The associated production of top quarks with W bosons (single top Wt) was modeled by the POWHEG BOX v2 generator at NLO in QCD using the five-flavor scheme and the NNPDF3.0NLO PDF set. [65]. The diagram removal scheme [75] was used to remove interference and overlap with $t\bar{t}$ production. The uncertainty on the single top yield due to the destructive interference between the $t\bar{t}$ and Wt processes is estimated by using inclusive $WWbb$ samples generated at leading order (LO) using MADGRAPH5_AMC@NLO 2.3.3 [70]. The events were interfaced to PYTHIA 8.230 [76] for the modeling of the parton shower (PS), hadronization and the underlying event (UE), using the A14 set of tuned parameters (tune) [77] and the NNPDF2.3LO set of PDFs [78].

Due to the majority of $t\bar{t}$ and single top events being produced with significantly lower H_{T} than the targeted signal region, special H_{T}-sliced $t\bar{t}$ and single top samples were utilized. H_{T} is defined as the scalar sum of the p_{T} of the decay products. These samples apply H_{T} requirements on produced events in order to boost available statistics at high H_{T}. This improves estimation of systematic uncertainties on the background in the signal regions with the highest values of the leading lepton-jet mass. Other than the additional H_{T} filter, the generation configuration is identical to the nominal samples.

MC samples modeling pairs of stops decaying into $b\ell$ are generated for use in optimizing the selections and estimating the analysis sensitivity. Signal samples are

[2] The h_{damp} parameter is a resummation damping factor and one of the parameters that controls the matching of POWHEG matrix elements to the parton shower and thus effectively regulates the high-p_{T} radiation against which the $t\bar{t}$ system recoils.

generated at LO in QCD for stop masses between 600 and 1900 GeV in increments of 50 GeV using MADGRAPH5_AMC@NLO 2.6.2 [70] interfaced with PYTHIA with the CTEQ6L1 PDF set [70,79]. Signal cross sections are calculated at NLO in QCD in the strong coupling constant, adding the resummation of soft-gluon emission at next-to-leading-logarithmic accuracy (NLO + NLL) [71–73]. The nominal cross sections and the uncertainty are taken from an envelope of cross section predictions using different PDF sets and factorization and normalization scales, as described in Ref. [80]. The stops are allowed to decay directly into a b-quark and either an electron, muon, or τ-lepton, with identical branching ratios given by $\mathcal{B}(\tilde{t} \to eb) = \mathcal{B}(\tilde{t} \to \mu b) = \mathcal{B}(\tilde{t} \to \tau b) = 1/3$. In the interpretation of the search results, various hypotheses were tested for the branching ratios by reweighting events with appropriate factors so that the branching ratios for all three charged lepton flavors sum to unity.

The modeling of c-hadron and b-hadron decays was performed with EVTGEN 1.6.0 [81]. EVTGEN is used for all samples except those generated with SHERPA. Events from all generators were propagated through a full simulation of the ATLAS detector using GEANT4 [82] to model the interactions of particles with the detector. The generation of the simulated event samples includes the effect of multiple pp interactions per bunch crossing, as well as the effect on the detector response due to interactions from bunch crossings before or after the one containing the hard interaction.

IV. PHYSICS OBJECT RECONSTRUCTION

Each event is required to have a primary reconstructed vertex with two or more associated tracks, where the primary vertex is chosen as the vertex with the highest Σp_{T}^2 of associated tracks [83]. Two stages of quality and kinematic requirements are applied to leptons and jets. The looser baseline requirements are applied first, and baseline leptons and jets are used to resolve any misidentification or overlap among electrons, muons, and jets. The subsequent tighter signal requirements are then applied to identify high-quality leptons and jets in the kinematic phase space of interest.

Electron candidates are reconstructed from energy deposits in the electromagnetic calorimeter matched to a charged-particle track in the ID. Baseline electron candidates must have $p_{\mathrm{T}} > 10$ GeV, $|\eta| < 2.47$, and satisfy a baseline *Loose* electron likelihood identification [84]. Each baseline electron must have a longitudinal impact parameter with respect to the primary vertex (z_0^{PV}) that satisfies $|z_0^{\mathrm{PV}} \sin\theta| < 0.5$ mm. Signal electrons must pass the baseline electron selection, have $p_{\mathrm{T}} > 40$ GeV, and satisfy a *Tight* electron likelihood identification. In addition, they must be isolated from nearby activity, satisfying a loose p_{T}-dependent track-based criterion [84]. Finally, their trajectory must be consistent with the primary vertex, such that their impact parameter in the transverse plane (d_0^{PV}) satisfies $|d_0^{\mathrm{PV}}|/\sigma_{d_0^{\mathrm{PV}}} < 5$, where $\sigma_{d_0^{\mathrm{PV}}}$ is the uncertainty in d_0^{PV}. Muon candidates are reconstructed by combining tracks in the ID with tracks in the MS. Baseline muon candidates must have $p_{\mathrm{T}} > 10\,\mathrm{GeV}$, $|\eta| < 2.7$, $|z_0^{\mathrm{PV}} \sin\theta| <$ 0.5 mm, and satisfy the *Medium* muon identification criteria [85]. Signal muons must pass the baseline muon selection, have $p_{\mathrm{T}} > 40$ GeV, $|\eta| < 2.7$ and $|d_0^{\mathrm{PV}}|/\sigma_{d_0^{\mathrm{PV}}} < 3$. As with electrons, muons must satisfy the p_{T}-dependent loose track-based isolation criteria [85]. Events containing a poorly measured signal muon, as determined by having incompatible momentum measurements in the ID and the MS, are rejected. Absolute requirements of $|z_0^{\mathrm{PV}}| < 1$ mm and $|d_0^{\mathrm{PV}}| < 0.2$ mm on the impact parameters of signal muons are applied to reject cosmic muons.

Reconstructed jets are identified by combining measurements from both the ID and the calorimeter using a particle flow (PFlow) algorithm [86]. PFlow objects defined by this algorithm are then passed as inputs to the anti-k_t algorithm [86,87] with a radius parameter $R = 0.4$. Jets are further calibrated to account for the predicted detector response in MC simulation, and a residual calibration of jets in data is derived through *in situ* measurements [88]. Baseline jet candidates are required to have $p_{\mathrm{T}} > 20$ GeV and $|\eta| < 4.5$. Jets with $p_{\mathrm{T}} < 60$ GeV and $|\eta| < 2.4$ must satisfy requirements on the jet vertex tagger [89], which is used to reject pileup jets. Signal jets must pass the baseline jet selection and have $p_{\mathrm{T}} > 60$ GeV. Events are rejected if they contain a jet that fails the *Loose* quality criteria [90], reducing contamination from noise bursts and noncollision backgrounds.

The identification of baseline jets containing b-hadrons (b-jets) is performed using the DL1r b-tagging algorithm [91]. The b-tagging requirements result in an efficiency of 85% for jets containing b-hadrons, as determined in a sample of simulated $t\bar{t}$ events with final states containing two leptons, and the corrections are consistent with unity with uncertainties at the level of a few percent over most of the jet p_{T} range. The 85% working point has a rejection factor of 3.1 and of 33 on charm and light-jets, respectively [92].

To avoid reconstructing a single detector signature in multiple ways, an overlap removal procedure is performed on baseline leptons and jets. The requirements are applied sequentially, and failing particles are removed from consideration in the subsequent steps. If an electron and muon share a track in the ID, the electron is removed. Any jet that is not b-tagged and is within a distance $\Delta R(e, \mathrm{jet}) \leq 0.2$ of an electron is removed. Any electron with $\Delta R(e, \mathrm{jet}) \leq 0.4$ from a baseline jet is removed since this electron is assumed to be a constituent of the jet. Any jet that is within $\Delta R(\mu, \mathrm{jet}) \leq 0.2$ and has less than three tracks is removed. If that jet is b-tagged, the muon is instead removed. Any muon with $\Delta R(\mu, \mathrm{jet}) \leq 0.4$ of a baseline jet is then removed.

TABLE II. Summary of the requirements used in signal, control, and validation regions. All regions require at least two jets and two oppositely charged leptons. In the CRZ both leptons are required to be of the same flavor.

Region	N_b	$m_{b\ell}^0$ [GeV]	$m_{b\ell}^{1,\mathrm{rej}}$ [GeV]	H_T [GeV]	$m_{b\ell}^{\mathrm{asym}}$	$m_{\ell\ell}$ [GeV]	$m_{b\ell}^{0,\mathrm{rej}}$ [GeV]
SR	≥ 1	> 400	> 150	> 1000	< 0.2	> 300 GeV	...
CRtt	≥ 1	[180, 500]	< 150	[500, 800]	< 0.2	> 200 GeV	< 180
CRst	$= 2$	[180, 500]	< 150	[400, 800]	< 0.2	> 200 GeV	> 180
CRZ	≥ 1	> 700	...	> 1000	< 0.2	[76.2, 106.2]	...
VR $m_{b\ell}^0$	≥ 1	> 500	< 150	[600, 800]	< 0.2	> 300 GeV	...
VR $m_{b\ell}^{1,\mathrm{rej}}$	≥ 1	[200, 500]	> 150	[600, 800]	< 0.2	> 300 GeV	...
VR H_T	≥ 1	[200, 500]	< 150	> 800	< 0.2	> 300 GeV	...
VRZ	$= 0$	[500, 800]	> 150	> 1000	< 0.2	> 300 GeV	...

The trigger, reconstruction, identification, and isolation efficiencies of electrons [84] and muons [85] in MC simulation are corrected using events in data with leptonic Z and J/ψ decays. Similarly, corrections to the b-tagging efficiency and mistag rate in MC simulation are derived from various control regions in data [92–94].

V. EVENT SELECTION

To identify the pair production of stops, events are required to have at least two leptons and two jets. If more than two leptons or two jets are found, the two highest-p_T leptons and jets are selected. At least one of the two leading jets must be b-tagged. The selected leptons are required to have opposite charge, and one of them must be consistent with the associated single-lepton trigger [95,96]. The lepton is not required to be the leading lepton in the event, but must exceed the offline p_T threshold for that trigger. The offline p_T requirement for each trigger is set to 1 GeV above online for electron triggers and 5% above for muon triggers. The trigger requirement is applied in both data and MC. To account for the difference in trigger efficiency, a trigger scale factor is applied to MC events that passed the trigger requirement [97]. This trigger requirement is highly efficient for signal events, with an efficiency of 93% for the $\mu\mu$ channel and 98% for the ee channel.

The lepton-jet pair from each stop decay reconstructs the invariant mass $m_{b\ell}$ of the original stop. In an event with two leptons and two jets, two pairings are possible: one that reconstructs the correct stop masses, and one which inverts the pairing and incorrectly reconstructs the masses. As the two masses for the correct pairing should be roughly equal, the pairing that minimizes the mass asymmetry between $m_{b\ell}^0$ and $m_{b\ell}^1$ is chosen, defined as

$$m_{b\ell}^{\mathrm{asym}} = \frac{m_{b\ell}^0 - m_{b\ell}^1}{m_{b\ell}^0 + m_{b\ell}^1}.$$

Here $m_{b\ell}^0$ is chosen to be the larger of the two masses. Events are further selected to have small mass asymmetry $m_{b\ell}^{\mathrm{asym}} < 0.2$. This reduces the contamination from background processes with a more uniform $m_{b\ell}^{\mathrm{asym}}$ distribution. The power of the asymmetry variable can be seen in the reference to the previous iteration of this search [40]. Several other kinematic selections are defined to reduce the contribution from the largest backgrounds. As the stop decay products are generally very energetic, a selection on their scalar p_T sum is applied such that $H_\mathrm{T} > 1000$ GeV, with H_T defined as the scalar sum of the p_T of the selected two leptons and two jets. To reduce contamination from $Z+$jets events, a requirement is placed on the invariant mass of two leptons of $m_{\ell\ell} > 300$ GeV. A large fraction of the background from processes involving a top quark is suppressed through the requirement on $m_{b\ell}^0$ and $m_{b\ell}^{\mathrm{asym}}$, with correctly paired top quark masses falling well below the signal region (SR) requirements. However, top quark decays in which the lepton and b-jet decay products are mispaired can enter the SRs if the invariant masses happen to be large. In such cases it is the rejected pairing that properly reconstructs the decay of a top quark, with one of the two $b\ell$ pair masses below the kinematic limit for a top quark decay. To suppress such backgrounds, events are rejected if the subleading $b\ell$ mass of the rejected pairing, $m_{b\ell}^{1,\mathrm{rej}}$, is indicative of that of a reconstructed top quark, with $m_{b\ell}^{1,\mathrm{rej}} < 150$ GeV.

All of the SRs require the leading lepton-jet mass to be above 400 GeV. A set of 15 variable-width bins in the leading lepton-jet mass were chosen from optimization studies based on simulated signal and backgrounds. The signal width of the reconstructed lepton-jet resonances increases with mass, from ~20–80 GeV for stop mass values of 600–1900 GeV. The optimization studies for the bin widths included the systematic uncertainty on the background separately for each bin. In contrast to the previous search with two nested SRs above 800 GeV and above 1100 GeV [40], this search extends the sensitivity to lower and higher values for the stop mass and to lower values for the stop decay branching ratio to an electron and a b-jet or to a muon and a b-jet. A full list of region selections is given in Table II.

VI. BACKGROUND ESTIMATION

For each of the relevant backgrounds in the signal regions, one of two methods is used to estimate the contribution. The small $W + \text{jets}$, $t\bar{t} + V$, diboson and triboson backgrounds are estimated directly from MC simulation and the normalization is corrected to the highest-order theoretical cross section available. For the dominant $t\bar{t}$, single top, and $Z + \text{jets}$ backgrounds, the expected yield in the signal regions (SRs) is estimated by scaling each MC prediction by a normalization factor derived from three dedicated control regions (CRs), one for each background process. Each CR is defined to be kinematically close to the SRs while inverting or relaxing specific selections. This enhances the contribution from the targeted background process in the CR designed for each major background while reducing the contamination from other backgrounds and the benchmark signals.

To derive a background-only estimate, the normalizations of the $t\bar{t}$, single top, and $Z + \text{jets}$ backgrounds are determined through a likelihood fit [98] performed simultaneously to the observed number of events in each CR. The expected yield in each region is given by the inclusive sum over all background processes in the ee, $e\mu$, and $\mu\mu$ channels. The normalization factors for each of the $t\bar{t}$, single top, and $Z + \text{jets}$ backgrounds are free parameters of the fit. The other systematic uncertainties are treated as nuisance parameters in the fit and are not significantly constrained.

Several validation regions (VRs) are defined to test the extrapolation from the CRs to SRs over the relevant kinematic variables. The VRs are disjoint from both the CRs and SRs, and are constructed to fall between one or more CRs and the SRs in one of the extrapolated variables. The VRs are not included in the fit, but provide a statistically independent cross-check of the background prediction. Four VRs are constructed to test the extrapolation in the $m_{b\ell}^{0}$, $m_{b\ell}^{1,\text{rej}}$, $m_{\ell\ell}$ and H_{T} observables. Validation regions show signal contamination generally below 10% for stop masses > 600 GeV. Details of the selection criteria in each CR and VR are provided in Table II.

A. Control regions

The $t\bar{t}$ CR (CRtt) has specific requirements to separate it from the SR. The SR selection on $m_{b\ell}^{1,\text{rej}}$ is inverted to $m_{b\ell}^{1,\text{rej}} < 150$ GeV. This enhances the fraction of $t\bar{t}$ events where the jets and leptons are mispaired. The average H_{T} value needs to be lower in CRtt with respect to the SRs to remove contamination from signal events: a selection of $500 \leq H_{\text{T}} \leq 800$ GeV is applied. The selection on $m_{\ell\ell}$ is loosened to $m_{\ell\ell} > 200$ GeV, and the $m_{b\ell}^{0}$ selection is restricted to between 180 and 500 GeV to enhance the $t\bar{t}$ contribution in the CRtt. This $t\bar{t}$ contribution comes from the incorrectly paired $m_{b\ell}$. The b-tagging requirement is kept the same as the SR. The expected distributions of $m_{b\ell}^{0}$, $m_{b\ell}{}^{1,\text{rej}}$, and H_{T} are shown in Figs. 2(a)–2(c) for the $t\bar{t}$ control region.

The $Z + \text{jets}$ control region (CRZ) places selections on the dilepton pair to isolate the leptons coming from a Z boson. The dilepton invariant mass must be consistent with the mass of the Z boson ($|m_{\ell\ell} - m_Z| \leq 15$ GeV) and the leptons are required to be of the same flavor, while still having opposite charge. The $m_{\ell\ell}$ selection is very effective at removing signal contamination, which makes it possible to keep the H_{T} and $m_{b\ell}^{0}$ of the CRZ events close to the SR. The requirements of $H_{\text{T}} > 1000$ GeV and $m_{b\ell}^{0} > 700$ GeV are placed. The $m_{b\ell}^{\text{asym}}$ is required to be less than 0.2.

As single top production has a smaller cross section than $t\bar{t}$, there is some difficulty with $t\bar{t}$ contamination in the single top CR (CRst). To allow the single top background to have lower purity, the $t\bar{t}$ CR was designed to have higher statistics to constrain the $t\bar{t}$ normalization factor. The purity for single top is about 30% in CRst. The main difference between the CRst and CRtt is that the selection on $m_{b\ell}^{0,\text{rej}}$ is inverted. While $t\bar{t}$ events are expected to have both $b\ell$ masses in the rejected pairing compatible with the top quark mass, only one is for single top backgrounds. This distinction allows for selecting the $m_{b\ell}^{0,\text{rej}}$ above the top quark mass to reject $t\bar{t}$ events in the CRst. This region additionally requires both leading jets to be b-tagged, as this strengthens the discriminating power of the higher $m_{b\ell}^{0,\text{rej}}$ requirement. The expected distribution of $m_{b\ell}^{0,\text{rej}}$ is shown in Fig. 2(d) for the CRst. In the case of $t\bar{t}$ events, requiring 2 b-tags improves the confidence that the correct jets are selected from the top quark decay, leading to at least one of the potential jet-lepton pairing schemes to properly reconstruct both top quarks. The selections $m_{b\ell}^{0} \geq 180$ GeV and $m_{b\ell}^{0,\text{rej}} \geq 180$ GeV are thus very effective at removing $t\bar{t}$ events. The values of H_{T}, $m_{\ell\ell}$ and $m_{b\ell}^{0}$ of the leading $b\ell$ pair are constrained to reduce signal contamination, as described in Table II.

B. Validation regions

Four disjoint validation regions are used to test the extrapolation of the background fit from the CRs to the SRs. A full list of the region selections is given in Table II. The main extrapolations are from the $t\bar{t}$ and single top CRs to the SR: in particular, there is a significant extrapolation on the invariant mass of the leading accepted $b\ell$ pair $m_{b\ell}^{0}$, on the invariant mass of the subleading rejected $b\ell$ pair $m_{b\ell}^{1,\text{rej}}$, and on the H_{T}. For this reason, three separate validation regions are defined by keeping all the $t\bar{t}$ CR selections, and reverting the selection on these three variables respectively. The upper bound on $m_{b\ell}^{0,\text{rej}}$ is also removed from the VRs. Such regions allow for validation of the extrapolations from the CRs to the SRs. The CRZ

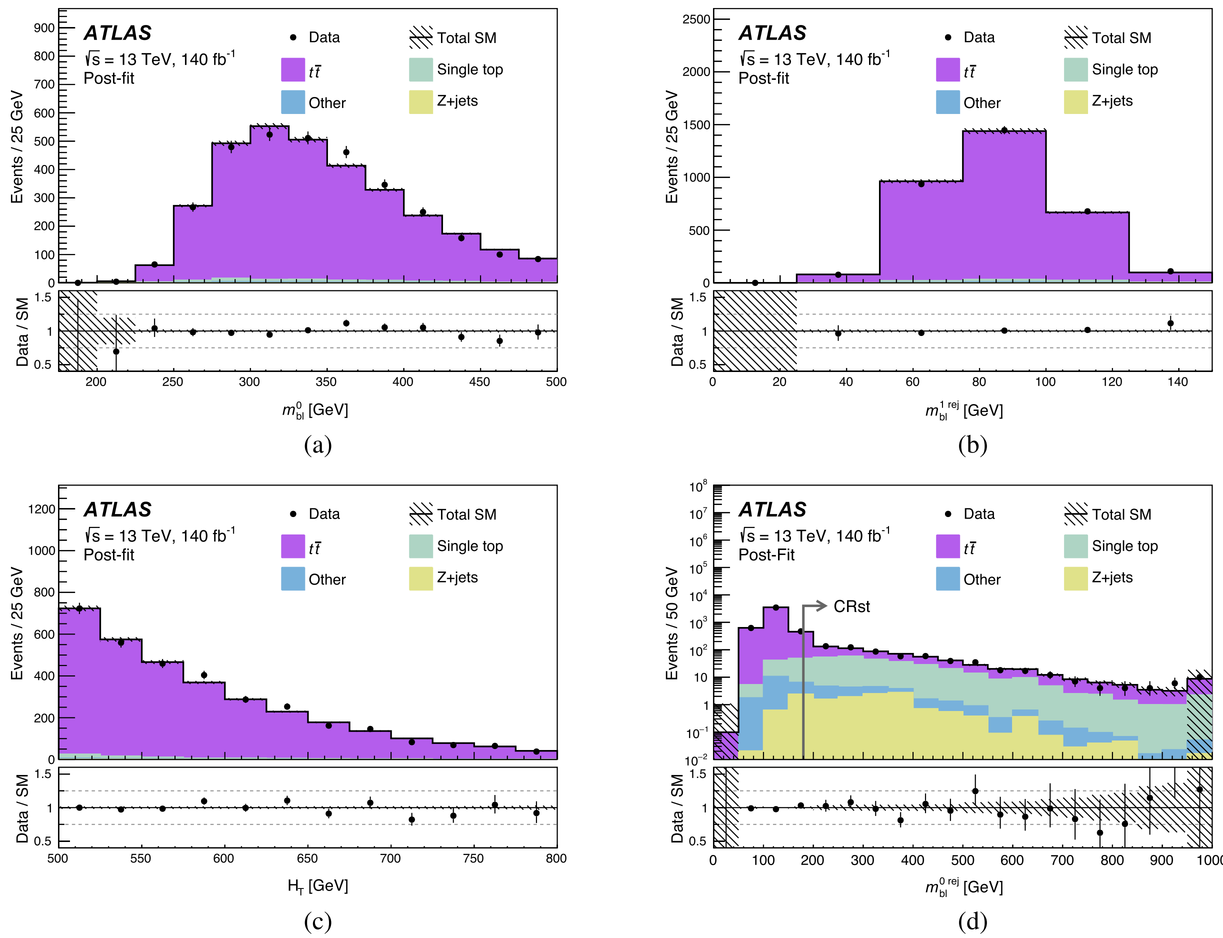

FIG. 2. Distributions of (a) $m_{b\ell}^{0}$ in the CRtt, (b) $m_{b\ell}^{1,\mathrm{rej}}$ in the CRtt, (c) H_{T} in the CRtt, and (d) $m_{b\ell}^{0,\mathrm{rej}}$ in the CRst for the data and post-fit MC prediction. Normalization factors are derived from the background-only fit configuration are applied to the dominant $t\bar{t}$, single top, and $Z+$jets processes. The "Other" category consists of $W+$jets, $t\bar{t}+V$, diboson, and triboson processes. Processes are listed from largest to smallest contribution to the given region reading left to right and then top to bottom. The relevant CR event selections are applied for each flavor inclusive distribution except the selection on the variable shown for (d). The arrow indicates the CR selection on the $m_{b\ell}^{0,\mathrm{rej}}$ variable. The hatched band represents statistical and theoretical uncertainties on the backgrounds. The bottom panel of each plot shows the ratio between the data and the post-fit MC prediction. The last bin includes the overflow events.

applies similar selections as the SR, with the exception of the $m_{\ell\ell}$ selection that needs to be modified to select the Z-boson peak. For this reason, a VR is defined with exactly zero b-tagged jets, to enhance the $Z+$jets background with respect to $t\bar{t}$ and single top. The VR$m_{b\ell}^{1,\mathrm{rej}}$ is divided into opposite-flavor leptons and same-flavor leptons, where the latter region allows a check of the estimate of the $Z+$jets background in the region with one or more b-tagged jets. All the other SR selections are applied, including $m_{\ell\ell} > 300$ GeV, with the only exception being $m_{b\ell}^{0}$, for which a window of [500, 800] GeV is used to reduce signal contamination.

The observed data yield and the post-fit background prediction for each CR and VR are shown in Fig. 3. Good agreement is seen in all validation regions, with differences between the data and SM prediction within 1σ. The modeling of the extrapolated variable for each VR is shown in Fig. 4, demonstrating good agreement in the shape of the variables of interest. The resulting normalization factors for the $t\bar{t}$, single top, and $Z+$jets backgrounds are 0.88 ± 0.03 for $t\bar{t}$, 1.35 ± 0.24 for single top, and 0.88 ± 0.08 for $Z+$jets. Normalization factors are obtained from the background-only fit (constrained only by CRs) considering all systematic uncertainties for each of the three main backgrounds.

VII. SYSTEMATIC UNCERTAINTIES

Systematic uncertainties in the signal and background predictions arise from theoretical uncertainties in the expected yield and MC modeling, and from experimental sources. Experimental uncertainties reflect the precision of the energy and momentum calibration of jets and leptons, as well as corrections for the identification and

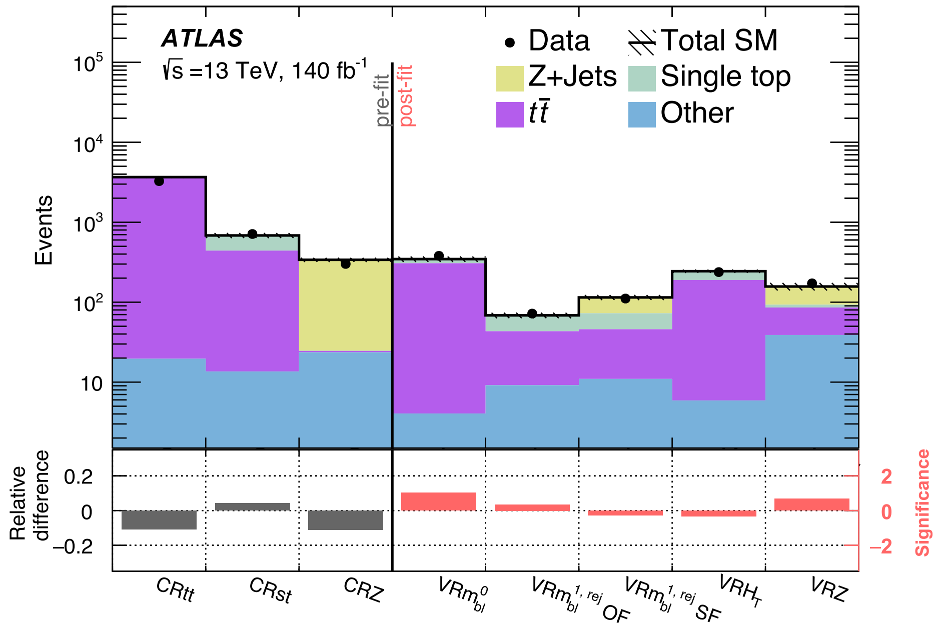

FIG. 3. Comparison of the observed data and expected numbers of events in the CRs (pre-fit) and VRs (post-fit). The "Other" category consists of $W+$jets, $t\bar{t}+V$, diboson and triboson processes. Processes are listed from largest to smallest contribution for the given region reading left to right and then top to bottom. The background prediction is derived with the background-only fit configuration. The bottom panel of the plot shows the relative difference, the difference between the observed data and total background divided by the observed data, for the CRs as well as the significance of the difference for the VRs. The significance is computed through a profile likelihood method [99].

reconstruction efficiencies in MC simulation. The dominant experimental uncertainties on the signal efficiency are related to jets, including those in the jet energy scale and resolution [88] and the calibration of the b-tagging efficiency [92–94]. The largest experimental uncertainties in the fitted background prediction in the SR are from the mistagging of light-flavor jets and the jet energy resolution. The experimental uncertainties associated with leptons each have a small impact on the final measurement, and include uncertainties in the efficiency, energy scale and resolution of electrons [84] and muons [85,100], and the calibration of the lepton trigger, identification, reconstruction, and isolation efficiencies.

Theoretical and MC modeling uncertainties of the $t\bar{t}$ and single top backgrounds account for the choice of event generator, underlying-event tune, and their parameters. The uncertainties are derived separately for each background process and are treated as uncorrelated nuisance parameters. For $t\bar{t}$ and single top backgrounds the theory systematics uncertainties considered arise from renormalization and factorization scale choices, PDF, α_s, MC generator, and parton shower modeling. For the $Z+$jets background only uncertainties from renormalization and factorization scale choices, PDF and α_s are considered. As the normalization for the $t\bar{t}$, single top and $Z+$jets background is constrained in the likelihood fits, the uncertainties are derived from the normalization factor of the relevant CR to each SR bin independently by comparing CR-to-SR yield ratios in alternative models. The uncertainty in the background estimate due to the choice of MC event generator is estimated for $t\bar{t}$ and single top backgrounds by comparing the CR-to-SR yield ratios derived using the nominal $t\bar{t}$ sample with another event sample produced with the MADGRAPH5_AMC@NLO 2.6.2 generator at NLO in QCD using the five-flavor scheme and the NNPDF2.3NLO PDF set. The events were interfaced with PYTHIA 8.230, using the A14 set of tuned parameters and the NNPDF2.3LO PDF. The uncertainty due to the parton shower and hadronization model was evaluated by comparing the nominal sample of events with a sample where events generated with the POWHEG BOX v2 generator were interfaced to HERWIG 7.04 [101,102], using the H7UE set of tuned parameters [102] and the MMHT2014LO PDF set [103].

An uncertainty in the single top yield due to the destructive interference between the $t\bar{t}$ and Wt processes is estimated by using inclusive $WWbb$ samples generated at LO using MADGRAPH5_AMC@NLO split by different requirements on the presence of resonant top quarks. The yields for each set of requirements is calculated in each SR bin and compared to one another to calculate a relative uncertainty on the Wt yields. This relative uncertainty is applied as an uncertainty on the transfer of the normalization factor from the CRst to each SR bin. For background processes that are not normalized in the CRs ($W+$jets, $t\bar{t}+V$, diboson, triboson), the theoretical uncertainty on the NLO cross section is applied.

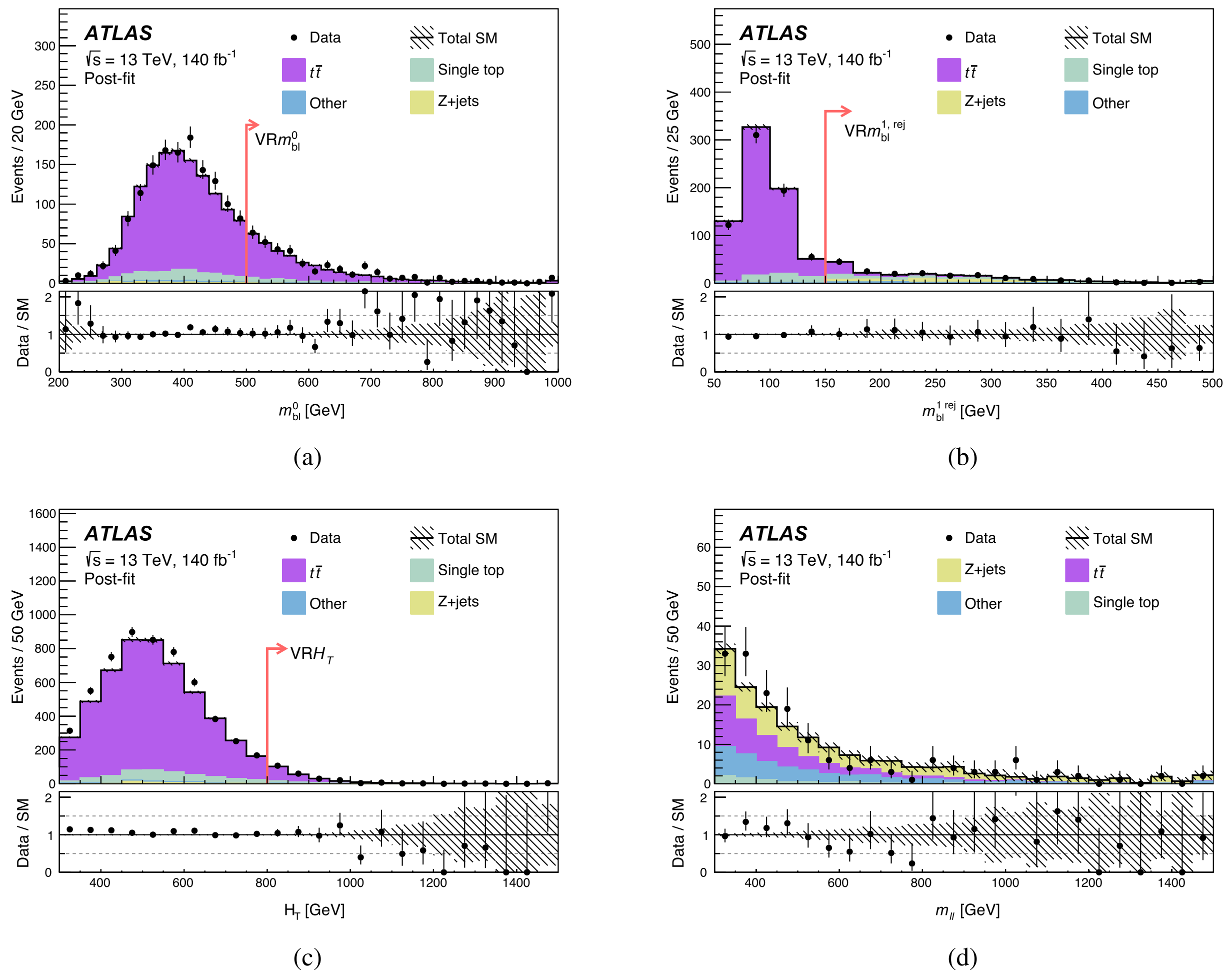

FIG. 4. Flavor-inclusive distributions of (a) $m^0_{b\ell}$ in the VR$m^0_{b\ell}$, (b) $m^{1,\mathrm{rej}}_{b\ell}$ in the VR$m^{1,\mathrm{rej}}_{b\ell}$, (c) H_T in the VRH_T, and (d) $m_{\ell\ell}$ in the VRZ for the data and post-fit MC prediction. Normalization factors are derived from the background-only fit configuration and are applied to the dominant $t\bar{t}$, single top, and $Z+$jets processes. The "Other" category consists of $W+$jets, $t\bar{t}+V$, diboson and triboson processes. Processes are listed from largest to smallest contribution to the given region reading left to right and then top to bottom. The relevant VR event selections are applied for each flavor-inclusive distribution except the selection on the variable shown for (a) $m^0_{b\ell}$ in the VR$m^0_{b\ell}$, (b) $m^{1,\mathrm{rej}}_{b\ell}$ in the VR$m^{1,\mathrm{rej}}_{b\ell}$, and (c) H_T in the VRH_T. Figure 4(d) includes all relevant VR event selections. Regions outside of the proposed cut may show slight discrepancy from applying normalization factors designed for the regions of interest. The hatched band represents statistical and theoretical uncertainties on the backgrounds. The arrow indicates the VR selection on the variable shown. The bottom panel of each plot shows the ratio between the data and the post-fit MC prediction. The last bin includes the overflow events.

Uncertainties in the expected yields of the stop signal samples are derived for each $m^0_{b\ell}$ bin of the SR as the envelope of variations to the renormalization and factorization scales, α_S, and PDF set. A theoretical uncertainty on the stop cross section is independently applied by varying the signal yield in all regions, and ranges from 8% to 22% for stop mass values from 600 to 1900 GeV. Uncertainties that affect the signal acceptance include the electron efficiency, with uncertainties calculated between 3% and 4% for the various stop masses when assuming $\mathcal{B}(\tilde{t}\to be)=\mathcal{B}(\tilde{t}\to b\mu)=50\%$, and are between 5% and 8% when assuming $\mathcal{B}(\tilde{t}\to be)=100\%$. Similarly, the muon efficiency uncertainties are between 2% and 4% when assuming $\mathcal{B}(\tilde{t}\to be)=\mathcal{B}(\tilde{t}\to b\mu)=50\%$, and rise to 6% when assuming $\mathcal{B}(\tilde{t}\to b\mu)=100\%$. The electron, muon, and jet energy scale and resolution uncertainties are generally below 1% for the stop signal models, reaching 1% for masses near the $m_{b\ell}$ threshold of 800 GeV. The b-tagging efficiency uncertainties are between 1% and 3%, reaching the largest value for the 600 GeV signal model.

VIII. RESULTS

To evaluate the presence of signal in this analysis, a multibin fit is used to maximize the likelihood function

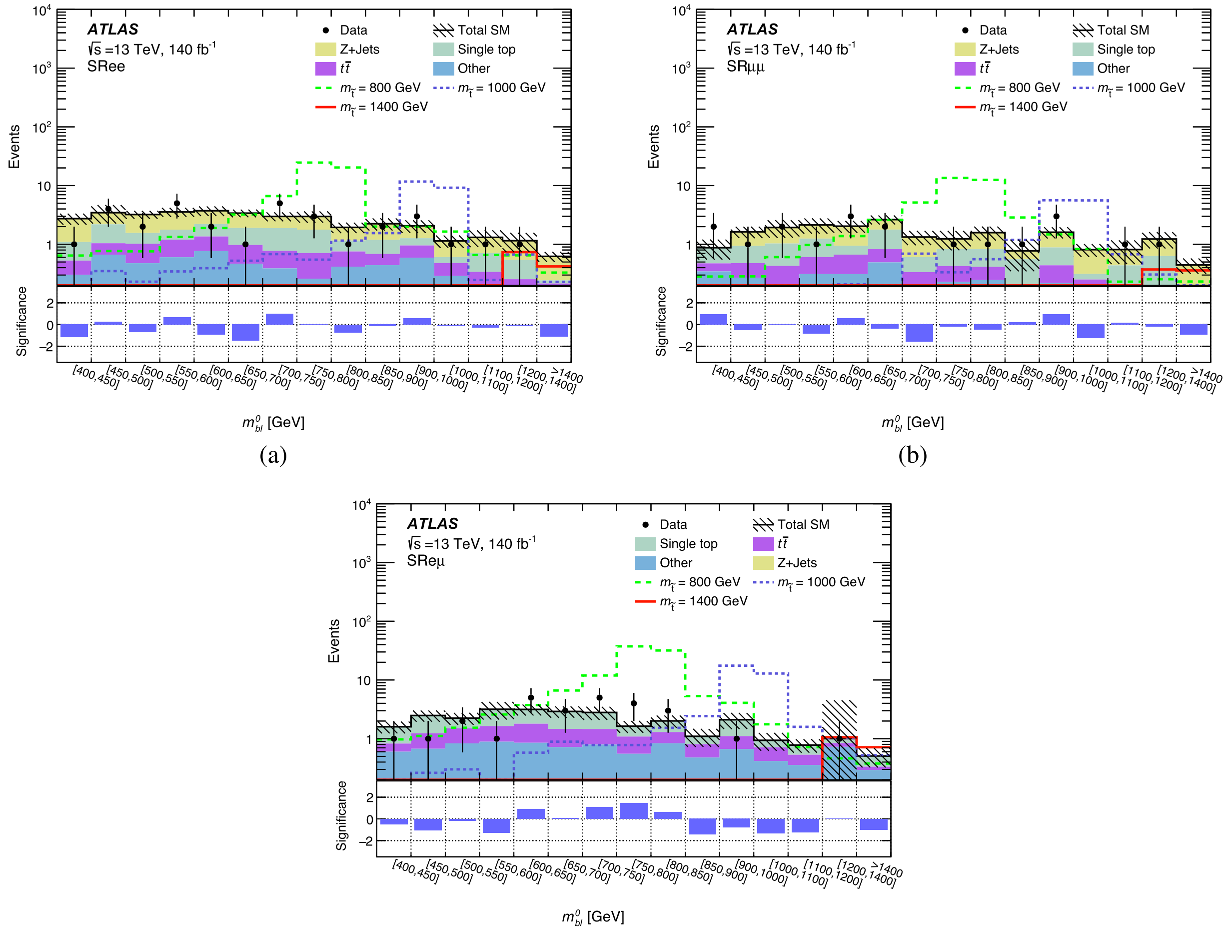

(a) (b) (c)

FIG. 5. The observed data and post-fit Monte Carlo expectation for SM processes in each SR bin for the flavor-aware configuration in (a) the ee channel, (b) the $\mu\mu$ channel, and (c) the $e\mu$ channel. Each plot shows the yields for a single flavor channel of the 45-bin background-only fit. All systematic uncertainties are applied in this fit. The "Other" category consists of $W+$jets, $t\bar{t}+V$, diboson and triboson processes. Processes are listed from largest to smallest contribution to the given region reading left to right and then top to bottom. The bottom panel of each plot shows the significance of the difference between the expected yields and observed data. Expected signal contributions for different stop mass hypotheses are shown, assuming equal branching ratios to electron, muon and τ-leptons. The significance is computed through a profile likelihood method [99].

$\mathcal{L}(\mu_{\text{sig}}, \theta)$. The likelihood function is a product of Poisson distributions for each bin and depends on the parameter of interest, μ_{sig}. This parameter, referred to as the signal strength, is defined by the ratio of the fitted signal cross section versus the theoretical cross section. The effect of systematic uncertainties in the signal and background predictions are described by nuisance parameters subject to Gaussian penalty terms in the likelihood function. For model dependent results, two exclusion fits were performed for each lepton branching ratio point probed: one inclusive 15-bin fit, which is agnostic to lepton final state, and one 45-bin fit simultaneously across all three lepton flavor channels ($e\mu, \mu\mu, ee$) as separate SRs. For each stop mass and branching ratio, the configuration that provides the strongest expected limit on the signal strength will be used. The flavor-agnostic configuration typically has the stronger expected sensitivity when $\mathcal{B}(\tilde{t} \to be)$, $\mathcal{B}(\tilde{t} \to b\mu)$, and $\mathcal{B}(\tilde{t} \to b\tau)$ are similar in size, while the flavor-aware configuration is more sensitive in the corners of the branching ratio plane.

The observed yields and fitted background predictions for the SRs are shown in Fig. 5 for the 45-bin fit and in Fig. 6 for the 15-bin fit. Yields for the 45-bin SR configurations are split across three plots (one for each lepton flavor channel). Estimated background is in agreement with observed data within 1σ over almost all signal bins. Validation regions show that background is modeled well. Model-dependent limits are given in Fig. 7 for a range of assumed stop masses. The model-dependent results show observed limits that are stronger than the expected

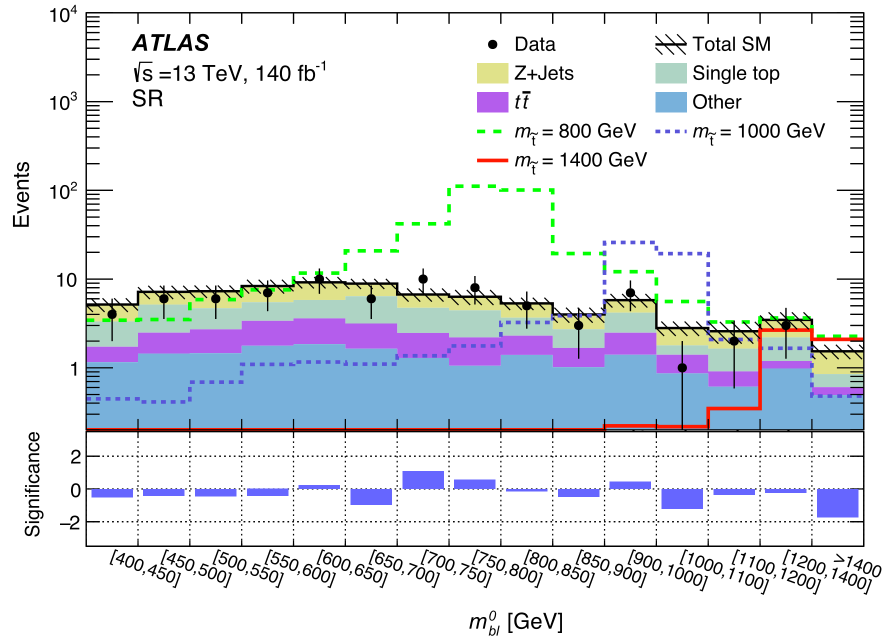

FIG. 6. The observed data and post-fit Monte Carlo expectation for SM processes in each SR bin for the flavor-agnostic configuration. The results are obtained from the SRs using the 15-bin background-only fit. All systematic uncertainties are applied in this fit. The "Other" category consists of $W+$jets, $t\bar{t}+V$, diboson and triboson processes. Processes are listed from largest to smallest contribution to the given region reading left to right and then top to bottom. The bottom panel of the plot shows the significance of the difference between the expected yields and observed data. Expected signal contributions for different stop mass hypotheses are shown assuming equal branching ratios to electron, muon and τ-leptons. The significance is computed through a profile likelihood method [99].

limits at the 1σ level, primarily due to the highest mass signal bin where zero events are observed while 2.14 ± 0.60 events are expected from background predictions. The behavior of the limits shown in Fig. 7 is driven by the highest mass bin of the SR, which has low statistics but an observed deficit.

Exclusion limits are derived at 95% CL for stop pair production. Limits are obtained through an exclusion fit based on a profile log-likelihood ratio test using the $\mathrm{CL_s}$ prescription [104] and asymptotic approximation [105], following the simultaneous fit to the CRs and SRs [98]. The signal contributions in both the SRs and CRs are accounted for in the fit, although they are negligible in the latter. Exclusion fits are performed separately for various branching ratio assumptions, sampling, in steps of 5%, values of $\mathcal{B}(\tilde{t} \to be)$, $\mathcal{B}(\tilde{t} \to b\mu)$, and $\mathcal{B}(\tilde{t} \to b\tau)$ whose sum is unity and reweighting events in the signal samples according to the generated decays. The limits are strongest at low values of $\mathcal{B}(\tilde{t} \to b\tau)$, where the expected number of events with electrons or muons in the final state is largest. Expected limits are slightly stronger for increasing $\mathcal{B}(\tilde{t} \to be)$, reflecting a higher trigger efficiency for electrons than for muons. Stops with $\mathcal{B}(\tilde{t} \to b\tau)$ up to 100% are excluded for masses below 800 GeV, while those with $\mathcal{B}(\tilde{t} \to b\mu)$ up to 100% are excluded up to 1800 GeV and those with $\mathcal{B}(\tilde{t} \to be)$ up to 100% are excluded up to 1900 GeV. Observed limits are stronger than expected, reflecting the lower-than-expected event yield at high $m_{b\ell}$. Exclusion contours reflecting the highest stop mass excluded at a 95% CL for a given point in the branching ratio plane are shown in Fig. 8, which emphasizes this search's ability to probe different branching ratio regions. These branching ratio regions can inform theoretical predictions for the normal versus inverted neutrino mass ordering [51]. One-dimensional limit plots for different branching ratio benchmarks are shown in Fig. 9. Cross-section limits for the stop decaying into a b-jet and lepton with democratic branching ratio to each of the lepton flavors without systematic uncertainties would be 2 times stronger for lower stop masses and 1.2 times stronger for higher stop masses.

In addition to using the aforementioned SR definitions for model-dependent results, a second set of regions were defined to produce model-independent results. These model-independent regions use the same baseline SR selections as the regions with the orthogonal bins in $m^0_{b\ell}$ replaced by 15 inclusive, nested bins in $m^0_{b\ell}$. Each nested bin starts at the lower bin edge of the respective nominal SR definition. For each inclusive

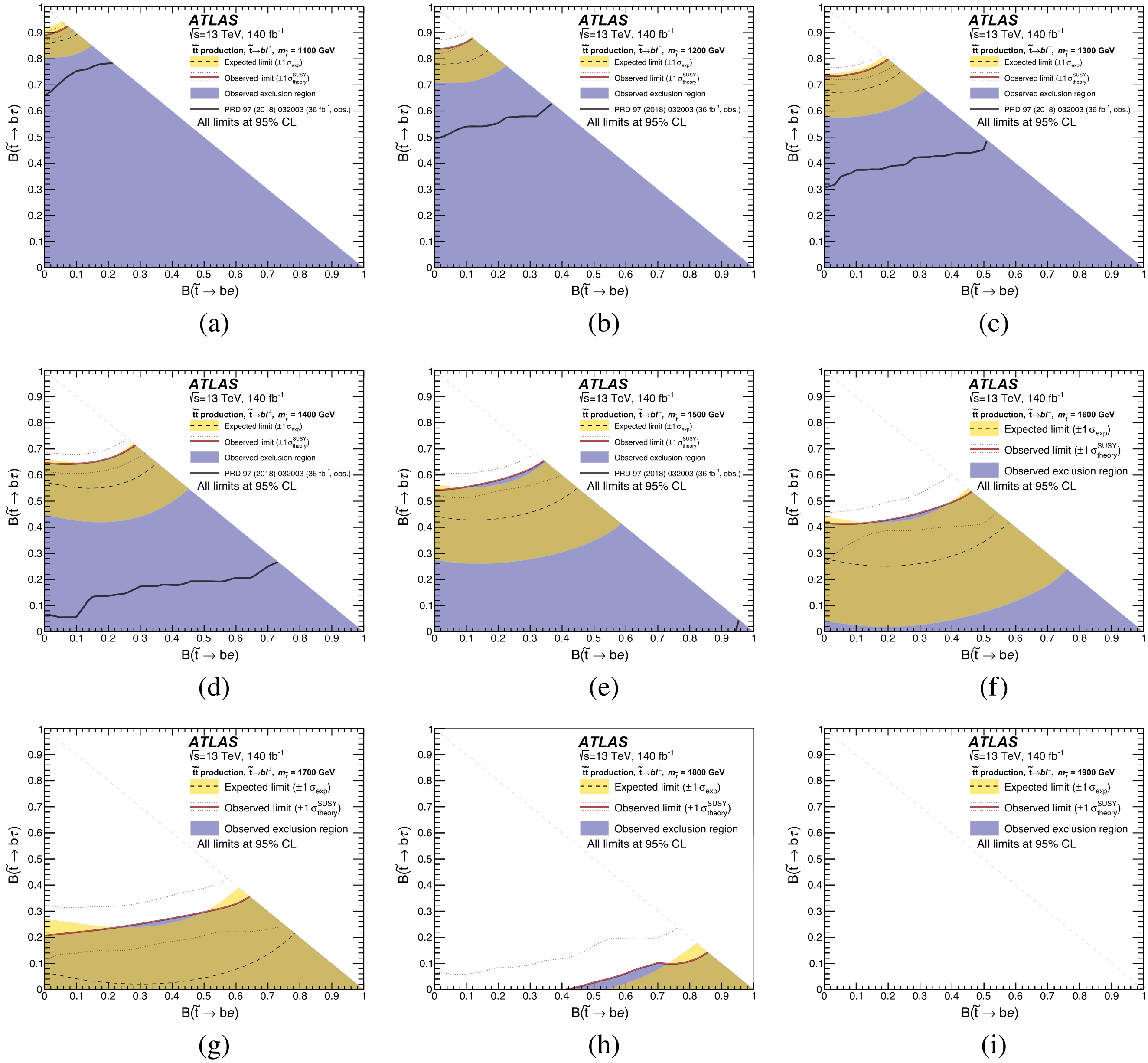

FIG. 7. Observed (solid red) and expected (dashed black) 95% CL exclusions in the $\mathcal{B}(\tilde{t} \to b\tau)$ vs. $\mathcal{B}(\tilde{t} \to be)$ plane for various mass values between 1100 and 1900 GeV (a)–(i). The sum of $\mathcal{B}(\tilde{t} \to be)$, $\mathcal{B}(\tilde{t} \to b\mu)$, and $\mathcal{B}(\tilde{t} \to b\tau)$ is assumed to be unity everywhere; hence, the $\mathcal{B}(\tilde{t} \to b\mu)$ can be inferred for each point in the figure. The yellow band reflects the $\pm 1\sigma$ uncertainty of the expected limit due to theoretical, experimental, and MC statistical uncertainties. The shaded purple area represents the branching ratios that are observed to be excluded. The dotted red lines correspond to the $\pm 1\sigma$ cross section uncertainty of the observed limit derived by varying the signal cross section by the theoretical uncertainties. The black solid line represents previous limits placed by the early Run 2 analysis [40]. In figures that do not have previous limits shown, there was no sensitivity for this mass range in the previous analysis. The chosen branching ratio plane to interpret the results allows an easier comparison with the results of the scan over the neutrino mass hierarchy presented in Ref. [51].

SR, model-independent upper limits are derived on the visible cross section of potential beyond-the-SM (BSM) processes at a 95% CL. The visible cross section is defined to be $\sigma \cdot \epsilon \cdot A$, where σ is the cross section, ϵ is the efficiency, and A is the detector acceptance. A likelihood fit is performed to the number of observed events in all three CRs and the target SR where a generic BSM process is assumed to contribute to the SR only. The p-value of this statistical test is obtained using pseudo-experiments. No theoretical or systematic uncertainties are considered for the potential BSM signal except the luminosity uncertainty from 2015 to 2018. The observed (S^{95}_{obs}) and

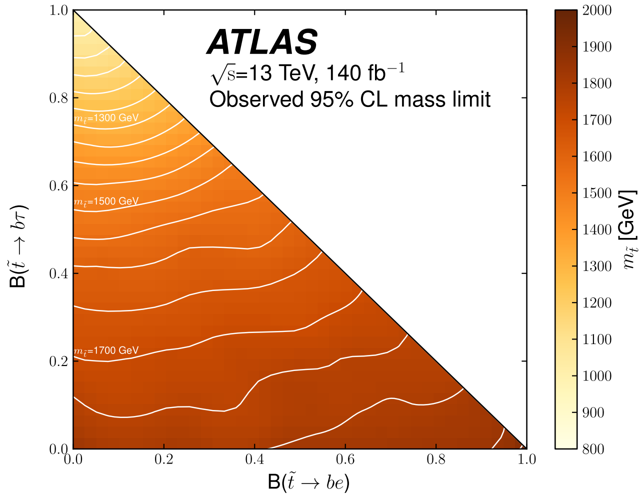

FIG. 8. The observed lower limits on the $\tilde{t}$ mass at 95% CL as a function of $\tilde{t}$ branching ratios. The sum of $\mathcal{B}(\tilde{t} \to be)$, $\mathcal{B}(\tilde{t} \to b\mu)$, and $\mathcal{B}(\tilde{t} \to b\tau)$ is assumed to be unity everywhere; hence, the $\mathcal{B}(\tilde{t} \to b\mu)$ can be inferred for each point in the figure. As the branching ratio $\mathcal{B}(\tilde{t} \to b\tau)$ increases, the observed number of events with electrons or muons in the final state decreases, reducing the sensitivity of the search. Benchmark stop masses are provided in 50 GeV intervals.

expected ($S^{95}_{\rm exp}$) limits on the number of BSM events are derived at 95% CL inclusively across flavor channels to avoid assumptions on the underlying model. These results are shown in Table III. Also shown are the observed limits on the visible cross section $\sigma_{\rm vis}$, defined as $S^{95}_{\rm obs}$ normalized to the integrated luminosity, and representing the product of the production cross section, acceptance, and selection efficiency of a generic BSM signal. Limits on $\sigma_{\rm vis}$ are set between 0.02 and 0.16 fb, depending on the $m_{b\ell}$ requirement.

IX. CONCLUSION

This paper presents the full Run 2 ATLAS results on the search for stop pair production, with each stop decaying via an RPV coupling to a b-quark and a lepton. The search uses 140 fb^{-1} of $\sqrt{s} = 13$ TeV proton-proton collision data collected with the ATLAS detector at the LHC from 2015 to 2018. The resulting final state is characterized by two jets, at least one of which is b-tagged, and two light, opposite-charge leptons (electron or muon). This signal is searched for in the distribution of the leading invariant mass of the lepton-jet resonance reconstructing the stop pair. No significant excess of events over the SM prediction is

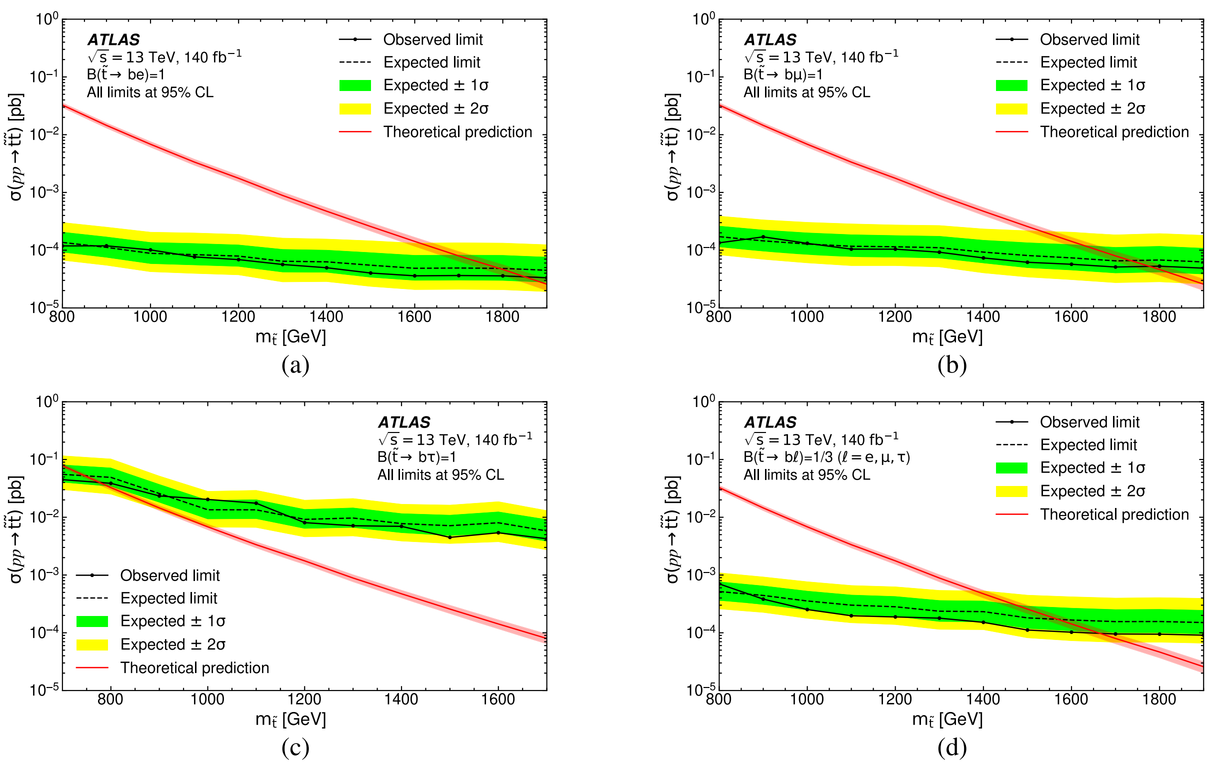

FIG. 9. Observed (solid black) and expected (dashed black) 95% CL upper limits on the stop pair production cross section as a function of stop mass for different branching ratio hypotheses: (a) 100% to a b-quark and an electron, (b) 100% to a b-quark and a muon, (c) 100% to a b-quark and a tau, and (d) democratic branching ratios for this decay. The red line represents theory prediction for the stop cross section, and corresponding uncertainty is represented by a lighter red band [39].

TABLE III. Left to right: the number of events expected by the SM, the number of events observed, 95% CL upper limits on the visible cross section ($\langle\epsilon\sigma\rangle^{95}_{\mathrm{obs}}$) and on the number of signal events (S^{95}_{obs}). The fifth column (S^{95}_{exp}) shows the 95% CL upper limit on the number of signal events, given the expected number (and $\pm1\sigma$ excursions on the expectation) of background events. The last column indicates the CL_b value, i.e. the confidence level observed for the background-only hypothesis. The discovery p-value [$p(s=0)$] is 0.50 with significance (Z) of 0 for all presented mass ranges. The discovery limits were derived using 10,000 pseudo-experiments.

Mass range [GeV]	$N^{\mathrm{SM}}_{\mathrm{exp}}$	N_{obs}	$\langle\epsilon\sigma\rangle^{95}_{\mathrm{obs}}$[fb]	S^{95}_{obs}	S^{95}_{exp}	CL_b
≥ 400	84.0 ± 8.2	78	0.16	22	32^{+11}_{-8}	0.09
≥ 450	81.8 ± 7.6	74	0.13	19	29^{+10}_{-8}	0.06
≥ 500	72.7 ± 7.9	68	0.15	22	30^{+10}_{-7}	0.12
≥ 550	67.7 ± 7.3	62	0.13	18	27^{+9}_{-7}	0.11
≥ 600	59.9 ± 6.8	55	0.13	18	25^{+9}_{-6}	0.12
≥ 650	50.2 ± 5.9	45	0.11	15	22^{+8}_{-6}	0.11
≥ 700	43.4 ± 5.4	39	0.10	14	20^{+7}_{-5}	0.15
≥ 750	33.3 ± 4.6	29	0.08	12	17^{+6}_{-5}	0.12
≥ 800	26.6 ± 3.6	21	0.06	8.9	14^{+6}_{-4}	0.07
≥ 850	20.1 ± 3.2	16	0.06	8.3	13^{+5}_{-3}	0.10
≥ 900	16.9 ± 2.8	13	0.05	7.4	11^{+5}_{-3}	0.11
≥ 1000	9.9 ± 1.8	6	0.04	5.1	8.4^{+4}_{-3}	0.08
≥ 1100	8.5 ± 1.6	5	0.03	4.9	7.8^{+4}_{-2}	0.09
≥ 1200	5.3 ± 1.3	3	0.03	4.2	6.4^{+3}_{-2}	0.14
≥ 1400	1.8 ± 0.5	0	0.02	3.0	4.2^{+2}_{-1}	0.11

observed, and limits are set on the stop mass under different hypotheses for the branching ratios at 95% confidence level. Limits are set on stop masses up to 800 GeV for a $b\tau$ branching ratio of 100%, 1800 GeV for a $b\mu$ branching ratio of 100% and 1900 GeV for a be branching ratio of 100%. These results significantly extend the mass exclusion limits from previous searches. The improvement in sensitivity is due to the larger dataset, performing a fit to the distribution of the mass of the leading lepton-jet pair, increasing the threshold for the highest bin from 1100 to 1400 GeV, and reducing the impact of systematic uncertainties with improved control regions. Model-independent upper limits are set on the cross section of potential BSM processes inclusive in the ee, $e\mu$, and $\mu\mu$ channels and between 0.02 and 0.16 fb.

ACKNOWLEDGMENTS

We thank CERN for the very successful operation of the LHC and its injectors, as well as the support staff at CERN and at our institutions worldwide without whom ATLAS could not be operated efficiently. The crucial computing support from all WLCG partners is acknowledged gratefully, in particular from CERN, the ATLAS Tier-1 facilities at TRIUMF/SFU (Canada), NDGF (Denmark, Norway, Sweden), CC-IN2P3 (France), KIT/GridKA (Germany), INFN-CNAF (Italy), NL-T1 (Netherlands), PIC (Spain), RAL (UK) and BNL (USA), the Tier-2 facilities worldwide and large non-WLCG resource providers. Major contributors of computing resources are listed in Ref. [106]. We gratefully acknowledge the support of ANPCyT, Argentina; YerPhI, Armenia; ARC, Australia; BMWFW and FWF, Austria; ANAS, Azerbaijan; CNPq and FAPESP, Brazil; NSERC, NRC and CFI, Canada; CERN; ANID, Chile; CAS, MOST and NSFC, China; Minciencias, Colombia; MEYS CR, Czech Republic; DNRF and DNSRC, Denmark; IN2P3-CNRS and CEA-DRF/IRFU, France; SRNSFG, Georgia; BMBF, HGF and MPG, Germany; GSRI, Greece; RGC and Hong Kong SAR, China; ISF and Benoziyo Center, Israel; INFN, Italy; MEXT and JSPS, Japan; CNRST, Morocco; NWO, Netherlands; RCN, Norway; MNiSW, Poland; FCT, Portugal; MNE/IFA, Romania; MESTD, Serbia; MSSR, Slovakia; ARIS and MVZI, Slovenia; DSI/NRF, South Africa; MICIU/AEI, Spain; SRC and Wallenberg Foundation, Sweden; SERI, SNSF and Cantons of Bern and Geneva, Switzerland; NSTC, Taipei; TENMAK, Türkiye; STFC/UKRI, United Kingdom; DOE and NSF, United States of America. Individual groups and members have received support from BCKDF, CANARIE, CRC and DRAC, Canada; CERN-CZ, FORTE and PRIMUS, Czech Republic; COST, ERC, ERDF, Horizon 2020, ICSC-NextGenerationEU and Marie Skłodowska-Curie Actions, European Union; Investissements d'Avenir Labex, Investissements d'Avenir Idex and ANR, France; DFG and AvH Foundation, Germany; Herakleitos, Thales and Aristeia programmes co-financed by EU-ESF and the Greek NSRF, Greece; BSF-NSF and MINERVA, Israel; NCN and NAWA, Poland; La Caixa Banking Foundation, CERCA Programme Generalitat de Catalunya and PROMETEO and GenT Programmes Generalitat Valenciana, Spain; Göran Gustafssons Stiftelse, Sweden; The Royal Society and Leverhulme Trust, United Kingdom. In addition, individual members wish to acknowledge support from Armenia: Yerevan Physics Institute (FAPERJ); CERN: European Organization for Nuclear Research (CERN PJAS); Chile: Agencia Nacional de Investigación y Desarrollo (FONDECYT 1230812, FONDECYT 1230987, FONDECYT 1240864); China: Chinese Ministry of Science and Technology (MOST-2023YFA1605700), National Natural Science Foundation of China (NSFC—12175119, NSFC 12275265, NSFC-12075060); Czech Republic: Czech Science Foundation (GACR—24-11373S), Ministry of Education Youth and Sports (FORTE CZ.02.01.01/00/22_008/0004632), PRIMUS Research Programme (PRIMUS/21/SCI/017); EU: H2020 European Research Council (ERC—101002463); European Union: European Research Council (ERC—948254, ERC 101089007), Horizon 2020 Framework Programme (MUCCA—CHIST-ERA-19-XAI-00), European Union, Future Artificial Intelligence Research (FAIR-NextGenerationEU PE00000013), Italian Center for High Performance Computing, Big Data and Quantum Computing (ICSC, NextGenerationEU); France: Agence Nationale de la Recherche (ANR-20-CE31-0013, ANR-21-CE31-0013, ANR-21-CE31-0022, ANR-22-EDIR-0002), Investissements d'Avenir Labex (ANR-11-LABX-0012); Germany: Baden-Württemberg Stiftung (BW Stiftung-Postdoc Eliteprogramme), Deutsche Forschungsgemeinschaft (DFG—469666862, DFG—CR 312/5-2); Italy: Istituto Nazionale di Fisica Nucleare (ICSC, NextGenerationEU), Ministero dell'Università e della Ricerca (PRIN—20223N7F8K—PNRR M4.C2.1.1); Japan: Japan Society for the Promotion of Science (JSPS KAKENHI JP22H01227, JSPS KAKENHI JP22H04944, JSPS KAKENHI JP22KK0227, JSPS KAKENHI JP23KK0245); Netherlands: Netherlands Organisation for Scientific Research (NWO Veni 2020—VI.Veni.202.179); Norway: Research Council of Norway (RCN-314472); Poland: Ministry of Science and Higher Education (IDUB AGH, POB8, D4 no 9722), Polish National Agency for Academic Exchange (PPN/PPO/2020/1/00002/U/00001), Polish National Science Centre (NCN 2021/42/E/ST2/00350, NCN OPUS No. 2022/47/B/ST2/03059, NCN UMO-2019/34/E/ST2/00393, UMO-2020/37/B/ST2/01043, UMO-2021/40/C/ST2/00187, UMO-2022/47/O/ST2/00148, UMO-2023/49/B/ST2/04085); Slovenia: Slovenian Research Agency (ARIS Grant No. J1-3010); Spain: Generalitat Valenciana (Artemisa, FEDER, IDIFEDER/2018/048), Ministry of Science and Innovation (MCIN & NextGenEU PCI2022-135018-2, MICIN & FEDER PID2021-125273NB, RYC2019-028510-I, RYC2020-030254-I, RYC2021-031273-I, RYC2022-038164-I), PROMETEO and GenT Programmes Generalitat Valenciana (CIDEGENT/2019/027); Sweden: Swedish Research Council (Swedish Research Council 2023-04654, VR 2018-00482, VR 2022-03845, VR 2022-04683, VR 2023-03403, VR 2021-03651), Knut and Alice Wallenberg Foundation (KAW 2018.0157, KAW 2018.0458, KAW 2019.0447, KAW 2022.0358); Switzerland: Swiss National Science Foundation (SNSF—PCEFP2_194658); United Kingdom: Leverhulme Trust (Leverhulme Trust RPG-2020-004), Royal Society (NIF-R1-231091); United States of America: U.S. Department of Energy (ECA DE-AC02-76SF00515), Neubauer Family Foundation.

---

[1] H. Miyazawa, Baryon number changing currents, Prog. Theor. Phys. **36**, 1266 (1966).
[2] P. Ramond, Dual theory for free fermions, Phys. Rev. D **3**, 2415 (1971).
[3] Y. A. Golfand and E. P. Likhtman, Extension of the algebra of poincare group generators and violation of P-invariance, JETP Lett. **13**, 323 (1971).
[4] A. Neveu and J. H. Schwarz, Factorizable dual model of pions, Nucl. Phys. **B31**, 86 (1971).
[5] A. Neveu and J. H. Schwarz, Quark model of dual pions, Phys. Rev. D **4**, 1109 (1971).
[6] J.-L. Gervais and B. Sakita, Field theory interpretation of supergauges in dual models, Nucl. Phys. **B34**, 632 (1971).
[7] D. V. Volkov and V. P. Akulov, Is the neutrino a goldstone particle?, Phys. Lett. **46B**, 109 (1973).
[8] J. Wess and B. Zumino, A Lagrangian model invariant under supergauge transformations, Phys. Lett. **49B**, 52 (1974).
[9] J. Wess and B. Zumino, Supergauge transformations in four dimensions, Nucl. Phys. **B70**, 39 (1974).
[10] P. Fayet, Supersymmetry and weak, electromagnetic and strong interactions, Phys. Lett. **64B**, 159 (1976).
[11] P. Fayet, Spontaneously broken supersymmetric theories of weak, electromagnetic and strong interactions, Phys. Lett. **69B**, 489 (1977).
[12] G. R. Farrar and P. Fayet, Phenomenology of the production, decay, and detection of new hadronic states associated with supersymmetry, Phys. Lett. **76B**, 575 (1978).
[13] P. Fayet, Relations between the masses of the superpartners of leptons and quarks, the goldstino coupling and the neutral currents, Phys. Lett. **84B**, 416 (1979).

[14] S. Dimopoulos and H. Georgi, Softly broken supersymmetry and SU(5), Nucl. Phys. **B193**, 150 (1981).

[15] J. R. Ellis, J. S. Hagelin, D. V. Nanopoulos, K. A. Olive, and M. Srednicki, Supersymmetric relics from the big bang, Nucl. Phys. **B238**, 453 (1984).

[16] M. Pospelov, Particle physics catalysis of thermal big bang nucleosynthesis, Phys. Rev. Lett. **98**, 231301 (2007).

[17] P. F. Pérez and S. Spinner, Spontaneous R-parity breaking and left-right symmetry, Phys. Lett. B **673**, 251 (2009).

[18] V. Barger, P. F. Pérez, and S. Spinner, Minimal gauged $U(1)_{B-L}$ model with spontaneous R parity violation, Phys. Rev. Lett. **102**, 181802 (2009).

[19] P. F. Pérez and S. Spinner, Spontaneous R-parity breaking in supersymmetric models, Phys. Rev. D **80**, 015004 (2009).

[20] L. L. Everett, P. F. Pérez, and S. Spinner, Right side of TeV scale spontaneous R-parity violation, Phys. Rev. D **80**, 055007 (2009).

[21] M. Evans and B. A. Ovrut, The world sheet supergravity of the heterotic string, Phys. Lett. B **171**, 177 (1986).

[22] A. Lukas, B. A. Ovrut, K. Stelle, and D. Waldram, Universe as a domain wall, Phys. Rev. D **59**, 086001 (1999).

[23] V. Braun, Y.-H. He, B. A. Ovrut, and T. Pantev, A heterotic standard model, Phys. Lett. B **618**, 252 (2005).

[24] V. Braun, Y.-H. He, B. A. Ovrut, and T. Pantev, The exact MSSM spectrum from string theory, J. High Energy Phys. 05 (2006) 043.

[25] V. Braun, Y.-H. He, and B. A. Ovrut, Stability of the minimal heterotic standard model bundle, J. High Energy Phys. 06 (2006) 032.

[26] M. Ambroso and B. Ovrut, The B-L/electroweak hierarchy in heterotic string and M-theory, J. High Energy Phys. 10 (2009) 011.

[27] M. Ambroso and B. A. Ovrut, The mass spectra, hierarchy and cosmology of B-L MSSM heterotic compactifications, Int. J. Mod. Phys. A **26**, 1569 (2011).

[28] B. A. Ovrut, A. Purves, and S. Spinner, Wilson lines and a canonical basis of SU(4) heterotic standard models, J. High Energy Phys. 11 (2012) 026.

[29] R. Deen, B. A. Ovrut, and A. Purves, The minimal SUSY B-L model: Simultaneous Wilson lines and string thresholds, J. High Energy Phys. 07 (2016) 043.

[30] R. Deen, B. A. Ovrut, and A. Purves, Supersymmetric sneutrino-Higgs inflation, Phys. Lett. B **762**, 441 (2016).

[31] A. Atre, V. Barger, and T. Han, Upper bounds on lepton-number violating processes, Phys. Rev. D **71**, 113014 (2005).

[32] P. F. Pérez and S. Spinner, The minimal theory for R-parity violation at the LHC, J. High Energy Phys. 04 (2012) 118.

[33] P. Fileviez Perez and S. Spinner, Supersymmetry at the LHC and the theory of R-parity, Phys. Lett. B **728**, 489 (2014).

[34] B. A. Ovrut, A. Purves, and S. Spinner, A statistical analysis of the minimal SUSY B–L theory, Mod. Phys. Lett. A **30**, 1550085 (2015).

[35] B. A. Ovrut, A. Purves, and S. Spinner, The minimal SUSY B-L model: From the unification scale to the LHC, J. High Energy Phys. 06 (2015) 182.

[36] R. Barbieri and G. Giudice, Upper bounds on supersymmetric particle masses, Nucl. Phys. **B306**, 63 (1988).

[37] B. de Carlos and J. A. Casas, One-loop analysis of the electroweak breaking in supersymmetric models and the fine-tuning problem, Phys. Lett. B **309**, 320 (1993).

[38] B. Allanach and H. E. Haber, Supersymmetry, part I (theory), arXiv:2401.03827.

[39] W. Beenakker, C. Borschensky, M. Krämer, A. Kulesza, and E. Laenen, NNLL-fast: Predictions for coloured supersymmetric particle production at the LHC with threshold and Coulomb resummation, J. High Energy Phys. 12 (2016) 133.

[40] ATLAS Collaboration, Search for $B-L$ R-parity-violating top squarks in $\sqrt{s}=13$ TeV pp collisions with the ATLAS experiment, Phys. Rev. D **97**, 032003 (2018).

[41] ATLAS Collaboration, Search for trilepton resonances from chargino and neutralino pair production in $\sqrt{s}=13$ TeV pp collisions with the ATLAS detector, Phys. Rev. D **103**, 112003 (2021).

[42] CMS Collaboration, Search for top squarks in final states with two top quarks and several light-flavor jets in proton–proton collisions at $\sqrt{s}=13$ TeV, Phys. Rev. D **104**, 032006 (2021).

[43] ATLAS Collaboration, Search for pairs of scalar leptoquarks decaying into quarks and electrons or muons in $\sqrt{s}=13$ TeV pp collisions with the ATLAS detector, J. High Energy Phys. 10 (2020) 112.

[44] ATLAS Collaboration, Combination of searches for pair-produced leptoquarks at $\sqrt{s}=13$ TeV with the ATLAS detector, Phys. Lett. B **854**, 138736 (2024).

[45] ATLAS Collaboration, Search for pair-produced scalar and vector leptoquarks decaying into third-generation quarks and first- or second-generation leptons in pp collisions with the ATLAS detector, J. High Energy Phys. 06 (2023) 188.

[46] ATLAS Collaboration, Search for pair production of third-generation scalar leptoquarks decaying into a top quark and a τ-lepton in pp collisions at $\sqrt{s}=13$ TeV with the ATLAS detector, J. High Energy Phys. 06 (2021) 179.

[47] ATLAS Collaboration, Search for pair production of scalar leptoquarks decaying into first- or second-generation leptons and top quarks in proton–proton collisions at $\sqrt{s}=13$ TeV with the ATLAS detector, Eur. Phys. J. C **81**, 313 (2021).

[48] CMS Collaboration, Search for a third-generation leptoquark coupled to a τ lepton and a b quark through single, pair, and nonresonant production in proton-proton collisions at $\sqrt{s}=13$ TeV, J. High Energy Phys. 05 (2024) 311.

[49] CMS Collaboration, Search for long-lived particles using displaced jets in proton–proton collisions at $\sqrt{s}=13$ TeV, Phys. Rev. D **104**, 012015 (2021).

[50] Z. Marshall, B. A. Ovrut, A. Purves, and S. Spinner, LSP squark decays at the LHC and the neutrino mass hierarchy, Phys. Rev. D **90**, 015034 (2014).

[51] Z. Marshall, B. A. Ovrut, A. Purves, and S. Spinner, Spontaneous R-parity breaking, stop LSP decays and the neutrino mass hierarchy, Phys. Lett. B **732**, 325 (2014).

[52] ATLAS Collaboration, The ATLAS experiment at the CERN large hadron collider, J. Instrum. **3**, S08003 (2008).

[53] ATLAS Collaboration, ATLAS insertable B-layer: Technical design report, Reports No. ATLAS-TDR-19, No. CERN-LHCC-2010-013, 2010, https://cds.cern.ch/record/1291633.Addendum: Reports No. ATLAS-TDR-19-ADD-1, No. CERN-LHCC-2012-009, 2012, https://cds.cern.ch/record/1451888.
[54] B. Abbott *et al.*, Production and integration of the ATLAS insertable B-layer, J. Instrum. **13**, T05008 (2018).
[55] ATLAS Collaboration, Performance of the ATLAS trigger system in 2015, Eur. Phys. J. C **77**, 317 (2017).
[56] ATLAS Collaboration, Software and computing for Run 3 of the ATLAS experiment at the LHC, arXiv:2404.06335.
[57] ATLAS Collaboration, Luminosity determination in pp collisions at $\sqrt{s} = 13$ TeV using the ATLAS detector at the LHC, Eur. Phys. J. C **83**, 982 (2023).
[58] G. Avoni *et al.*, The new LUCID-2 detector for luminosity measurement and monitoring in ATLAS, J. Instrum. **13**, P07017 (2018).
[59] ATLAS Collaboration, ATLAS data quality operations and performance for 2015–2018 data-taking, J. Instrum. **15**, P04003 (2020).
[60] P. Nason, A new method for combining NLO QCD with shower Monte Carlo algorithms, J. High Energy Phys. 11 (2004) 040.
[61] S. Frixione, P. Nason, and C. Oleari, Matching NLO QCD computations with parton shower simulations: The POWHEG method, J. High Energy Phys. 11 (2007) 070.
[62] S. Alioli, P. Nason, C. Oleari, and E. Re, A general framework for implementing NLO calculations in shower Monte Carlo programs: The POWHEG BOX, J. High Energy Phys. 06 (2010) 043.
[63] S. Frixione, G. Ridolfi, and P. Nason, A positive-weight next-to-leading-order Monte Carlo for heavy flavour hadroproduction, J. High Energy Phys. 09 (2007) 126.
[64] E. Re, Single-top Wt-channel production matched with parton showers using the POWHEG method, Eur. Phys. J. C **71**, 1547 (2011).
[65] R. D. Ball *et al.* (NNPDF Collaboration), Parton distributions for the LHC run II, J. High Energy Phys. 04 (2015) 040.
[66] E. Bothmann *et al.*, Event generation with SHERPA 2.2, SciPost Phys. **7**, 034 (2019).
[67] C. Anastasiou, L. Dixon, K. Melnikov, and F. Petriello, High-precision QCD at hadron colliders: Electroweak gauge boson rapidity distributions at next-to-next-to leading order, Phys. Rev. D **69**, 094008 (2004).
[68] T. Gleisberg and S. Höche, Comix, a new matrix element generator, J. High Energy Phys. 12 (2008) 039.
[69] S. Schumann and F. Krauss, A parton shower algorithm based on Catani–Seymour dipole factorisation, J. High Energy Phys. 03 (2008) 038.
[70] J. Alwall, R. Frederix, S. Frixione, V. Hirschi, F. Maltoni, O. Mattelaer, H.-S. Shao, T. Stelzer, P. Torrielli, and M. Zaro, The automated computation of tree-level and next-to-leading order differential cross sections, and their matching to parton shower simulations, J. High Energy Phys. 07 (2014) 079.
[71] W. Beenakker, M. Krämer, T. Plehn, M. Spira, and P. Zerwas, Stop production at hadron colliders, Nucl. Phys. **B515**, 3 (1998).
[72] W. Beenakker, S. Brensing, M. Krämer, A. Kulesza, E. Laenen, and I. Niessen, Supersymmetric top and bottom squark production at hadron colliders, J. High Energy Phys. 08 (2010) 098.
[73] W. Beenakker, S. Brensing, M. Krämer, A. kulesza, E. Laenen, L. Motyka, and I. Niessen, Squark and gluino hadroproduction, Int. J. Mod. Phys. A **26**, 2637 (2011).
[74] ATLAS Collaboration, Studies on top-quark Monte Carlo modelling for Top2016, Report No. ATL-PHYS-PUB-2016-020, 2016, https://cds.cern.ch/record/2216168.
[75] S. Frixione, E. Laenen, P. Motylinski, C. White, and B. R. Webber, Single-top hadroproduction in association with a W boson, J. High Energy Phys. 07 (2008) 029.
[76] T. Sjöstrand, S. Ask, J. R. Christiansen, R. Corke, N. Desai, P. Ilten, S. Mrenna, S. Prestel, C. O. Rasmussen, and P. Z. Skands, An introduction to PYTHIA 8.2, Comput. Phys. Commun. **191**, 159 (2015).
[77] ATLAS Collaboration, ATLAS PYTHIA 8 tunes to 7 TeV data, Report No. ATL-PHYS-PUB-2014-021, 2014, https://cds.cern.ch/record/1966419.
[78] R. D. Ball *et al.* (NNPDF Collaboration), Parton distributions with LHC data, Nucl. Phys. **B867**, 244 (2013).
[79] J. Pumplin, D. R. Stump, J. Huston, H.-L. Lai, P. Nadolsky, and W.-K. Tung, New generation of parton distributions with uncertainties from global QCD analysis, J. High Energy Phys. 07 (2002) 012.
[80] C. Borschensky, M. Krämer, A. Kulesza, M. Mangano, S. Padhi, T. Plehn, and X. Portell, Squark and gluino production cross sections in pp collisions at $\sqrt{s} = 13$, 14, 33 and 100 TeV, Eur. Phys. J. C **74**, 3174 (2014).
[81] D. J. Lange, The EVTGEN particle decay simulation package, Nucl. Instrum. Methods Phys. Res., Sect. A **462**, 152 (2001).
[82] S. Agostinelli *et al.*, GEANT4—a simulation toolkit, Nucl. Instrum. Methods Phys. Res., Sect. A **506**, 250 (2003).
[83] ATLAS Collaboration, Vertex reconstruction performance of the ATLAS detector at $\sqrt{s} = 13$ TeV, Report No. ATL-PHYS-PUB-2015-026, 2015, https://cds.cern.ch/record/2037717.
[84] ATLAS Collaboration, Electron and photon performance measurements with the ATLAS detector using the 2015–2017 LHC proton–proton collision data, J. Instrum. **14**, P12006 (2019).
[85] ATLAS Collaboration, Muon reconstruction and identification efficiency in ATLAS using the full Run 2 pp collision data set at $\sqrt{s} = 13$ TeV, Eur. Phys. J. C **81**, 578 (2021).
[86] ATLAS Collaboration, Jet reconstruction and performance using particle flow with the ATLAS detector, Eur. Phys. J. C **77**, 466 (2017).
[87] M. Cacciari, G. P. Salam, and G. Soyez, FastJet user manual, Eur. Phys. J. C **72**, 1896 (2012).
[88] ATLAS Collaboration, Jet energy scale and resolution measured in proton–proton collisions at $\sqrt{s} = 13$ TeV with the ATLAS detector, Eur. Phys. J. C **81**, 689 (2021).
[89] ATLAS Collaboration, Performance of pile-up mitigation techniques for jets in pp collisions at $\sqrt{s} = 8$ TeV using the ATLAS detector, Eur. Phys. J. C **76**, 581 (2016).
[90] ATLAS Collaboration, Selection of jets produced in 13 TeV proton–proton collisions with the ATLAS detector, Report No. ATLAS-CONF-2015-029, 2015, https://cds.cern.ch/record/2037702.

[91] ATLAS Collaboration, ATLAS flavour-tagging algorithms for the LHC Run 2 pp collision dataset, Eur. Phys. J. C **83**, 681 (2023).

[92] ATLAS Collaboration, ATLAS b-jet identification performance and efficiency measurement with $t\bar{t}$ events in pp collisions at $\sqrt{s} = 13$ TeV, Eur. Phys. J. C **79**, 970 (2019).

[93] ATLAS Collaboration, Calibration of the light-flavour jet mistagging efficiency of the b-tagging algorithms with $Z+$jets events using 139 fb^{-1} of ATLAS proton–proton collision data at $\sqrt{s} = 13$ TeV, Eur. Phys. J. C **83**, 728 (2023).

[94] ATLAS Collaboration, Measurement of the c-jet mistagging efficiency in $t\bar{t}$ events using pp collision data at $\sqrt{s} = 13$ TeV collected with the ATLAS detector, Eur. Phys. J. C **82**, 95 (2022).

[95] ATLAS Collaboration, Performance of electron and photon triggers in ATLAS during LHC Run 2, Eur. Phys. J. C **80**, 47 (2020).

[96] ATLAS Collaboration, Performance of the ATLAS muon triggers in Run 2, J. Instrum. **15**, P09015 (2020).

[97] ATLAS Collaboration, Operation of the ATLAS trigger system in Run 2, J. Instrum. **15**, P10004 (2020).

[98] M. Baak, G. J. Besjes, D. Côté, A. Koutsman, J. Lorenz, and D. Short, HistFitter software framework for statistical data analysis, Eur. Phys. J. C **75**, 153 (2015).

[99] R. D. Cousins, J. T. Linnemann, and J. Tucker, Evaluation of three methods for calculating statistical significance when incorporating a systematic uncertainty into a test of the background-only hypothesis for a Poisson process, Nucl. Instrum. Methods Phys. Res., Sect. A **595**, 480 (2008).

[100] ATLAS Collaboration, Studies of the muon momentum calibration and performance of the ATLAS detector with pp collisions at $\sqrt{s} = 13$ TeV, Eur. Phys. J. C **83**, 686 (2023).

[101] M. Bähr *et al.*, HERWIG++ physics and manual, Eur. Phys. J. C **58**, 639 (2008).

[102] J. Bellm *et al.*, HERWIG7.0/HERWIG++ 3.0 release note, Eur. Phys. J. C **76**, 196 (2016).

[103] L. A. Harland-Lang, A. D. Martin, P. Motylinski, and R. S. Thorne, Parton distributions in the LHC era: MMHT 2014 PDFs, Eur. Phys. J. C **75**, 204 (2015).

[104] A. L. Read, Presentation of search results: the CL_S technique, J. Phys. G **28**, 2693 (2002).

[105] G. Cowan, K. Cranmer, E. Gross, and O. Vitells, Asymptotic formulae for likelihood-based tests of new physics, Eur. Phys. J. C **71**, 1554 (2011).

[106] ATLAS Collaboration, ATLAS computing acknowledgements, Report No. ATL-SOFT-PUB-2023-001, 2023, https://cds.cern.ch/record/2869272.

G. Aad,[104] E. Aakvaag,[17] B. Abbott,[123] S. Abdelhameed,[119a] K. Abeling,[56] N. J. Abicht,[50] S. H. Abidi,[30] M. Aboelela,[45] A. Aboulhorma,[36e] H. Abramowicz,[154] H. Abreu,[153] Y. Abulaiti,[120] B. S. Acharya,[70a,70b,b] A. Ackermann,[64a] C. Adam Bourdarios,[4] L. Adamczyk,[87a] S. V. Addepalli,[27] M. J. Addison,[103] J. Adelman,[118] A. Adiguzel,[22c] T. Adye,[137] A. A. Affolder,[139] Y. Afik,[40] M. N. Agaras,[13] J. Agarwala,[74a,74b] A. Aggarwal,[102] C. Agheorghiesei,[28c] F. Ahmadov,[39,c] W. S. Ahmed,[106] S. Ahuja,[97] X. Ai,[63e] G. Aielli,[77a,77b] A. Aikot,[166] M. Ait Tamlihat,[36e] B. Aitbenchikh,[36a] M. Akbiyik,[102] T. P. A. Åkesson,[100] A. V. Akimov,[38] D. Akiyama,[171] N. N. Akolkar,[25] S. Aktas,[22a] K. Al Khoury,[42] G. L. Alberghi,[24b] J. Albert,[168] P. Albicocco,[54] G. L. Albouy,[61] S. Alderweireldt,[53] Z. L. Alegria,[124] M. Aleksa,[37] I. N. Aleksandrov,[39] C. Alexa,[28b] T. Alexopoulos,[10] F. Alfonsi,[24b] M. Algren,[57] M. Alhroob,[170] B. Ali,[135] H. M. J. Ali,[93] S. Ali,[32] S. W. Alibocus,[94] M. Aliev,[34c] G. Alimonti,[72a] W. Alkakhi,[56] C. Allaire,[67] B. M. M. Allbrooke,[149] J. F. Allen,[53] C. A. Allendes Flores,[140f] P. P. Allport,[21] A. Aloisio,[73a,73b] F. Alonso,[92] C. Alpigiani,[141] Z. M. K. Alsolami,[93] M. Alvarez Estevez,[101] A. Alvarez Fernandez,[102] M. Alves Cardoso,[57] M. G. Alviggi,[73a,73b] M. Aly,[103] Y. Amaral Coutinho,[84b] A. Ambler,[106] C. Amelung,[37] M. Amerl,[103] C. G. Ames,[111] D. Amidei,[108] B. Amini,[55] K. J. Amirie,[158] S. P. Amor Dos Santos,[133a] K. R. Amos,[166] D. Amperiadou,[155] S. An,[85] V. Ananiev,[128] C. Anastopoulos,[142] T. Andeen,[11] J. K. Anders,[37] A. C. Anderson,[60] S. Y. Andrean,[48a,48b] A. Andreazza,[72a,72b] S. Angelidakis,[9] A. Angerami,[42] A. V. Anisenkov,[38] A. Annovi,[75a] C. Antel,[57] E. Antipov,[148] M. Antonelli,[54] F. Anulli,[76a] M. Aoki,[85] T. Aoki,[156] M. A. Aparo,[149] L. Aperio Bella,[49] C. Appelt,[19] A. Apyan,[27] S. J. Arbiol Val,[88] C. Arcangeletti,[54] A. T. H. Arce,[52] J-F. Arguin,[110] S. Argyropoulos,[55] J.-H. Arling,[49] O. Arnaez,[4] H. Arnold,[148] G. Artoni,[76a,76b] H. Asada,[113] K. Asai,[121] S. Asai,[156] N. A. Asbah,[37] R. A. Ashby Pickering,[170] K. Assamagan,[30] R. Astalos,[29a] K. S. V. Astrand,[100] S. Atashi,[162] R. J. Atkin,[34a] M. Atkinson,[165] H. Atmani,[36f] P. A. Atmasiddha,[131] K. Augsten,[135] S. Auricchio,[73a,73b] A. D. Auriol,[21] V. A. Austrup,[103] G. Avolio,[37] K. Axiotis,[57] G. Azuelos,[110,d] D. Babal,[29b] H. Bachacou,[138] K. Bachas,[155,e] A. Bachiu,[35] F. Backman,[48a,48b] A. Badea,[40] T. M. Baer,[108] P. Bagnaia,[76a,76b] M. Bahmani,[19] D. Bahner,[55] K. Bai,[126] J. T. Baines,[137] L. Baines,[96] O. K. Baker,[175] E. Bakos,[16] D. Bakshi Gupta,[8] L. E. Balabram Filho,[84b] V. Balakrishnan,[123] R. Balasubramanian,[117] E. M. Baldin,[38] P. Balek,[87a] E. Ballabene,[24b,24a] F. Balli,[138] L. M. Baltes,[64a] W. K. Balunas,[33] J. Balz,[102]

I. Bamwidhi,[119b] E. Banas,[88] M. Bandieramonte,[132] A. Bandyopadhyay,[25] S. Bansal,[25] L. Barak,[154] M. Barakat,[49] E. L. Barberio,[107] D. Barberis,[58b,58a] M. Barbero,[104] M. Z. Barel,[117] T. Barillari,[112] M-S. Barisits,[37] T. Barklow,[146] P. Baron,[125] D. A. Baron Moreno,[103] A. Baroncelli,[63a] A. J. Barr,[129] J. D. Barr,[98] F. Barreiro,[101] J. Barreiro Guimarães da Costa,[14] U. Barron,[154] M. G. Barros Teixeira,[133a] S. Barsov,[38] F. Bartels,[64a] R. Bartoldus,[146] A. E. Barton,[93] P. Bartos,[29a] A. Basan,[102] M. Baselga,[50] A. Bassalat,[67,f] M. J. Basso,[159a] S. Bataju,[45] R. Bate,[167] R. L. Bates,[60] S. Batlamous,[101] B. Batool,[144] M. Battaglia,[139] D. Battulga,[19] M. Bauce,[76a,76b] M. Bauer,[80] P. Bauer,[25] L. T. Bazzano Hurrell,[31] J. B. Beacham,[52] T. Beau,[130] J. Y. Beaucamp,[92] P. H. Beauchemin,[161] P. Bechtle,[25] H. P. Beck,[20,g] K. Becker,[170] A. J. Beddall,[83] V. A. Bednyakov,[39] C. P. Bee,[148] L. J. Beemster,[16] T. A. Beermann,[37] M. Begalli,[84d] M. Begel,[30] A. Behera,[148] J. K. Behr,[49] J. F. Beirer,[37] F. Beisiegel,[25] M. Belfkir,[119b] G. Bella,[154] L. Bellagamba,[24b] A. Bellerive,[35] P. Bellos,[21] K. Beloborodov,[38] D. Benchekroun,[36a] F. Bendebba,[36a] Y. Benhammou,[154] K. C. Benkendorfer,[62] L. Beresford,[49] M. Beretta,[54] E. Bergeaas Kuutmann,[164] N. Berger,[4] B. Bergmann,[135] J. Beringer,[18a] G. Bernardi,[5] C. Bernius,[146] F. U. Bernlochner,[25] F. Bernon,[37,104] A. Berrocal Guardia,[13] T. Berry,[97] P. Berta,[136] A. Berthold,[51] S. Bethke,[112] A. Betti,[76a,76b] A. J. Bevan,[96] N. K. Bhalla,[55] S. Bhatta,[148] D. S. Bhattacharya,[169] P. Bhattarai,[146] K. D. Bhide,[55] V. S. Bhopatkar,[124] R. M. Bianchi,[132] G. Bianco,[24b,24a] O. Biebel,[111] R. Bielski,[126] M. Biglietti,[78a] C. S. Billingsley,[45] Y. Bimgdi,[36f] M. Bindi,[56] A. Bingul,[22b] C. Bini,[76a,76b] G. A. Bird,[33] M. Birman,[172] M. Biros,[136] S. Biryukov,[149] T. Bisanz,[50] E. Bisceglie,[44b,44a] J. P. Biswal,[137] D. Biswas,[144] I. Bloch,[49] A. Blue,[60] U. Blumenschein,[96] J. Blumenthal,[102] V. S. Bobrovnikov,[38] M. Boehler,[55] B. Boehm,[169] D. Bogavac,[37] A. G. Bogdanchikov,[38] L. S. Boggia,[130] C. Bohm,[48a] V. Boisvert,[97] P. Bokan,[37] T. Bold,[87a] M. Bomben,[5] M. Bona,[96] M. Boonekamp,[138] C. D. Booth,[97] A. G. Borbély,[60] I. S. Bordulev,[38] G. Borissov,[93] D. Bortoletto,[129] D. Boscherini,[24b] M. Bosman,[13] J. D. Bossio Sola,[37] K. Bouaouda,[36a] N. Bouchhar,[166] L. Boudet,[4] J. Boudreau,[132] E. V. Bouhova-Thacker,[93] D. Boumediene,[41] R. Bouquet,[58b,58a] A. Boveia,[122] J. Boyd,[37] D. Boye,[30] I. R. Boyko,[39] L. Bozianu,[57] J. Bracinik,[21] N. Brahimi,[4] G. Brandt,[174] O. Brandt,[33] F. Braren,[49] B. Brau,[105] J. E. Brau,[126] R. Brener,[172] L. Brenner,[117] R. Brenner,[164] S. Bressler,[172] G. Brianti,[79a,79b] D. Britton,[60] D. Britzger,[112] I. Brock,[25] R. Brock,[109] G. Brooijmans,[42] E. M. Brooks,[159b] E. Brost,[30] L. M. Brown,[168] L. E. Bruce,[62] T. L. Bruckler,[129] P. A. Bruckman de Renstrom,[88] B. Brüers,[49] A. Bruni,[24b] G. Bruni,[24b] M. Bruschi,[24b] N. Bruscino,[76a,76b] T. Buanes,[17] Q. Buat,[141] D. Buchin,[112] A. G. Buckley,[60] O. Bulekov,[38] B. A. Bullard,[146] S. Burdin,[94] C. D. Burgard,[50] A. M. Burger,[37] B. Burghgrave,[8] O. Burlayenko,[55] J. Burleson,[165] J. T. P. Burr,[33] J. C. Burzynski,[145] E. L. Busch,[42] V. Büscher,[102] P. J. Bussey,[60] J. M. Butler,[26] C. M. Buttar,[60] J. M. Butterworth,[98] W. Buttinger,[137] C. J. Buxo Vazquez,[109] A. R. Buzykaev,[38] S. Cabrera Urbán,[166] L. Cadamuro,[67] D. Caforio,[59] H. Cai,[132] Y. Cai,[14,114c] Y. Cai,[114a] V. M. M. Cairo,[37] O. Cakir,[3a] N. Calace,[37] P. Calafiura,[18a] G. Calderini,[130] P. Calfayan,[69] G. Callea,[60] L. P. Caloba,[84b] D. Calvet,[41] S. Calvet,[41] M. Calvetti,[75a,75b] R. Camacho Toro,[130] S. Camarda,[37] D. Camarero Munoz,[27] P. Camarri,[77a,77b] M. T. Camerlingo,[73a,73b] D. Cameron,[37] C. Camincher,[168] M. Campanelli,[98] A. Camplani,[43] V. Canale,[73a,73b] A. C. Canbay,[3a] E. Canonero,[97] J. Cantero,[166] Y. Cao,[165] F. Capocasa,[27] M. Capua,[44b,44a] A. Carbone,[72a,72b] R. Cardarelli,[77a] J. C. J. Cardenas,[8] G. Carducci,[44b,44a] T. Carli,[37] G. Carlino,[73a] J. I. Carlotto,[13] B. T. Carlson,[132,h] E. M. Carlson,[168,159a] J. Carmignani,[94] L. Carminati,[72a,72b] A. Carnelli,[138] M. Carnesale,[76a,76b] S. Caron,[116] E. Carquin,[140f] S. Carrá,[72a] G. Carratta,[24b,24a] A. M. Carroll,[126] T. M. Carter,[53] M. P. Casado,[13,i] M. Caspar,[49] F. L. Castillo,[4] L. Castillo Garcia,[13] V. Castillo Gimenez,[166] N. F. Castro,[133a,133e] A. Catinaccio,[37] J. R. Catmore,[128] T. Cavaliere,[4] V. Cavaliere,[30] N. Cavalli,[24b,24a] L. J. Caviedes Betancourt,[23b] Y. C. Cekmecelioglu,[49] E. Celebi,[83] S. Cella,[37] F. Celli,[129] M. S. Centonze,[71a,71b] V. Cepaitis,[57] K. Cerny,[125] A. S. Cerqueira,[84a] A. Cerri,[149] L. Cerrito,[77a,77b] F. Cerutti,[18a] B. Cervato,[144] A. Cervelli,[24b] G. Cesarini,[54] S. A. Cetin,[83] D. Chakraborty,[118] J. Chan,[18a] W. Y. Chan,[156] J. D. Chapman,[33] E. Chapon,[138] B. Chargeishvili,[152b] D. G. Charlton,[21] M. Chatterjee,[20] C. Chauhan,[136] Y. Che,[114a] S. Chekanov,[6] S. V. Chekulaev,[159a] G. A. Chelkov,[39,j] A. Chen,[108] B. Chen,[154] B. Chen,[168] H. Chen,[114a] H. Chen,[30] J. Chen,[63c] J. Chen,[145] M. Chen,[129] S. Chen,[156] S. J. Chen,[114a] X. Chen,[63c] X. Chen,[15,k] Y. Chen,[63a] C. L. Cheng,[173] H. C. Cheng,[65a] S. Cheong,[146] A. Cheplakov,[39] E. Cheremushkina,[49] E. Cherepanova,[117] R. Cherkaoui El Moursli,[36e] E. Cheu,[7] K. Cheung,[66] L. Chevalier,[138] V. Chiarella,[54] G. Chiarelli,[75a] N. Chiedde,[104] G. Chiodini,[71a] A. S. Chisholm,[21] A. Chitan,[28b] M. Chitishvili,[166] M. V. Chizhov,[39,l] K. Choi,[11]

Y. Chou,[141] E. Y. S. Chow,[116] K. L. Chu,[172] M. C. Chu,[65a] X. Chu,[14,114c] Z. Chubinidze,[54] J. Chudoba,[134] J. J. Chwastowski,[88] D. Cieri,[112] K. M. Ciesla,[87a] V. Cindro,[95] A. Ciocio,[18a] F. Cirotto,[73a,73b] Z. H. Citron,[172] M. Citterio,[72a] D. A. Ciubotaru,[28b] A. Clark,[57] P. J. Clark,[53] N. Clarke Hall,[98] C. Clarry,[158] J. M. Clavijo Columbie,[49] S. E. Clawson,[49] C. Clement,[48a,48b] Y. Coadou,[104] M. Cobal,[70a,70c] A. Coccaro,[58b] R. F. Coelho Barrue,[133a] R. Coelho Lopes De Sa,[105] S. Coelli,[72a] B. Cole,[42] J. Collot,[61] P. Conde Muiño,[133a,133g] M. P. Connell,[34c] S. H. Connell,[34c] E. I. Conroy,[129] F. Conventi,[73a,m] H. G. Cooke,[21] A. M. Cooper-Sarkar,[129] F. A. Corchia,[24b,24a] A. Cordeiro Oudot Choi,[130] L. D. Corpe,[41] M. Corradi,[76a,76b] F. Corriveau,[106,n] A. Cortes-Gonzalez,[19] M. J. Costa,[166] F. Costanza,[4] D. Costanzo,[142] B. M. Cote,[122] J. Couthures,[4] G. Cowan,[97] K. Cranmer,[173] D. Cremonini,[24b,24a] S. Crépé-Renaudin,[61] F. Crescioli,[130] M. Cristinziani,[144] M. Cristoforetti,[79a,79b] V. Croft,[117] J. E. Crosby,[124] G. Crosetti,[44b,44a] A. Cueto,[101] H. Cui,[98] Z. Cui,[7] W. R. Cunningham,[60] F. Curcio,[166] J. R. Curran,[53] P. Czodrowski,[37] M. J. Da Cunha Sargedas De Sousa,[58b,58a] J. V. Da Fonseca Pinto,[84b] C. Da Via,[103] W. Dabrowski,[87a] T. Dado,[37] S. Dahbi,[151] T. Dai,[108] D. Dal Santo,[20] C. Dallapiccola,[105] M. Dam,[43] G. D'amen,[30] V. D'Amico,[111] J. Damp,[102] J. R. Dandoy,[35] D. Dannheim,[37] M. Danninger,[145] V. Dao,[148] G. Darbo,[58b] S. J. Das,[30,o] F. Dattola,[49] S. D'Auria,[72a,72b] A. D'Avanzo,[73a,73b] C. David,[34a] T. Davidek,[136] I. Dawson,[96] H. A. Day-hall,[135] K. De,[8] R. De Asmundis,[73a] N. De Biase,[49] S. De Castro,[24b,24a] N. De Groot,[116] P. de Jong,[117] H. De la Torre,[118] A. De Maria,[114a] A. De Salvo,[76a] U. De Sanctis,[77a,77b] F. De Santis,[71a,71b] A. De Santo,[149] J. B. De Vivie De Regie,[61] J. Debevc,[95] D. V. Dedovich,[39] J. Degens,[94] A. M. Deiana,[45] F. Del Corso,[24b,24a] J. Del Peso,[101] L. Delagrange,[130] F. Deliot,[138] C. M. Delitzsch,[50] M. Della Pietra,[73a,73b] D. Della Volpe,[57] A. Dell'Acqua,[37] L. Dell'Asta,[72a,72b] M. Delmastro,[4] P. A. Delsart,[61] S. Demers,[175] M. Demichev,[39] S. P. Denisov,[38] L. D'Eramo,[41] D. Derendarz,[88] F. Derue,[130] P. Dervan,[94] K. Desch,[25] C. Deutsch,[25] F. A. Di Bello,[58b,58a] A. Di Ciaccio,[77a,77b] L. Di Ciaccio,[4] A. Di Domenico,[76a,76b] C. Di Donato,[73a,73b] A. Di Girolamo,[37] G. Di Gregorio,[37] A. Di Luca,[79a,79b] B. Di Micco,[78a,78b] R. Di Nardo,[78a,78b] K. F. Di Petrillo,[40] M. Diamantopoulou,[35] F. A. Dias,[117] T. Dias Do Vale,[145] M. A. Diaz,[140a,140b] F. G. Diaz Capriles,[25] A. R. Didenko,[39] M. Didenko,[166] E. B. Diehl,[108] S. Díez Cornell,[49] C. Diez Pardos,[144] C. Dimitriadi,[164] A. Dimitrievska,[21] J. Dingfelder,[25] T. Dingley,[129] I-M. Dinu,[28b] S. J. Dittmeier,[64b] F. Dittus,[37] M. Divisek,[136] B. Dixit,[94] F. Djama,[104] T. Djobava,[152b] C. Doglioni,[103,100] A. Dohnalova,[29a] J. Dolejsi,[136] Z. Dolezal,[136] K. Domijan,[87a] K. M. Dona,[40] M. Donadelli,[84d] B. Dong,[109] J. Donini,[41] A. D'Onofrio,[73a,73b] M. D'Onofrio,[94] J. Dopke,[137] A. Doria,[73a] N. Dos Santos Fernandes,[133a] P. Dougan,[103] M. T. Dova,[92] A. T. Doyle,[60] M. A. Draguet,[129] E. Dreyer,[172] I. Drivas-koulouris,[10] M. Drnevich,[120] M. Drozdova,[57] D. Du,[63a] T. A. du Pree,[117] F. Dubinin,[38] M. Dubovsky,[29a] E. Duchovni,[172] G. Duckeck,[111] O. A. Ducu,[28b] D. Duda,[53] A. Dudarev,[37] E. R. Duden,[27] M. D'uffizi,[103] L. Duflot,[67] M. Dührssen,[37] I. Duminica,[28g] A. E. Dumitriu,[28b] M. Dunford,[64a] S. Dungs,[50] K. Dunne,[48a,48b] A. Duperrin,[104] H. Duran Yildiz,[3a] M. Düren,[59] A. Durglishvili,[152b] B. L. Dwyer,[118] G. I. Dyckes,[18a] M. Dyndal,[87a] B. S. Dziedzic,[37] Z. O. Earnshaw,[149] G. H. Eberwein,[129] B. Eckerova,[29a] S. Eggebrecht,[56] E. Egidio Purcino De Souza,[84e] L. F. Ehrke,[57] G. Eigen,[17] K. Einsweiler,[18a] T. Ekelof,[164] P. A. Ekman,[100] S. El Farkh,[36b] Y. El Ghazali,[63a] H. El Jarrari,[37] A. El Moussaouy,[36a] V. Ellajosyula,[164] M. Ellert,[164] F. Ellinghaus,[174] N. Ellis,[37] J. Elmsheuser,[30] M. Elsawy,[119a] M. Elsing,[37] D. Emeliyanov,[137] Y. Enari,[85] I. Ene,[18a] S. Epari,[13] P. A. Erland,[88] D. Ernani Martins Neto,[88] M. Errenst,[174] M. Escalier,[67] C. Escobar,[166] E. Etzion,[154] G. Evans,[133a] H. Evans,[69] L. S. Evans,[97] A. Ezhilov,[38] S. Ezzarqtouni,[36a] F. Fabbri,[24b,24a] L. Fabbri,[24b,24a] G. Facini,[98] V. Fadeyev,[139] R. M. Fakhrutdinov,[38] D. Fakoudis,[102] S. Falciano,[76a] L. F. Falda Ulhoa Coelho,[37] F. Fallavollita,[112] G. Falsetti,[44b,44a] J. Faltova,[136] C. Fan,[165] K. Y. Fan,[65b] Y. Fan,[14] Y. Fang,[14,114c] M. Fanti,[72a,72b] M. Faraj,[70a,70b] Z. Farazpay,[99] A. Farbin,[8] A. Farilla,[78a] T. Farooque,[109] S. M. Farrington,[53] F. Fassi,[36e] D. Fassouliotis,[9] M. Facci Giannelli,[77a,77b] W. J. Fawcett,[33] L. Fayard,[67] P. Federic,[136] P. Federicova,[134] O. L. Fedin,[38,j] M. Feickert,[173] L. Feligioni,[104] D. E. Fellers,[126] C. Feng,[63b] Z. Feng,[117] M. J. Fenton,[162] L. Ferencz,[49] R. A. M. Ferguson,[93] S. I. Fernandez Luengo,[140f] P. Fernandez Martinez,[13] M. J. V. Fernoux,[104] J. Ferrando,[93] A. Ferrari,[164] P. Ferrari,[117,116] R. Ferrari,[74a] D. Ferrere,[57] C. Ferretti,[108] D. Fiacco,[76a,76b] F. Fiedler,[102] P. Fiedler,[135] A. Filipčič,[95] E. K. Filmer,[1] F. Filthaut,[116] M. C. N. Fiolhais,[133a,133c,p] L. Fiorini,[166] W. C. Fisher,[109] T. Fitschen,[103] P. M. Fitzhugh,[138] I. Fleck,[144] P. Fleischmann,[108] T. Flick,[174] M. Flores,[34d,q] L. R. Flores Castillo,[65a] L. Flores Sanz De Acedo,[37]

F. M. Follega,[79a,79b] N. Fomin,[33] J. H. Foo,[158] A. Formica,[138] A. C. Forti,[103] E. Fortin,[37] A. W. Fortman,[18a] M. G. Foti,[18a] L. Fountas,[9,r] D. Fournier,[67] H. Fox,[93] P. Francavilla,[75a,75b] S. Francescato,[62] S. Franchellucci,[57] M. Franchini,[24b,24a] S. Franchino,[64a] D. Francis,[37] L. Franco,[116] V. Franco Lima,[37] L. Franconi,[49] M. Franklin,[62] G. Frattari,[27] Y. Y. Frid,[154] J. Friend,[60] N. Fritzsche,[37] A. Froch,[55] D. Froidevaux,[37] J. A. Frost,[129] Y. Fu,[63a] S. Fuenzalida Garrido,[140f] M. Fujimoto,[104] K. Y. Fung,[65a] E. Furtado De Simas Filho,[84e] M. Furukawa,[156] J. Fuster,[166] A. Gaa,[56] A. Gabrielli,[24b,24a] A. Gabrielli,[158] P. Gadow,[37] G. Gagliardi,[58b,58a] L. G. Gagnon,[18a] S. Gaid,[163] S. Galantzan,[154] J. Gallagher,[1] E. J. Gallas,[129] B. J. Gallop,[137] K. K. Gan,[122] S. Ganguly,[156] Y. Gao,[53] F. M. Garay Walls,[140a,140b] B. Garcia,[30] C. García,[166] A. Garcia Alonso,[117] A. G. Garcia Caffaro,[175] J. E. García Navarro,[166] M. Garcia-Sciveres,[18a] G. L. Gardner,[131] R. W. Gardner,[40] N. Garelli,[161] D. Garg,[81] R. B. Garg,[146] J. M. Gargan,[53] C. A. Garner,[158] C. M. Garvey,[34a] V. K. Gassmann,[161] G. Gaudio,[74a] V. Gautam,[13] P. Gauzzi,[76a,76b] J. Gavranovic,[95] I. L. Gavrilenko,[38] A. Gavrilyuk,[38] C. Gay,[167] G. Gaycken,[126] E. N. Gazis,[10] A. A. Geanta,[28b] C. M. Gee,[139] A. Gekow,[122] C. Gemme,[58b] M. H. Genest,[61] A. D. Gentry,[115] S. George,[97] W. F. George,[21] T. Geralis,[47] P. Gessinger-Befurt,[37] M. E. Geyik,[174] M. Ghani,[170] K. Ghorbanian,[96] A. Ghosal,[144] A. Ghosh,[162] A. Ghosh,[7] B. Giacobbe,[24b] S. Giagu,[76a,76b] T. Giani,[117] A. Giannini,[63a] S. M. Gibson,[97] M. Gignac,[139] D. T. Gil,[87b] A. K. Gilbert,[87a] B. J. Gilbert,[42] D. Gillberg,[35] G. Gilles,[117] L. Ginabat,[130] D. M. Gingrich,[2,d] M. P. Giordani,[70a,70c] P. F. Giraud,[138] G. Giugliarelli,[70a,70c] D. Giugni,[72a] F. Giuli,[37] I. Gkialas,[9,r] L. K. Gladilin,[38] C. Glasman,[101] G. R. Gledhill,[126] G. Glemža,[49] M. Glisic,[126] I. Gnesi,[44b,s] Y. Go,[30] M. Goblirsch-Kolb,[37] B. Gocke,[50] D. Godin,[110] B. Gokturk,[22a] S. Goldfarb,[107] T. Golling,[57] M. G. D. Gololo,[34g] D. Golubkov,[38] J. P. Gombas,[109] A. Gomes,[133a,133b] G. Gomes Da Silva,[144] A. J. Gomez Delegido,[166] R. Gonçalo,[133a] L. Gonella,[21] A. Gongadze,[152c] F. Gonnella,[21] J. L. Gonski,[146] R. Y. González Andana,[53] S. González de la Hoz,[166] R. Gonzalez Lopez,[94] C. Gonzalez Renteria,[18a] M. V. Gonzalez Rodrigues,[49] R. Gonzalez Suarez,[164] S. Gonzalez-Sevilla,[57] L. Goossens,[37] B. Gorini,[37] E. Gorini,[71a,71b] A. Gorišek,[95] T. C. Gosart,[131] A. T. Goshaw,[52] M. I. Gostkin,[39] S. Goswami,[124] C. A. Gottardo,[37] S. A. Gotz,[111] M. Gouighri,[36b] V. Goumarre,[49] A. G. Goussiou,[141] N. Govender,[34c] R. P. Grabarczyk,[129] I. Grabowska-Bold,[87a] K. Graham,[35] E. Gramstad,[128] S. Grancagnolo,[71a,71b] C. M. Grant,[1,138] P. M. Gravila,[28f] F. G. Gravili,[71a,71b] H. M. Gray,[18a] M. Greco,[71a,71b] M. J. Green,[1] C. Grefe,[25] A. S. Grefsrud,[17] I. M. Gregor,[49] K. T. Greif,[162] P. Grenier,[146] S. G. Grewe,[112] A. A. Grillo,[139] K. Grimm,[32] S. Grinstein,[13,t] J.-F. Grivaz,[67] E. Gross,[172] J. Grosse-Knetter,[56] L. Guan,[108] J. G. R. Guerrero Rojas,[166] G. Guerrieri,[37] R. Gugel,[102] J. A. M. Guhit,[108] A. Guida,[19] E. Guilloton,[170] S. Guindon,[37] F. Guo,[14,114c] J. Guo,[63c] L. Guo,[49] Y. Guo,[108] R. Gupta,[132] S. Gurbuz,[25] S. S. Gurdasani,[55] G. Gustavino,[76a,76b] P. Gutierrez,[123] L. F. Gutierrez Zagazeta,[131] M. Gutsche,[51] C. Gutschow,[98] C. Gwenlan,[129] C. B. Gwilliam,[94] E. S. Haaland,[128] A. Haas,[120] M. Habedank,[49] C. Haber,[18a] H. K. Hadavand,[8] A. Hadef,[51] S. Hadzic,[112] A. I. Hagan,[93] J. J. Hahn,[144] E. H. Haines,[98] M. Haleem,[169] J. Haley,[124] J. J. Hall,[142] G. D. Hallewell,[104] L. Halser,[20] K. Hamano,[168] M. Hamer,[25] G. N. Hamity,[53] E. J. Hampshire,[97] J. Han,[63b] K. Han,[63a] L. Han,[114a] L. Han,[63a] S. Han,[18a] Y. F. Han,[158] K. Hanagaki,[85] M. Hance,[139] D. A. Hangal,[42] H. Hanif,[145] M. D. Hank,[131] J. B. Hansen,[43] P. H. Hansen,[43] D. Harada,[57] T. Harenberg,[174] S. Harkusha,[38] M. L. Harris,[105] Y. T. Harris,[25] J. Harrison,[13] N. M. Harrison,[122] P. F. Harrison,[170] N. M. Hartman,[112] N. M. Hartmann,[111] R. Z. Hasan,[97,137] Y. Hasegawa,[143] F. Haslbeck,[129] S. Hassan,[17] R. Hauser,[109] C. M. Hawkes,[21] R. J. Hawkings,[37] Y. Hayashi,[156] D. Hayden,[109] C. Hayes,[108] R. L. Hayes,[117] C. P. Hays,[129] J. M. Hays,[96] H. S. Hayward,[94] F. He,[63a] M. He,[14,114c] Y. He,[49] Y. He,[98] N. B. Heatley,[96] V. Hedberg,[100] A. L. Heggelund,[128] N. D. Hehir,[96,a] C. Heidegger,[55] K. K. Heidegger,[55] J. Heilman,[35] S. Heim,[49] T. Heim,[18a] J. G. Heinlein,[131] J. J. Heinrich,[126] L. Heinrich,[112,u] J. Hejbal,[134] A. Held,[173] S. Hellesund,[17] C. M. Helling,[167] S. Hellman,[48a,48b] R. C. W. Henderson,[93] L. Henkelmann,[33] A. M. Henriques Correia,[37] H. Herde,[100] Y. Hernández Jiménez,[148] L. M. Herrmann,[25] T. Herrmann,[51] G. Herten,[55] R. Hertenberger,[111] L. Hervas,[37] M. E. Hesping,[102] N. P. Hessey,[159a] M. Hidaoui,[36b] N. Hidic,[136] E. Hill,[158] S. J. Hillier,[21] J. R. Hinds,[109] F. Hinterkeuser,[25] M. Hirose,[127] S. Hirose,[160] D. Hirschbuehl,[174] T. G. Hitchings,[103] B. Hiti,[95] J. Hobbs,[148] R. Hobincu,[28e] N. Hod,[172] M. C. Hodgkinson,[142] B. H. Hodkinson,[129] A. Hoecker,[37] D. D. Hofer,[108] J. Hofer,[49] T. Holm,[25] M. Holzbock,[37] L. B. A. H. Hommels,[33] B. P. Honan,[103] J. J. Hong,[69] J. Hong,[63c] T. M. Hong,[132] B. H. Hooberman,[165] W. H. Hopkins,[6] M. C. Hoppesch,[165] Y. Horii,[113] S. Hou,[151] A. S. Howard,[95] J. Howarth,[60]

J. Hoya,[6] M. Hrabovsky,[125] A. Hrynevich,[49] T. Hryn'ova,[4] P. J. Hsu,[66] S.-C. Hsu,[141] T. Hsu,[67] M. Hu,[18a] Q. Hu,[63a] S. Huang,[65b] X. Huang,[14,114c] Y. Huang,[142] Y. Huang,[102] Y. Huang,[14] Z. Huang,[103] Z. Hubacek,[135] M. Huebner,[25] F. Huegging,[25] T. B. Huffman,[129] C. A. Hugli,[49] M. Huhtinen,[37] S. K. Huiberts,[17] R. Hulsken,[106] N. Huseynov,[12,v] J. Huston,[109] J. Huth,[62] R. Hyneman,[146] G. Iacobucci,[57] G. Iakovidis,[30] L. Iconomidou-Fayard,[67] J. P. Iddon,[37] P. Iengo,[73a,73b] R. Iguchi,[156] Y. Iiyama,[156] T. Iizawa,[129] Y. Ikegami,[85] N. Ilic,[158] H. Imam,[84c] G. Inacio Goncalves,[84d] M. Ince Lezki,[57] T. Ingebretsen Carlson,[48a,48b] J. M. Inglis,[96] G. Introzzi,[74a,74b] M. Iodice,[78a] V. Ippolito,[76a,76b] R. K. Irwin,[94] M. Ishino,[156] W. Islam,[173] C. Issever,[19,49] S. Istin,[22a,w] H. Ito,[171] R. Iuppa,[79a,79b] A. Ivina,[172] J. M. Izen,[46] V. Izzo,[73a] P. Jacka,[134] P. Jackson,[1] C. S. Jagfeld,[111] G. Jain,[159a] P. Jain,[49] K. Jakobs,[55] T. Jakoubek,[172] J. Jamieson,[60] W. Jang,[156] M. Javurkova,[105] P. Jawahar,[103] L. Jeanty,[126] J. Jejelava,[152a,x] P. Jenni,[55,y] C. E. Jessiman,[35] C. Jia,[63b] J. Jia,[148] X. Jia,[14,114c] Z. Jia,[114a] C. Jiang,[53] S. Jiggins,[49] J. Jimenez Pena,[13] S. Jin,[114a] A. Jinaru,[28b] O. Jinnouchi,[157] P. Johansson,[142] K. A. Johns,[7] J. W. Johnson,[139] F. A. Jolly,[49] D. M. Jones,[149] E. Jones,[49] K. S. Jones,[8] P. Jones,[33] R. W. L. Jones,[93] T. J. Jones,[94] H. L. Joos,[56,37] R. Joshi,[122] J. Jovicevic,[16] X. Ju,[18a] J. J. Junggeburth,[105] T. Junkermann,[64a] A. Juste Rozas,[13,t] M. K. Juzek,[88] S. Kabana,[140e] A. Kaczmarska,[88] M. Kado,[112] H. Kagan,[122] M. Kagan,[146] A. Kahn,[131] C. Kahra,[102] T. Kaji,[156] E. Kajomovitz,[153] N. Kakati,[172] I. Kalaitzidou,[55] C. W. Kalderon,[30] N. J. Kang,[139] D. Kar,[34g] K. Karava,[129] M. J. Kareem,[159b] E. Karentzos,[55] O. Karkout,[117] S. N. Karpov,[39] Z. M. Karpova,[39] V. Kartvelishvili,[93] A. N. Karyukhin,[38] E. Kasimi,[155] J. Katzy,[49] S. Kaur,[35] K. Kawade,[143] M. P. Kawale,[123] C. Kawamoto,[89] T. Kawamoto,[63a] E. F. Kay,[37] F. I. Kaya,[161] S. Kazakos,[109] V. F. Kazanin,[38] Y. Ke,[148] J. M. Keaveney,[34a] R. Keeler,[168] G. V. Kehris,[62] J. S. Keller,[35] A. S. Kelly,[98] J. J. Kempster,[149] P. D. Kennedy,[102] O. Kepka,[134] B. P. Kerridge,[137] S. Kersten,[174] B. P. Kerševan,[95] L. Keszeghova,[29a] S. Ketabchi Haghighat,[158] R. A. Khan,[132] A. Khanov,[124] A. G. Kharlamov,[38] T. Kharlamova,[38] E. E. Khoda,[141] M. Kholodenko,[133a] T. J. Khoo,[19] G. Khoriauli,[169] J. Khubua,[152b,a] Y. A. R. Khwaira,[130] B. Kibirige,[34g] D. Kim,[6] D. W. Kim,[48a,48b] Y. K. Kim,[40] N. Kimura,[98] M. K. Kingston,[56] A. Kirchhoff,[56] C. Kirfel,[25] F. Kirfel,[25] J. Kirk,[137] A. E. Kiryunin,[112] C. Kitsaki,[10] O. Kivernyk,[25] M. Klassen,[161] C. Klein,[35] L. Klein,[169] M. H. Klein,[45] S. B. Klein,[57] U. Klein,[94] P. Klimek,[37] A. Klimentov,[30] T. Klioutchnikova,[37] P. Kluit,[117] S. Kluth,[112] E. Kneringer,[80] T. M. Knight,[158] A. Knue,[50] D. Kobylianskii,[172] S. F. Koch,[129] M. Kocian,[146] P. Kodyš,[136] D. M. Koeck,[126] P. T. Koenig,[25] T. Koffas,[35] O. Kolay,[51] I. Koletsou,[4] T. Komarek,[88] K. Köneke,[55] A. X. Y. Kong,[1] T. Kono,[121] N. Konstantinidis,[98] P. Kontaxakis,[57] B. Konya,[100] R. Kopeliansky,[42] S. Koperny,[87a] K. Korcyl,[88] K. Kordas,[155,z] A. Korn,[98] S. Korn,[56] I. Korolkov,[13] N. Korotkova,[38] B. Kortman,[117] O. Kortner,[112] S. Kortner,[112] W. H. Kostecka,[118] V. V. Kostyukhin,[144] A. Kotsokechagia,[37] A. Kotwal,[52] A. Koulouris,[37] A. Kourkoumeli-Charalampidi,[74a,74b] C. Kourkoumelis,[9] E. Kourlitis,[112,u] O. Kovanda,[126] R. Kowalewski,[168] W. Kozanecki,[126] A. S. Kozhin,[38] V. A. Kramarenko,[38] G. Kramberger,[95] P. Kramer,[102] M. W. Krasny,[130] A. Krasznahorkay,[37] A. C. Kraus,[118] J. W. Kraus,[174] J. A. Kremer,[49] T. Kresse,[51] L. Kretschmann,[174] J. Kretzschmar,[94] K. Kreul,[19] P. Krieger,[158] M. Krivos,[136] K. Krizka,[21] K. Kroeninger,[50] H. Kroha,[112] J. Kroll,[134] J. Kroll,[131] K. S. Krowpman,[109] U. Kruchonak,[39] H. Krüger,[25] N. Krumnack,[82] M. C. Kruse,[52] O. Kuchinskaia,[38] S. Kuday,[3a] S. Kuehn,[37] R. Kuesters,[55] T. Kuhl,[49] V. Kukhtin,[39] Y. Kulchitsky,[38,j] S. Kuleshov,[140d,140b] M. Kumar,[34g] N. Kumari,[49] P. Kumari,[159b] A. Kupco,[134] T. Kupfer,[50] A. Kupich,[38] O. Kuprash,[55] H. Kurashige,[86] L. L. Kurchaninov,[159a] O. Kurdysh,[67] Y. A. Kurochkin,[38] A. Kurova,[38] M. Kuze,[157] A. K. Kvam,[105] J. Kvita,[125] T. Kwan,[106] N. G. Kyriacou,[108] L. A. O. Laatu,[104] C. Lacasta,[166] F. Lacava,[76a,76b] H. Lacker,[19] D. Lacour,[130] N. N. Lad,[98] E. Ladygin,[39] A. Lafarge,[41] B. Laforge,[130] T. Lagouri,[175] F. Z. Lahbabi,[36a] S. Lai,[56] J. E. Lambert,[168] S. Lammers,[69] W. Lampl,[7] C. Lampoudis,[155,z] G. Lamprinoudis,[102] A. N. Lancaster,[118] E. Lançon,[30] U. Landgraf,[55] M. P. J. Landon,[96] V. S. Lang,[55] O. K. B. Langrekken,[128] A. J. Lankford,[162] F. Lanni,[37] K. Lantzsch,[25] A. Lanza,[74a] M. Lanzac Berrocal,[166] J. F. Laporte,[138] T. Lari,[72a] F. Lasagni Manghi,[24b] M. Lassnig,[37] V. Latonova,[134] A. Laurier,[153] S. D. Lawlor,[142] Z. Lawrence,[103] R. Lazaridou,[170] M. Lazzaroni,[72a,72b] B. Le,[103] E. M. Le Boulicaut,[52] L. T. Le Pottier,[18a] B. Leban,[24b,24a] A. Lebedev,[82] M. LeBlanc,[103] F. Ledroit-Guillon,[61] S. C. Lee,[151] S. Lee,[48a,48b] T. F. Lee,[94] L. L. Leeuw,[34c] H. P. Lefebvre,[97] M. Lefebvre,[168] C. Leggett,[18a] G. Lehmann Miotto,[37] M. Leigh,[57] W. A. Leight,[105] W. Leinonen,[116] A. Leisos,[155,aa] M. A. L. Leite,[84c] C. E. Leitgeb,[19] R. Leitner,[136] K. J. C. Leney,[45] T. Lenz,[25] S. Leone,[75a] C. Leonidopoulos,[53] A. Leopold,[147]

R. Les,[109] C. G. Lester,[33] M. Levchenko,[38] J. Levêque,[4] L. J. Levinson,[172] G. Levrini,[24b,24a] M. P. Lewicki,[88] C. Lewis,[141] D. J. Lewis,[4] L. Lewitt,[142] A. Li,[5] B. Li,[63b] C. Li,[63a] C-Q. Li,[112] H. Li,[63a] H. Li,[63b] H. Li,[114a] H. Li,[15] H. Li,[63b] J. Li,[63c] K. Li,[141] L. Li,[63c] M. Li,[14,114c] S. Li,[14,114c] S. Li,[63d,63c] T. Li,[5] X. Li,[106] Z. Li,[129] Z. Li,[156] Z. Li,[14,114c] Z. Li,[63a] S. Liang,[14,114c] Z. Liang,[14] M. Liberatore,[138] B. Liberti,[77a] K. Lie,[65c] J. Lieber Marin,[84e] H. Lien,[69] H. Lin,[108] K. Lin,[109] R. E. Lindley,[7] J. H. Lindon,[2] J. Ling,[62] E. Lipeles,[131] A. Lipniacka,[17] A. Lister,[167] J. D. Little,[69] B. Liu,[14] B. X. Liu,[114b] D. Liu,[63d,63c] E. H. L. Liu,[21] J. B. Liu,[63a] J. K. K. Liu,[33] K. Liu,[63d] K. Liu,[63d,63c] M. Liu,[63a] M. Y. Liu,[63a] P. Liu,[14] Q. Liu,[63d,141,63c] X. Liu,[63a] X. Liu,[63b] Y. Liu,[114b,114c] Y. L. Liu,[63b] Y. W. Liu,[63a] S. L. Lloyd,[96] E. M. Lobodzinska,[49] P. Loch,[7] T. Lohse,[19] K. Lohwasser,[142] E. Loiacono,[49] M. Lokajicek,[134,a] J. D. Lomas,[21] J. D. Long,[165] I. Longarini,[162] R. Longo,[165] I. Lopez Paz,[68] A. Lopez Solis,[49] N. A. Lopez-canelas,[7] N. Lorenzo Martinez,[4] A. M. Lory,[111] M. Losada,[119a] G. Löschcke Centeno,[149] O. Loseva,[38] X. Lou,[48a,48b] X. Lou,[14,114c] A. Lounis,[67] P. A. Love,[93] G. Lu,[14,114c] M. Lu,[67] S. Lu,[131] Y. J. Lu,[66] H. J. Lubatti,[141] C. Luci,[76a,76b] F. L. Lucio Alves,[114a] F. Luehring,[69] I. Luise,[148] O. Lukianchuk,[67] O. Lundberg,[147] B. Lund-Jensen,[147,a] N. A. Luongo,[6] M. S. Lutz,[37] A. B. Lux,[26] D. Lynn,[30] R. Lysak,[134] E. Lytken,[100] V. Lyubushkin,[39] T. Lyubushkina,[39] M. M. Lyukova,[148] M. Firdaus M. Soberi,[53] H. Ma,[30] K. Ma,[63a] L. L. Ma,[63b] W. Ma,[63a] Y. Ma,[124] J. C. MacDonald,[102] P. C. Machado De Abreu Farias,[84e] R. Madar,[41] T. Madula,[98] J. Maeda,[86] T. Maeno,[30] H. Maguire,[142] V. Maiboroda,[138] A. Maio,[133a,133b,133d] K. Maj,[87a] O. Majersky,[49] S. Majewski,[126] N. Makovec,[67] V. Maksimovic,[16] B. Malaescu,[130] Pa. Malecki,[88] V. P. Maleev,[38] F. Malek,[61,bb] M. Mali,[95] D. Malito,[97] U. Mallik,[81,a] S. Maltezos,[10] S. Malyukov,[39] J. Mamuzic,[13] G. Mancini,[54] M. N. Mancini,[27] G. Manco,[74a,74b] J. P. Mandalia,[96] S. S. Mandarry,[149] I. Mandić,[95] L. Manhaes de Andrade Filho,[84a] I. M. Maniatis,[172] J. Manjarres Ramos,[91] D. C. Mankad,[172] A. Mann,[111] S. Manzoni,[37] L. Mao,[63c] X. Mapekula,[34c] A. Marantis,[155,aa] G. Marchiori,[5] M. Marcisovsky,[134] C. Marcon,[72a] M. Marinescu,[21] S. Marium,[49] M. Marjanovic,[123] A. Markhoos,[55] M. Markovitch,[67] E. J. Marshall,[93] Z. Marshall,[18a] S. Marti-Garcia,[166] J. Martin,[98] T. A. Martin,[137] V. J. Martin,[53] B. Martin dit Latour,[17] L. Martinelli,[76a,76b] M. Martinez,[13,t] P. Martinez Agullo,[166] V. I. Martinez Outschoorn,[105] P. Martinez Suarez,[13] S. Martin-Haugh,[137] G. Martinovicova,[136] V. S. Martoiu,[28b] A. C. Martyniuk,[98] A. Marzin,[37] D. Mascione,[79a,79b] L. Masetti,[102] J. Masik,[103] A. L. Maslennikov,[38] P. Massarotti,[73a,73b] P. Mastrandrea,[75a,75b] A. Mastroberardino,[44b,44a] T. Masubuchi,[127] T. Mathisen,[164] J. Matousek,[136] J. Maurer,[28b] A. J. Maury,[67] B. Maček,[95] D. A. Maximov,[38] A. E. May,[103] R. Mazini,[151] I. Maznas,[118] M. Mazza,[109] S. M. Mazza,[139] E. Mazzeo,[72a,72b] C. Mc Ginn,[30] J. P. Mc Gowan,[168] S. P. Mc Kee,[108] C. C. McCracken,[167] E. F. McDonald,[107] A. E. McDougall,[117] J. A. Mcfayden,[149] R. P. McGovern,[131] R. P. Mckenzie,[34g] T. C. Mclachlan,[49] D. J. Mclaughlin,[98] S. J. McMahon,[137] C. M. Mcpartland,[94] R. A. McPherson,[168,n] S. Mehlhase,[111] A. Mehta,[94] D. Melini,[166] B. R. Mellado Garcia,[34g] A. H. Melo,[56] F. Meloni,[49] A. M. Mendes Jacques Da Costa,[103] H. Y. Meng,[158] L. Meng,[93] S. Menke,[112] M. Mentink,[37] E. Meoni,[44b,44a] G. Mercado,[118] S. Merianos,[155] C. Merlassino,[70a,70c] L. Merola,[73a,73b] C. Meroni,[72a,72b] J. Metcalfe,[6] A. S. Mete,[6] E. Meuser,[102] C. Meyer,[69] J-P. Meyer,[138] R. P. Middleton,[137] L. Mijović,[53] G. Mikenberg,[172] M. Mikestikova,[134] M. Mikuž,[95] H. Mildner,[102] A. Milic,[37] D. W. Miller,[40] E. H. Miller,[146] L. S. Miller,[35] A. Milov,[172] D. A. Milstead,[48a,48b] T. Min,[114a] A. A. Minaenko,[38] I. A. Minashvili,[152b] L. Mince,[60] A. I. Mincer,[120] B. Mindur,[87a] M. Mineev,[39] Y. Mino,[89] L. M. Mir,[13] M. Miralles Lopez,[60] M. Mironova,[18a] M. C. Missio,[116] A. Mitra,[170] V. A. Mitsou,[166] Y. Mitsumori,[113] O. Miu,[158] P. S. Miyagawa,[96] T. Mkrtchyan,[64a] M. Mlinarevic,[98] T. Mlinarevic,[98] M. Mlynarikova,[37] S. Mobius,[20] P. Mogg,[111] M. H. Mohamed Farook,[115] A. F. Mohammed,[14,114c] S. Mohapatra,[42] G. Mokgatitswane,[34g] L. Moleri,[172] B. Mondal,[144] S. Mondal,[135] K. Mönig,[49] E. Monnier,[104] L. Monsonis Romero,[166] J. Montejo Berlingen,[13] A. Montella,[48a,48b] M. Montella,[122] F. Montereali,[78a,78b] F. Monticelli,[92] S. Monzani,[70a,70c] A. Morancho Tarda,[43] N. Morange,[67] A. L. Moreira De Carvalho,[49] M. Moreno Llácer,[166] C. Moreno Martinez,[57] J. M. Moreno Perez,[23b] P. Morettini,[58b] S. Morgenstern,[37] M. Morii,[62] M. Morinaga,[156] F. Morodei,[76a,76b] L. Morvaj,[37] P. Moschovakos,[37] B. Moser,[129] M. Mosidze,[152b] T. Moskalets,[45] P. Moskvitina,[116] J. Moss,[32,cc] P. Moszkowicz,[87a] A. Moussa,[36d] E. J. W. Moyse,[105] O. Mtintsilana,[34g] S. Muanza,[104] J. Mueller,[132] D. Muenstermann,[93] R. Müller,[37] G. A. Mullier,[164] A. J. Mullin,[33] J. J. Mullin,[131] D. P. Mungo,[158] D. Munoz Perez,[166] F. J. Munoz Sanchez,[103] M. Murin,[103] W. J. Murray,[170,137] M. Muškinja,[95] C. Mwewa,[30] A. G. Myagkov,[38,j] A. J. Myers,[8] G. Myers,[108] M. Myska,[135] B. P. Nachman,[18a]

O. Nackenhorst,[50] K. Nagai,[129] K. Nagano,[85] J. L. Nagle,[30,o] E. Nagy,[104] A. M. Nairz,[37] Y. Nakahama,[85] K. Nakamura,[85] K. Nakkalil,[5] H. Nanjo,[127] E. A. Narayanan,[115] I. Naryshkin,[38] L. Nasella,[72a,72b] M. Naseri,[35] S. Nasri,[119b] C. Nass,[25] G. Navarro,[23a] J. Navarro-Gonzalez,[166] R. Nayak,[154] A. Nayaz,[19] P. Y. Nechaeva,[38] S. Nechaeva,[24b,24a] F. Nechansky,[49] L. Nedic,[129] T. J. Neep,[21] A. Negri,[74a,74b] M. Negrini,[24b] C. Nellist,[117] C. Nelson,[106] K. Nelson,[108] S. Nemecek,[134] M. Nessi,[37,dd] M. S. Neubauer,[165] F. Neuhaus,[102] J. Neundorf,[49] P. R. Newman,[21] C. W. Ng,[132] Y. W. Y. Ng,[49] B. Ngair,[119a] H. D. N. Nguyen,[110] R. B. Nickerson,[129] R. Nicolaidou,[138] J. Nielsen,[139] M. Niemeyer,[56] J. Niermann,[56] N. Nikiforou,[37] V. Nikolaenko,[38,j] I. Nikolic-Audit,[130] K. Nikolopoulos,[21] P. Nilsson,[30] I. Ninca,[49] G. Ninio,[154] A. Nisati,[76a] N. Nishu,[2] R. Nisius,[112] J-E. Nitschke,[51] E. K. Nkadimeng,[34g] T. Nobe,[156] T. Nommensen,[150] M. B. Norfolk,[142] B. J. Norman,[35] M. Noury,[36a] J. Novak,[95] T. Novak,[95] L. Novotny,[135] R. Novotny,[115] L. Nozka,[125] K. Ntekas,[162] N. M. J. Nunes De Moura Junior,[84b] J. Ocariz,[130] A. Ochi,[86] I. Ochoa,[133a] S. Oerdek,[49,ee] J. T. Offermann,[40] A. Ogrodnik,[136] A. Oh,[103] C. C. Ohm,[147] H. Oide,[85] R. Oishi,[156] M. L. Ojeda,[49] Y. Okumura,[156] L. F. Oleiro Seabra,[133a] I. Oleksiyuk,[57] S. A. Olivares Pino,[140d] G. Oliveira Correa,[13] D. Oliveira Damazio,[30] J. L. Oliver,[162] Ö. O. Öncel,[55] A. P. O'Neill,[20] A. Onofre,[133a,133e] P. U. E. Onyisi,[11] M. J. Oreglia,[40] G. E. Orellana,[92] D. Orestano,[78a,78b] N. Orlando,[13] R. S. Orr,[158] L. M. Osojnak,[131] R. Ospanov,[63a] G. Otero y Garzon,[31] H. Otono,[90] P. S. Ott,[64a] G. J. Ottino,[18a] M. Ouchrif,[36d] F. Ould-Saada,[128] T. Ovsiannikova,[141] M. Owen,[60] R. E. Owen,[137] V. E. Ozcan,[22a] F. Ozturk,[88] N. Ozturk,[8] S. Ozturk,[83] H. A. Pacey,[129] A. Pacheco Pages,[13] C. Padilla Aranda,[13] G. Padovano,[76a,76b] S. Pagan Griso,[18a] G. Palacino,[69] A. Palazzo,[71a,71b] J. Pampel,[25] J. Pan,[175] T. Pan,[65a] D. K. Panchal,[11] C. E. Pandini,[117] J. G. Panduro Vazquez,[137] H. D. Pandya,[1] H. Pang,[15] P. Pani,[49] G. Panizzo,[70a,70c] L. Panwar,[130] L. Paolozzi,[57] S. Parajuli,[165] A. Paramonov,[6] C. Paraskevopoulos,[54] D. Paredes Hernandez,[65b] A. Pareti,[74a,74b] K. R. Park,[42] T. H. Park,[158] M. A. Parker,[33] F. Parodi,[58b,58a] E. W. Parrish,[118] V. A. Parrish,[53] J. A. Parsons,[42] U. Parzefall,[55] B. Pascual Dias,[110] L. Pascual Dominguez,[101] E. Pasqualucci,[76a] S. Passaggio,[58b] F. Pastore,[97] P. Patel,[88] U. M. Patel,[52] J. R. Pater,[103] T. Pauly,[37] C. I. Pazos,[161] J. Pearkes,[146] M. Pedersen,[128] R. Pedro,[133a] S. V. Peleganchuk,[38] O. Penc,[37] E. A. Pender,[53] S. Peng,[15] G. D. Penn,[175] K. E. Penski,[111] M. Penzin,[38] B. S. Peralva,[84d] A. P. Pereira Peixoto,[141] L. Pereira Sanchez,[146] D. V. Perepelitsa,[30,o] G. Perera,[105] E. Perez Codina,[159a] M. Perganti,[10] H. Pernegger,[37] S. Perrella,[76a,76b] O. Perrin,[41] K. Peters,[49] R. F. Y. Peters,[103] B. A. Petersen,[37] T. C. Petersen,[43] E. Petit,[104] V. Petousis,[135] C. Petridou,[155,z] T. Petru,[136] A. Petrukhin,[144] M. Pettee,[18a] A. Petukhov,[38] K. Petukhova,[37] R. Pezoa,[140f] L. Pezzotti,[37] G. Pezzullo,[175] T. M. Pham,[173] T. Pham,[107] P. W. Phillips,[137] G. Piacquadio,[148] E. Pianori,[18a] F. Piazza,[126] R. Piegaia,[31] D. Pietreanu,[28b] A. D. Pilkington,[103] M. Pinamonti,[70a,70c] J. L. Pinfold,[2] B. C. Pinheiro Pereira,[133a] J. Pinol Bel,[13] A. E. Pinto Pinoargote,[138,138] L. Pintucci,[70a,70c] K. M. Piper,[149] A. Pirttikoski,[57] D. A. Pizzi,[35] L. Pizzimento,[65b] A. Pizzini,[117] M.-A. Pleier,[30] V. Pleskot,[136] E. Plotnikova,[39] G. Poddar,[96] R. Poettgen,[100] L. Poggioli,[130] I. Pokharel,[56] S. Polacek,[136] G. Polesello,[74a] A. Poley,[145,159a] A. Polini,[24b] C. S. Pollard,[170] Z. B. Pollock,[122] E. Pompa Pacchi,[76a,76b] N. I. Pond,[98] D. Ponomarenko,[69] L. Pontecorvo,[37] S. Popa,[28a] G. A. Popeneciu,[28d] A. Poreba,[37] D. M. Portillo Quintero,[159a] S. Pospisil,[135] M. A. Postill,[142] P. Postolache,[28c] K. Potamianos,[170] P. A. Potepa,[87a] I. N. Potrap,[39] C. J. Potter,[33] H. Potti,[150] J. Poveda,[166] M. E. Pozo Astigarraga,[37] A. Prades Ibanez,[77a,77b] J. Pretel,[168] D. Price,[103] M. Primavera,[71a] L. Primomo,[70a,70c] M. A. Principe Martin,[101] R. Privara,[125] T. Procter,[60] M. L. Proffitt,[141] N. Proklova,[131] K. Prokofiev,[65c] G. Proto,[112] J. Proudfoot,[6] M. Przybycien,[87a] W. W. Przygoda,[87b] A. Psallidas,[47] J. E. Puddefoot,[142] D. Pudzha,[55] D. Pyatiizbyantseva,[38] J. Qian,[108] D. Qichen,[103] Y. Qin,[13] T. Qiu,[53] A. Quadt,[56] M. Queitsch-Maitland,[103] G. Quetant,[57] R. P. Quinn,[167] G. Rabanal Bolanos,[62] D. Rafanoharana,[55] F. Raffaeli,[77a,77b] F. Ragusa,[72a,72b] J. L. Rainbolt,[40] J. A. Raine,[57] S. Rajagopalan,[30] E. Ramakoti,[38] L. Rambelli,[58b,58a] I. A. Ramirez-Berend,[35] K. Ran,[49,114c] D. S. Rankin,[131] N. P. Rapheeha,[34g] H. Rasheed,[28b] V. Raskina,[130] D. F. Rassloff,[64a] A. Rastogi,[18a] S. Rave,[102] S. Ravera,[58b,58a] B. Ravina,[56] I. Ravinovich,[172] M. Raymond,[37] A. L. Read,[128] N. P. Readioff,[142] D. M. Rebuzzi,[74a,74b] G. Redlinger,[30] A. S. Reed,[112] K. Reeves,[27] J. A. Reidelsturz,[174] D. Reikher,[126] A. Rej,[50] C. Rembser,[37] M. Renda,[28b] F. Renner,[49] A. G. Rennie,[162] A. L. Rescia,[49] S. Resconi,[72a] M. Ressegotti,[58b,58a] S. Rettie,[37] J. G. Reyes Rivera,[109] E. Reynolds,[18a] O. L. Rezanova,[38] P. Reznicek,[136] H. Riani,[36d] N. Ribaric,[93] E. Ricci,[79a,79b] R. Richter,[112] S. Richter,[48a,48b] E. Richter-Was,[87b] M. Ridel,[130] S. Ridouani,[36d] P. Rieck,[120]

P. Riedler,[37] E. M. Riefel,[48a,48b] J. O. Rieger,[117] M. Rijssenbeek,[148] M. Rimoldi,[37] L. Rinaldi,[24b,24a] P. Rincke,[56,164] T. T. Rinn,[30] M. P. Rinnagel,[111] G. Ripellino,[164] I. Riu,[13] J. C. Rivera Vergara,[168] F. Rizatdinova,[124] E. Rizvi,[96] B. R. Roberts,[18a] S. S. Roberts,[139] S. H. Robertson,[106,n] D. Robinson,[33] M. Robles Manzano,[102] A. Robson,[60] A. Rocchi,[77a,77b] C. Roda,[75a,75b] S. Rodriguez Bosca,[37] Y. Rodriguez Garcia,[23a] A. Rodriguez Rodriguez,[55] A. M. Rodríguez Vera,[118] S. Roe,[37] J. T. Roemer,[37] A. R. Roepe-Gier,[139] O. Røhne,[128] R. A. Rojas,[105] C. P. A. Roland,[130] J. Roloff,[30] A. Romaniouk,[38] E. Romano,[74a,74b] M. Romano,[24b] A. C. Romero Hernandez,[165] N. Rompotis,[94] L. Roos,[130] S. Rosati,[76a] B. J. Rosser,[40] E. Rossi,[129] E. Rossi,[73a,73b] L. P. Rossi,[62] L. Rossini,[55] R. Rosten,[122] M. Rotaru,[28b] B. Rottler,[55] C. Rougier,[91] D. Rousseau,[67] D. Rousso,[49] A. Roy,[165] S. Roy-Garand,[158] A. Rozanov,[104] Z. M. A. Rozario,[60] Y. Rozen,[153] A. Rubio Jimenez,[166] A. J. Ruby,[94] V. H. Ruelas Rivera,[19] T. A. Ruggeri,[1] A. Ruggiero,[129] A. Ruiz-Martinez,[166] A. Rummler,[37] Z. Rurikova,[55] N. A. Rusakovich,[39] H. L. Russell,[168] G. Russo,[76a,76b] J. P. Rutherfoord,[7] S. Rutherford Colmenares,[33] M. Rybar,[136] E. B. Rye,[128] A. Ryzhov,[45] J. A. Sabater Iglesias,[57] H. F-W. Sadrozinski,[139] F. Safai Tehrani,[76a] B. Safarzadeh Samani,[137] S. Saha,[1] M. Sahinsoy,[83] A. Saibel,[166] M. Saimpert,[138] M. Saito,[156] T. Saito,[156] A. Sala,[72a,72b] D. Salamani,[37] A. Salnikov,[146] J. Salt,[166] A. Salvador Salas,[154] D. Salvatore,[44b,44a] F. Salvatore,[149] A. Salzburger,[37] D. Sammel,[55] E. Sampson,[93] D. Sampsonidis,[155,z] D. Sampsonidou,[126] J. Sánchez,[166] V. Sanchez Sebastian,[166] H. Sandaker,[128] C. O. Sander,[49] J. A. Sandesara,[105] M. Sandhoff,[174] C. Sandoval,[23b] L. Sanfilippo,[64a] D. P. C. Sankey,[137] T. Sano,[89] A. Sansoni,[54] L. Santi,[37,76b] C. Santoni,[41] H. Santos,[133a,133b] A. Santra,[172] E. Sanzani,[24b,24a] K. A. Saoucha,[163] J. G. Saraiva,[133a,133d] J. Sardain,[7] O. Sasaki,[85] K. Sato,[160] C. Sauer,[64b] E. Sauvan,[4] P. Savard,[158,d] R. Sawada,[156] C. Sawyer,[137] L. Sawyer,[99] C. Sbarra,[24b] A. Sbrizzi,[24b,24a] T. Scanlon,[98] J. Schaarschmidt,[141] U. Schäfer,[102] A. C. Schaffer,[67,45] D. Schaile,[111] R. D. Schamberger,[148] C. Scharf,[19] M. M. Schefer,[20] V. A. Schegelsky,[38] D. Scheirich,[136] M. Schernau,[162] C. Scheulen,[56] C. Schiavi,[58b,58a] M. Schioppa,[44b,44a] B. Schlag,[146,ff] K. E. Schleicher,[55] S. Schlenker,[37] J. Schmeing,[174] M. A. Schmidt,[174] K. Schmieden,[102] C. Schmitt,[102] N. Schmitt,[102] S. Schmitt,[49] L. Schoeffel,[138] A. Schoening,[64b] P. G. Scholer,[35] E. Schopf,[129] M. Schott,[25] J. Schovancova,[37] S. Schramm,[57] T. Schroer,[57] H-C. Schultz-Coulon,[64a] M. Schumacher,[55] B. A. Schumm,[139] Ph. Schune,[138] A. J. Schuy,[141] H. R. Schwartz,[139] A. Schwartzman,[146] T. A. Schwarz,[108] Ph. Schwemling,[138] R. Schwienhorst,[109] F. G. Sciacca,[20] A. Sciandra,[30] G. Sciolla,[27] F. Scuri,[75a] C. D. Sebastiani,[94] K. Sedlaczek,[118] S. C. Seidel,[115] A. Seiden,[139] B. D. Seidlitz,[42] C. Seitz,[49] J. M. Seixas,[84b] G. Sekhniaidze,[73a] L. Selem,[61] N. Semprini-Cesari,[24b,24a] D. Sengupta,[57] V. Senthilkumar,[166] L. Serin,[67] M. Sessa,[77a,77b] H. Severini,[123] F. Sforza,[58b,58a] A. Sfyrla,[57] Q. Sha,[14] E. Shabalina,[56] A. H. Shah,[33] R. Shaheen,[147] J. D. Shahinian,[131] D. Shaked Renous,[172] L. Y. Shan,[14] M. Shapiro,[18a] A. Sharma,[37] A. S. Sharma,[167] P. Sharma,[81] P. B. Shatalov,[38] K. Shaw,[149] S. M. Shaw,[103] Q. Shen,[63c] D. J. Sheppard,[145] P. Sherwood,[98] L. Shi,[98] X. Shi,[14] S. Shimizu,[85] C. O. Shimmin,[175] J. D. Shinner,[97] I. P. J. Shipsey,[129] S. Shirabe,[90] M. Shiyakova,[39,gg] M. J. Shochet,[40] D. R. Shope,[128] B. Shrestha,[123] S. Shrestha,[122,hh] M. J. Shroff,[168] P. Sicho,[134] A. M. Sickles,[165] E. Sideras Haddad,[34g] A. C. Sidley,[117] A. Sidoti,[24b] F. Siegert,[51] Dj. Sijacki,[16] F. Sili,[92] J. M. Silva,[53] I. Silva Ferreira,[84b] M. V. Silva Oliveira,[30] S. B. Silverstein,[48a] S. Simion,[67] R. Simoniello,[37] E. L. Simpson,[103] H. Simpson,[149] L. R. Simpson,[108] N. D. Simpson,[100] S. Simsek,[83] S. Sindhu,[56] P. Sinervo,[158] S. Singh,[158] S. Sinha,[49] S. Sinha,[103] M. Sioli,[24b,24a] I. Siral,[37] E. Sitnikova,[49] J. Sjölin,[48a,48b] A. Skaf,[56] E. Skorda,[21] P. Skubic,[123] M. Slawinska,[88] V. Smakhtin,[172] B. H. Smart,[137] S. Yu. Smirnov,[38] Y. Smirnov,[38] L. N. Smirnova,[38,j] O. Smirnova,[100] A. C. Smith,[42] D. R. Smith,[162] E. A. Smith,[40] J. L. Smith,[103] R. Smith,[146] M. Smizanska,[93] K. Smolek,[135] A. A. Snesarev,[38] S. R. Snider,[158] H. L. Snoek,[117] S. Snyder,[30] R. Sobie,[168,n] A. Soffer,[154] C. A. Solans Sanchez,[37] E. Yu. Soldatov,[38] U. Soldevila,[166] A. A. Solodkov,[38] S. Solomon,[27] A. Soloshenko,[39] K. Solovieva,[55] O. V. Solovyanov,[41] P. Sommer,[51] A. Sonay,[13] W. Y. Song,[159b] A. Sopczak,[135] A. L. Sopio,[98] F. Sopkova,[29b] J. D. Sorenson,[115] I. R. Sotarriva Alvarez,[157] V. Sothilingam,[64a] O. J. Soto Sandoval,[140c,140b] S. Sottocornola,[69] R. Soualah,[163] Z. Soumaimi,[36e] D. South,[49] N. Soybelman,[172] S. Spagnolo,[71a,71b] M. Spalla,[112] D. Sperlich,[55] G. Spigo,[37] B. Spisso,[73a,73b] D. P. Spiteri,[60] M. Spousta,[136] E. J. Staats,[35] R. Stamen,[64a] A. Stampekis,[21] M. Standke,[25] E. Stanecka,[88] W. Stanek-Maslouska,[49] M. V. Stange,[51] B. Stanislaus,[18a] M. M. Stanitzki,[49] B. Stapf,[49] E. A. Starchenko,[38] G. H. Stark,[139] J. Stark,[91] P. Staroba,[134] P. Starovoitov,[64a] S. Stärz,[106] R. Staszewski,[88] G. Stavropoulos,[47] A. Stefl,[37] P. Steinberg,[30] B. Stelzer,[145,159a]

H. J. Stelzer,[132] O. Stelzer-Chilton,[159a] H. Stenzel,[59] T. J. Stevenson,[149] G. A. Stewart,[37] J. R. Stewart,[124] M. C. Stockton,[37] G. Stoicea,[28b] M. Stolarski,[133a] S. Stonjek,[112] A. Straessner,[51] J. Strandberg,[147] S. Strandberg,[48a,48b] M. Stratmann,[174] M. Strauss,[123] T. Strebler,[104] P. Strizenec,[29b] R. Ströhmer,[169] D. M. Strom,[126] R. Stroynowski,[45] A. Strubig,[48a,48b] S. A. Stucci,[30] B. Stugu,[17] J. Stupak,[123] N. A. Styles,[49] D. Su,[146] S. Su,[63a] W. Su,[63d] X. Su,[63a] D. Suchy,[29a] K. Sugizaki,[156] V. V. Sulin,[38] M. J. Sullivan,[94] D. M. S. Sultan,[129] L. Sultanaliyeva,[38] S. Sultansoy,[3b] T. Sumida,[89] S. Sun,[173] O. Sunneborn Gudnadottir,[164] N. Sur,[104] M. R. Sutton,[149] H. Suzuki,[160] M. Svatos,[134] M. Swiatlowski,[159a] T. Swirski,[169] I. Sykora,[29a] M. Sykora,[136] T. Sykora,[136] D. Ta,[102] K. Tackmann,[49,ee] A. Taffard,[162] R. Tafirout,[159a] J. S. Tafoya Vargas,[67] Y. Takubo,[85] M. Talby,[104] A. A. Talyshev,[38] K. C. Tam,[65b] N. M. Tamir,[154] A. Tanaka,[156] J. Tanaka,[156] R. Tanaka,[67] M. Tanasini,[148] Z. Tao,[167] S. Tapia Araya,[140f] S. Tapprogge,[102] A. Tarek Abouelfadl Mohamed,[109] S. Tarem,[153] K. Tariq,[14] G. Tarna,[28b] G. F. Tartarelli,[72a] M. J. Tartarin,[91] P. Tas,[136] M. Tasevsky,[134] E. Tassi,[44b,44a] A. C. Tate,[165] G. Tateno,[156] Y. Tayalati,[36e,ii] G. N. Taylor,[107] W. Taylor,[159b] R. Teixeira De Lima,[146] P. Teixeira-Dias,[97] J. J. Teoh,[158] K. Terashi,[156] J. Terron,[101] S. Terzo,[13] M. Testa,[54] R. J. Teuscher,[158,n] A. Thaler,[80] O. Theiner,[57] N. Themistokleous,[53] T. Theveneaux-Pelzer,[104] O. Thielmann,[174] D. W. Thomas,[97] J. P. Thomas,[21] E. A. Thompson,[18a] P. D. Thompson,[21] E. Thomson,[131] R. E. Thornberry,[45] C. Tian,[63a] Y. Tian,[56] V. Tikhomirov,[38,j] Yu. A. Tikhonov,[38] S. Timoshenko,[38] D. Timoshyn,[136] E. X. L. Ting,[1] P. Tipton,[175] A. Tishelman-Charny,[30] S. H. Tlou,[34g] K. Todome,[157] S. Todorova-Nova,[136] S. Todt,[51] L. Toffolin,[70a,70c] M. Togawa,[85] J. Tojo,[90] S. Tokár,[29a] K. Tokushuku,[85] O. Toldaiev,[69] M. Tomoto,[85,113] L. Tompkins,[146,ff] K. W. Topolnicki,[87b] E. Torrence,[126] H. Torres,[91] E. Torró Pastor,[166] M. Toscani,[31] C. Tosciri,[40] M. Tost,[11] D. R. Tovey,[142] I. S. Trandafir,[28b] T. Trefzger,[169] A. Tricoli,[30] I. M. Trigger,[159a] S. Trincaz-Duvoid,[130] D. A. Trischuk,[27] B. Trocmé,[61] A. Tropina,[39] L. Truong,[34c] M. Trzebinski,[88] A. Trzupek,[88] F. Tsai,[148] M. Tsai,[108] A. Tsiamis,[155] P. V. Tsiareshka,[38] S. Tsigaridas,[159a] A. Tsirigotis,[155,aa] V. Tsiskaridze,[158] E. G. Tskhadadze,[152a] M. Tsopoulou,[155] Y. Tsujikawa,[89] I. I. Tsukerman,[38] V. Tsulaia,[18a] S. Tsuno,[85] K. Tsuri,[121] D. Tsybychev,[148] Y. Tu,[65b] A. Tudorache,[28b] V. Tudorache,[28b] A. N. Tuna,[62] S. Turchikhin,[58b,58a] I. Turk Cakir,[3a] R. Turra,[72a] T. Turtuvshin,[39] P. M. Tuts,[42] S. Tzamarias,[155,z] E. Tzovara,[102] F. Ukegawa,[160] P. A. Ulloa Poblete,[140c,140b] E. N. Umaka,[30] G. Unal,[37] A. Undrus,[30] G. Unel,[162] J. Urban,[29b] P. Urrejola,[140a] G. Usai,[8] R. Ushioda,[157] M. Usman,[110] F. Ustuner,[53] Z. Uysal,[83] V. Vacek,[135] B. Vachon,[106] T. Vafeiadis,[37] A. Vaitkus,[98] C. Valderanis,[111] E. Valdes Santurio,[48a,48b] M. Valente,[159a] S. Valentinetti,[24b,24a] A. Valero,[166] E. Valiente Moreno,[166] A. Vallier,[91] J. A. Valls Ferrer,[166] D. R. Van Arneman,[117] T. R. Van Daalen,[141] A. Van Der Graaf,[50] P. Van Gemmeren,[6] M. Van Rijnbach,[37] S. Van Stroud,[98] I. Van Vulpen,[117] P. Vana,[136] M. Vanadia,[77a,77b] W. Vandelli,[37] E. R. Vandewall,[124] D. Vannicola,[154] L. Vannoli,[54] R. Vari,[76a] E. W. Varnes,[7] C. Varni,[18b] T. Varol,[151] D. Varouchas,[67] L. Varriale,[166] K. E. Varvell,[150] M. E. Vasile,[28b] L. Vaslin,[85] G. A. Vasquez,[168] A. Vasyukov,[39] L. M. Vaughan,[124] R. Vavricka,[102] T. Vazquez Schroeder,[37] J. Veatch,[32] V. Vecchio,[103] M. J. Veen,[105] I. Veliscek,[30] L. M. Veloce,[158] F. Veloso,[133a,133c] S. Veneziano,[76a] A. Ventura,[71a,71b] S. Ventura Gonzalez,[138] A. Verbytskyi,[112] M. Verducci,[75a,75b] C. Vergis,[96] M. Verissimo De Araujo,[84b] W. Verkerke,[117] J. C. Vermeulen,[117] C. Vernieri,[146] M. Vessella,[105] M. C. Vetterli,[145,d] A. Vgenopoulos,[102] N. Viaux Maira,[140f] T. Vickey,[142] O. E. Vickey Boeriu,[142] G. H. A. Viehhauser,[129] L. Vigani,[64b] M. Vigl,[112] M. Villa,[24b,24a] M. Villaplana Perez,[166] E. M. Villhauer,[53] E. Vilucchi,[54] M. G. Vincter,[35] A. Visibile,[117] C. Vittori,[37] I. Vivarelli,[24b,24a] E. Voevodina,[112] F. Vogel,[111] J. C. Voigt,[51] P. Vokac,[135] Yu. Volkotrub,[87b] J. Von Ahnen,[49] E. Von Toerne,[25] B. Vormwald,[37] V. Vorobel,[136] K. Vorobev,[38] M. Vos,[166] K. Voss,[144] M. Vozak,[117] L. Vozdecky,[123] N. Vranjes,[16] M. Vranjes Milosavljevic,[16] M. Vreeswijk,[117] N. K. Vu,[63d,63c] R. Vuillermet,[37] O. Vujinovic,[102] I. Vukotic,[40] S. Wada,[160] C. Wagner,[105] J. M. Wagner,[18a] W. Wagner,[174] S. Wahdan,[174] H. Wahlberg,[92] J. Walder,[137] R. Walker,[111] W. Walkowiak,[144] A. Wall,[131] E. J. Wallin,[100] T. Wamorkar,[6] A. Z. Wang,[139] C. Wang,[102] C. Wang,[11] H. Wang,[18a] J. Wang,[65c] P. Wang,[98] R. Wang,[62] R. Wang,[6] S. M. Wang,[151] S. Wang,[63b] S. Wang,[14] T. Wang,[63a] W. T. Wang,[81] W. Wang,[14] X. Wang,[114a] X. Wang,[165] X. Wang,[63c] Y. Wang,[63d] Y. Wang,[114a] Y. Wang,[63a] Z. Wang,[108] Z. Wang,[63d,52,63c] Z. Wang,[108] A. Warburton,[106] R. J. Ward,[21] N. Warrack,[60] S. Waterhouse,[97] A. T. Watson,[21] H. Watson,[60] M. F. Watson,[21] E. Watton,[60,137] G. Watts,[141] B. M. Waugh,[98] J. M. Webb,[55] C. Weber,[30] H. A. Weber,[19] M. S. Weber,[20] S. M. Weber,[64a] C. Wei,[63a] Y. Wei,[55] A. R. Weidberg,[129] E. J. Weik,[120] J. Weingarten,[50] C. Weiser,[55] C. J. Wells,[49] T. Wenaus,[30]

B. Wendland,[50] T. Wengler,[37] N. S. Wenke,[112] N. Wermes,[25] M. Wessels,[64a] A. M. Wharton,[93] A. S. White,[62] A. White,[8] M. J. White,[1] D. Whiteson,[162] L. Wickremasinghe,[127] W. Wiedenmann,[173] M. Wielers,[137] C. Wiglesworth,[43] D. J. Wilbern,[123] H. G. Wilkens,[37] J. J. H. Wilkinson,[33] D. M. Williams,[42] H. H. Williams,[131] S. Williams,[33] S. Willocq,[105] B. J. Wilson,[103] P. J. Windischhofer,[40] F. I. Winkel,[31] F. Winklmeier,[126] B. T. Winter,[55] J. K. Winter,[103] M. Wittgen,[146] M. Wobisch,[99] T. Wojtkowski,[61] Z. Wolffs,[117] J. Wollrath,[162] M. W. Wolter,[88] H. Wolters,[133a,133c] M. C. Wong,[139] E. L. Woodward,[42] S. D. Worm,[49] B. K. Wosiek,[88] K. W. Woźniak,[88] S. Wozniewski,[56] K. Wraight,[60] C. Wu,[21] M. Wu,[114b] M. Wu,[116] S. L. Wu,[173] X. Wu,[57] Y. Wu,[63a] Z. Wu,[4] J. Wuerzinger,[112,u] T. R. Wyatt,[103] B. M. Wynne,[53] S. Xella,[43] L. Xia,[114a] M. Xia,[15] M. Xie,[63a] S. Xin,[14,114c] A. Xiong,[126] J. Xiong,[18a] D. Xu,[14] H. Xu,[63a] L. Xu,[63a] R. Xu,[131] T. Xu,[108] Y. Xu,[15] Z. Xu,[53] Z. Xu,[114a] B. Yabsley,[150] S. Yacoob,[34a] Y. Yamaguchi,[85] E. Yamashita,[156] H. Yamauchi,[160] T. Yamazaki,[18a] Y. Yamazaki,[86] J. Yan,[63c] S. Yan,[60] Z. Yan,[105] H. J. Yang,[63c,63d] H. T. Yang,[63a] S. Yang,[63a] T. Yang,[65c] X. Yang,[37] X. Yang,[14] Y. Yang,[45] Y. Yang,[63a] Z. Yang,[63a] W-M. Yao,[18a] H. Ye,[114a] H. Ye,[56] J. Ye,[14] S. Ye,[30] X. Ye,[63a] Y. Yeh,[98] I. Yeletskikh,[39] B. Yeo,[18b] M. R. Yexley,[98] T. P. Yildirim,[129] P. Yin,[42] K. Yorita,[171] S. Younas,[28b] C. J. S. Young,[37] C. Young,[146] C. Yu,[14,114c] Y. Yu,[63a] J. Yuan,[14,114c] M. Yuan,[108] R. Yuan,[63d,63c] L. Yue,[98] M. Zaazoua,[63a] B. Zabinski,[88] E. Zaid,[53] Z. K. Zak,[88] T. Zakareishvili,[166] S. Zambito,[57] J. A. Zamora Saa,[140d,140b] J. Zang,[156] D. Zanzi,[55] O. Zaplatilek,[135] C. Zeitnitz,[174] H. Zeng,[14] J. C. Zeng,[165] D. T. Zenger Jr.,[27] O. Zenin,[38] T. Ženiš,[29a] S. Zenz,[96] S. Zerradi,[36a] D. Zerwas,[67] M. Zhai,[14,114c] D. F. Zhang,[142] J. Zhang,[63b] J. Zhang,[6] K. Zhang,[14,114c] L. Zhang,[63a] L. Zhang,[114a] P. Zhang,[14,114c] R. Zhang,[173] S. Zhang,[108] S. Zhang,[91] T. Zhang,[156] X. Zhang,[63c] X. Zhang,[63b] Y. Zhang,[63c] Y. Zhang,[98] Y. Zhang,[114a] Z. Zhang,[18a] Z. Zhang,[63b] Z. Zhang,[67] H. Zhao,[141] T. Zhao,[63b] Y. Zhao,[139] Z. Zhao,[63a] Z. Zhao,[63a] A. Zhemchugov,[39] J. Zheng,[114a] K. Zheng,[165] X. Zheng,[63a] Z. Zheng,[146] D. Zhong,[165] B. Zhou,[108] H. Zhou,[7] N. Zhou,[63c] Y. Zhou,[15] Y. Zhou,[114a] Y. Zhou,[7] C. G. Zhu,[63b] J. Zhu,[108] X. Zhu,[63d] Y. Zhu,[63c] Y. Zhu,[63a] X. Zhuang,[14] K. Zhukov,[69] N. I. Zimine,[39] J. Zinsser,[64b] M. Ziolkowski,[144] L. Živković,[16] A. Zoccoli,[24b,24a] K. Zoch,[62] T. G. Zorbas,[142] O. Zormpa,[47] W. Zou,[42] and L. Zwalinski[37]

(ATLAS Collaboration)

[1]*Department of Physics, University of Adelaide, Adelaide, Australia*
[2]*Department of Physics, University of Alberta, Edmonton, Alberta, Canada*
[3a]*Department of Physics, Ankara University, Ankara, Türkiye*
[3b]*Division of Physics, TOBB University of Economics and Technology, Ankara, Türkiye*
[4]*LAPP, Université Savoie Mont Blanc, CNRS/IN2P3, Annecy, France*
[5]*APC, Université Paris Cité, CNRS/IN2P3, Paris, France*
[6]*High Energy Physics Division, Argonne National Laboratory, Argonne, Illinois, USA*
[7]*Department of Physics, University of Arizona, Tucson, Arizona, USA*
[8]*Department of Physics, University of Texas at Arlington, Arlington, Texas, USA*
[9]*Physics Department, National and Kapodistrian University of Athens, Athens, Greece*
[10]*Physics Department, National Technical University of Athens, Zografou, Greece*
[11]*Department of Physics, University of Texas at Austin, Austin, Texas, USA*
[12]*Institute of Physics, Azerbaijan Academy of Sciences, Baku, Azerbaijan*
[13]*Institut de Física d'Altes Energies (IFAE), Barcelona Institute of Science and Technology, Barcelona, Spain*
[14]*Institute of High Energy Physics, Chinese Academy of Sciences, Beijing, China*
[15]*Physics Department, Tsinghua University, Beijing, China*
[16]*Institute of Physics, University of Belgrade, Belgrade, Serbia*
[17]*Department for Physics and Technology, University of Bergen, Bergen, Norway*
[18a]*Physics Division, Lawrence Berkeley National Laboratory, Berkeley, California, USA*
[18b]*University of California, Berkeley, California, USA*
[19]*Institut für Physik, Humboldt Universität zu Berlin, Berlin, Germany*
[20]*Albert Einstein Center for Fundamental Physics and Laboratory for High Energy Physics, University of Bern, Bern, Switzerland*
[21]*School of Physics and Astronomy, University of Birmingham, Birmingham, United Kingdom*
[22a]*Department of Physics, Bogazici University, Istanbul, Türkiye*
[22b]*Department of Physics Engineering, Gaziantep University, Gaziantep, Türkiye*

[22c]Department of Physics, Istanbul University, Istanbul, Türkiye
[23a]Facultad de Ciencias y Centro de Investigaciónes, Universidad Antonio Nariño, Bogotá, Colombia
[23b]Departamento de Física, Universidad Nacional de Colombia, Bogotá, Colombia
[24a]Dipartimento di Fisica e Astronomia A. Righi, Università di Bologna, Bologna, Italy
[24b]INFN Sezione di Bologna, Italy
[25]Physikalisches Institut, Universität Bonn, Bonn, Germany
[26]Department of Physics, Boston University, Boston, Massachusetts, USA
[27]Department of Physics, Brandeis University, Waltham, Massachusetts, USA
[28a]Transilvania University of Brasov, Brasov, Romania
[28b]Horia Hulubei National Institute of Physics and Nuclear Engineering, Bucharest, Romania
[28c]Department of Physics, Alexandru Ioan Cuza University of Iasi, Iasi, Romania
[28d]National Institute for Research and Development of Isotopic and Molecular Technologies, Physics Department, Cluj-Napoca, Romania
[28e]National University of Science and Technology Politechnica, Bucharest, Romania
[28f]West University in Timisoara, Timisoara, Romania
[28g]Faculty of Physics, University of Bucharest, Bucharest, Romania
[29a]Faculty of Mathematics, Physics and Informatics, Comenius University, Bratislava, Slovak Republic
[29b]Department of Subnuclear Physics, Institute of Experimental Physics of the Slovak Academy of Sciences, Kosice, Slovak Republic
[30]Physics Department, Brookhaven National Laboratory, Upton, New York, USA
[31]Universidad de Buenos Aires, Facultad de Ciencias Exactas y Naturales, Departamento de Física, y CONICET, Instituto de Física de Buenos Aires (IFIBA), Buenos Aires, Argentina
[32]California State University, California, USA
[33]Cavendish Laboratory, University of Cambridge, Cambridge, United Kingdom
[34a]Department of Physics, University of Cape Town, Cape Town, South Africa
[34b]iThemba Labs, Western Cape, South Africa
[34c]Department of Mechanical Engineering Science, University of Johannesburg, Johannesburg, South Africa
[34d]National Institute of Physics, University of the Philippines Diliman (Philippines), Philippines
[34e]University of South Africa, Department of Physics, Pretoria, South Africa
[34f]University of Zululand, KwaDlangezwa, South Africa
[34g]School of Physics, University of the Witwatersrand, Johannesburg, South Africa
[35]Department of Physics, Carleton University, Ottawa, Ontario, Canada
[36a]Faculté des Sciences Ain Chock, Université Hassan II de Casablanca, Casablanca, Morocco
[36b]Faculté des Sciences, Université Ibn-Tofail, Kénitra, Morocco
[36c]Faculté des Sciences Semlalia, Université Cadi Ayyad, LPHEA-Marrakech, Morocco
[36d]LPMR, Faculté des Sciences, Université Mohamed Premier, Oujda, Morocco
[36e]Faculté des sciences, Université Mohammed V, Rabat, Morocco
[36f]Institute of Applied Physics, Mohammed VI Polytechnic University, Ben Guerir, Morocco
[37]CERN, Geneva, Switzerland
[38]Affiliated with an institute covered by a cooperation agreement with CERN
[39]Affiliated with an international laboratory covered by a cooperation agreement with CERN
[40]Enrico Fermi Institute, University of Chicago, Chicago, Illinois, USA
[41]LPC, Université Clermont Auvergne, CNRS/IN2P3, Clermont-Ferrand, France
[42]Nevis Laboratory, Columbia University, Irvington, New York, USA
[43]Niels Bohr Institute, University of Copenhagen, Copenhagen, Denmark
[44a]Dipartimento di Fisica, Università della Calabria, Rende, Italy
[44b]INFN Gruppo Collegato di Cosenza, Laboratori Nazionali di Frascati, Cosenza, Italy
[45]Physics Department, Southern Methodist University, Dallas, Texas, USA
[46]Physics Department, University of Texas at Dallas, Richardson, Texas, USA
[47]National Centre for Scientific Research "Demokritos", Agia Paraskevi, Greece
[48a]Department of Physics, Stockholm University, Stockholm, Sweden
[48b]Oskar Klein Centre, Stockholm, Sweden
[49]Deutsches Elektronen-Synchrotron DESY, Hamburg and Zeuthen, Germany
[50]Fakultät Physik, Technische Universität Dortmund, Dortmund, Germany
[51]Institut für Kern- und Teilchenphysik, Technische Universität Dresden, Dresden, Germany
[52]Department of Physics, Duke University, Durham, North Carolina, USA
[53]SUPA - School of Physics and Astronomy, University of Edinburgh, Edinburgh, United Kingdom
[54]INFN e Laboratori Nazionali di Frascati, Frascati, Italy
[55]Physikalisches Institut, Albert-Ludwigs-Universität Freiburg, Freiburg, Germany

[56]*II. Physikalisches Institut, Georg-August-Universität Göttingen, Göttingen, Germany*
[57]*Département de Physique Nucléaire et Corpusculaire, Université de Genève, Genève, Switzerland*
[58a]*Dipartimento di Fisica, Università di Genova, Genova, Italy*
[58b]*INFN Sezione di Genova, Genova, Italy*
[59]*II. Physikalisches Institut, Justus-Liebig-Universität Giessen, Giessen, Germany*
[60]*SUPA - School of Physics and Astronomy, University of Glasgow, Glasgow, United Kingdom*
[61]*LPSC, Université Grenoble Alpes, CNRS/IN2P3, Grenoble INP, Grenoble, France*
[62]*Laboratory for Particle Physics and Cosmology, Harvard University, Cambridge, Massachusetts, USA*
[63a]*Department of Modern Physics and State Key Laboratory of Particle Detection and Electronics, University of Science and Technology of China, Hefei, China*
[63b]*Institute of Frontier and Interdisciplinary Science and Key Laboratory of Particle Physics and Particle Irradiation (MOE), Shandong University, Qingdao, China*
[63c]*School of Physics and Astronomy, Shanghai Jiao Tong University, Key Laboratory for Particle Astrophysics and Cosmology (MOE), SKLPPC, Shanghai, China*
[63d]*Tsung-Dao Lee Institute, Shanghai, China*
[63e]*School of Physics and Microelectronics, Zhengzhou University, Zhengzhou, China*
[64a]*Kirchhoff-Institut für Physik, Ruprecht-Karls-Universität Heidelberg, Heidelberg, Germany*
[64b]*Physikalisches Institut, Ruprecht-Karls-Universität Heidelberg, Heidelberg, Germany*
[65a]*Department of Physics, Chinese University of Hong Kong, Shatin, New Territories, Hong Kong, China*
[65b]*Department of Physics, University of Hong Kong, Hong Kong, China*
[65c]*Department of Physics and Institute for Advanced Study, Hong Kong University of Science and Technology, Clear Water Bay, Kowloon, Hong Kong, China*
[66]*Department of Physics, National Tsing Hua University, Hsinchu, Taiwan*
[67]*IJCLab, Université Paris-Saclay, CNRS/IN2P3, 91405, Orsay, France*
[68]*Centro Nacional de Microelectrónica (IMB-CNM-CSIC), Barcelona, Spain*
[69]*Department of Physics, Indiana University, Bloomington, Indiana, USA*
[70a]*INFN Gruppo Collegato di Udine, Sezione di Trieste, Udine, Italy*
[70b]*ICTP, Trieste, Italy*
[70c]*Dipartimento Politecnico di Ingegneria e Architettura, Università di Udine, Udine, Italy*
[71a]*INFN Sezione di Lecce, Lecce, Italy*
[71b]*Dipartimento di Matematica e Fisica, Università del Salento, Lecce, Italy*
[72a]*INFN Sezione di Milano, Milano, Italy*
[72b]*Dipartimento di Fisica, Università di Milano, Milano, Italy*
[73a]*INFN Sezione di Napoli, Napoli, Italy*
[73b]*Dipartimento di Fisica, Università di Napoli, Napoli, Italy*
[74a]*INFN Sezione di Pavia, Pavia, Italy*
[74b]*Dipartimento di Fisica, Università di Pavia, Pavia, Italy*
[75a]*INFN Sezione di Pisa, Pisa, Italy*
[75b]*Dipartimento di Fisica E. Fermi, Università di Pisa, Pisa, Italy*
[76a]*INFN Sezione di Roma, Roma, Italy*
[76b]*Dipartimento di Fisica, Sapienza Università di Roma, Roma, Italy*
[77a]*INFN Sezione di Roma Tor Vergata, Roma, Italy*
[77b]*Dipartimento di Fisica, Università di Roma Tor Vergata, Roma, Italy*
[78a]*INFN Sezione di Roma Tre, Roma, Italy*
[78b]*Dipartimento di Matematica e Fisica, Università Roma Tre, Roma, Italy*
[79a]*INFN-TIFPA, Trento, Italy*
[79b]*Università degli Studi di Trento, Trento, Italy*
[80]*Universität Innsbruck, Department of Astro and Particle Physics, Innsbruck, Austria*
[81]*University of Iowa, Iowa City, Iowa, USA*
[82]*Department of Physics and Astronomy, Iowa State University, Ames, Iowa, USA*
[83]*Istinye University, Sariyer, Istanbul, Türkiye*
[84a]*Departamento de Engenharia Elétrica, Universidade Federal de Juiz de Fora (UFJF), Juiz de Fora, Brazil*
[84b]*Universidade Federal do Rio De Janeiro COPPE/EE/IF, Rio de Janeiro, Brazil*
[84c]*Instituto de Física, Universidade de São Paulo, São Paulo, Brazil*
[84d]*Rio de Janeiro State University, Rio de Janeiro, Brazil*
[84e]*Federal University of Bahia, Bahia, Brazil*
[85]*KEK, High Energy Accelerator Research Organization, Tsukuba, Japan*
[86]*Graduate School of Science, Kobe University, Kobe, Japan*
[87a]*AGH University of Krakow, Faculty of Physics and Applied Computer Science, Krakow, Poland*

[87b]Marian Smoluchowski Institute of Physics, Jagiellonian University, Krakow, Poland
[88]Institute of Nuclear Physics Polish Academy of Sciences, Krakow, Poland
[89]Faculty of Science, Kyoto University, Kyoto, Japan
[90]Research Center for Advanced Particle Physics and Department of Physics, Kyushu University, Fukuoka, Japan
[91]L2IT, Université de Toulouse, CNRS/IN2P3, UPS, Toulouse, France
[92]Instituto de Física La Plata, Universidad Nacional de La Plata and CONICET, La Plata, Argentina
[93]Physics Department, Lancaster University, Lancaster, United Kingdom
[94]Oliver Lodge Laboratory, University of Liverpool, Liverpool, United Kingdom
[95]Department of Experimental Particle Physics, Jožef Stefan Institute and Department of Physics, University of Ljubljana, Ljubljana, Slovenia
[96]School of Physics and Astronomy, Queen Mary University of London, London, United Kingdom
[97]Department of Physics, Royal Holloway University of London, Egham, United Kingdom
[98]Department of Physics and Astronomy, University College London, London, United Kingdom
[99]Louisiana Tech University, Ruston, Louisiana, USA
[100]Fysiska institutionen, Lunds universitet, Lund, Sweden
[101]Departamento de Física Teorica C-15 and CIAFF, Universidad Autónoma de Madrid, Madrid, Spain
[102]Institut für Physik, Universität Mainz, Mainz, Germany
[103]School of Physics and Astronomy, University of Manchester, Manchester, United Kingdom
[104]CPPM, Aix-Marseille Université, CNRS/IN2P3, Marseille, France
[105]Department of Physics, University of Massachusetts, Amherst, Massachusetts, USA
[106]Department of Physics, McGill University, Montreal, Québec, Canada
[107]School of Physics, University of Melbourne, Victoria, Australia
[108]Department of Physics, University of Michigan, Ann Arbor, Michigan, USA
[109]Department of Physics and Astronomy, Michigan State University, East Lansing, Michigan, USA
[110]Group of Particle Physics, University of Montreal, Montreal, Québec, Canada
[111]Fakultät für Physik, Ludwig-Maximilians-Universität München, München, Germany
[112]Max-Planck-Institut für Physik (Werner-Heisenberg-Institut), München, Germany
[113]Graduate School of Science and Kobayashi-Maskawa Institute, Nagoya University, Nagoya, Japan
[114a]Department of Physics, Nanjing University, Nanjing, China
[114b]School of Science, Shenzhen Campus of Sun Yat-sen University, Shenzhen, China
[114c]University of Chinese Academy of Science (UCAS), Beijing, China
[115]Department of Physics and Astronomy, University of New Mexico, Albuquerque, New Mexico, USA
[116]Institute for Mathematics, Astrophysics and Particle Physics, Radboud University/Nikhef, Nijmegen, Netherlands
[117]Nikhef National Institute for Subatomic Physics and University of Amsterdam, Amsterdam, Netherlands
[118]Department of Physics, Northern Illinois University, DeKalb, Illinois, USA
[119a]New York University Abu Dhabi, Abu Dhabi, United Arab Emirates
[119b]United Arab Emirates University, Al Ain, United Arab Emirates
[120]Department of Physics, New York University, New York, New York, USA
[121]Ochanomizu University, Otsuka, Bunkyo-ku, Tokyo, Japan
[122]The Ohio State University, Columbus, Ohio, USA
[123]Homer L. Dodge Department of Physics and Astronomy, University of Oklahoma, Norman, Oklahoma, USA
[124]Department of Physics, Oklahoma State University, Stillwater, Oklahoma, USA
[125]Palacký University, Joint Laboratory of Optics, Olomouc, Czech Republic
[126]Institute for Fundamental Science, University of Oregon, Eugene, Oregon, USA
[127]Graduate School of Science, Osaka University, Osaka, Japan
[128]Department of Physics, University of Oslo, Oslo, Norway
[129]Department of Physics, Oxford University, Oxford, United Kingdom
[130]LPNHE, Sorbonne Université, Université Paris Cité, CNRS/IN2P3, Paris, France
[131]Department of Physics, University of Pennsylvania, Philadelphia, Pennsylvania, USA
[132]Department of Physics and Astronomy, University of Pittsburgh, Pittsburgh, Pennsylvania, USA
[133a]Laboratório de Instrumentação e Física Experimental de Partículas - LIP, Lisboa, Portugal
[133b]Departamento de Física, Faculdade de Ciências, Universidade de Lisboa, Lisboa, Portugal
[133c]Departamento de Física, Universidade de Coimbra, Coimbra, Portugal
[133d]Centro de Física Nuclear da Universidade de Lisboa, Lisboa, Portugal
[133e]Departamento de Física, Universidade do Minho, Braga, Portugal
[133f]Departamento de Física Teórica y del Cosmos, Universidad de Granada, Granada (Spain), Spain
[133g]Departamento de Física, Instituto Superior Técnico, Universidade de Lisboa, Lisboa, Portugal

[134]*Institute of Physics of the Czech Academy of Sciences, Prague, Czech Republic*
[135]*Czech Technical University in Prague, Prague, Czech Republic*
[136]*Charles University, Faculty of Mathematics and Physics, Prague, Czech Republic*
[137]*Particle Physics Department, Rutherford Appleton Laboratory, Didcot, United Kingdom*
[138]*IRFU, CEA, Université Paris-Saclay, Gif-sur-Yvette, France*
[139]*Santa Cruz Institute for Particle Physics, University of California Santa Cruz, Santa Cruz, California, USA*
[140a]*Departamento de Física, Pontificia Universidad Católica de Chile, Santiago, Chile*
[140b]*Millennium Institute for Subatomic physics at high energy frontier (SAPHIR), Santiago, Chile*
[140c]*Instituto de Investigación Multidisciplinario en Ciencia y Tecnología, y Departamento de Física, Universidad de La Serena, Chile*
[140d]*Universidad Andres Bello, Department of Physics, Santiago, Chile*
[140e]*Instituto de Alta Investigación, Universidad de Tarapacá, Arica, Chile*
[140f]*Departamento de Física, Universidad Técnica Federico Santa María, Valparaíso, Chile*
[141]*Department of Physics, University of Washington, Seattle, Washington, USA*
[142]*Department of Physics and Astronomy, University of Sheffield, Sheffield, United Kingdom*
[143]*Department of Physics, Shinshu University, Nagano, Japan*
[144]*Department Physik, Universität Siegen, Siegen, Germany*
[145]*Department of Physics, Simon Fraser University, Burnaby, British Columbia, Canada*
[146]*SLAC National Accelerator Laboratory, Stanford, California, USA*
[147]*Department of Physics, Royal Institute of Technology, Stockholm, Sweden*
[148]*Departments of Physics and Astronomy, Stony Brook University, Stony Brook, New York, USA*
[149]*Department of Physics and Astronomy, University of Sussex, Brighton, United Kingdom*
[150]*School of Physics, University of Sydney, Sydney, Australia*
[151]*Institute of Physics, Academia Sinica, Taipei, Taiwan*
[152a]*E. Andronikashvili Institute of Physics, Iv. Javakhishvili Tbilisi State University, Tbilisi, Georgia*
[152b]*High Energy Physics Institute, Tbilisi State University, Tbilisi, Georgia*
[152c]*University of Georgia, Tbilisi, Georgia*
[153]*Department of Physics, Technion, Israel Institute of Technology, Haifa, Israel*
[154]*Raymond and Beverly Sackler School of Physics and Astronomy, Tel Aviv University, Tel Aviv, Israel*
[155]*Department of Physics, Aristotle University of Thessaloniki, Thessaloniki, Greece*
[156]*International Center for Elementary Particle Physics and Department of Physics, University of Tokyo, Tokyo, Japan*
[157]*Department of Physics, Tokyo Institute of Technology, Tokyo, Japan*
[158]*Department of Physics, University of Toronto, Toronto, Ontario, Canada*
[159a]*TRIUMF, Vancouver, British Columbia, Canada*
[159b]*Department of Physics and Astronomy, York University, Toronto, Ontario, Canada*
[160]*Division of Physics and Tomonaga Center for the History of the Universe, Faculty of Pure and Applied Sciences, University of Tsukuba, Tsukuba, Japan*
[161]*Department of Physics and Astronomy, Tufts University, Medford, Massachusetts, USA*
[162]*Department of Physics and Astronomy, University of California Irvine, Irvine, California, USA*
[163]*University of Sharjah, Sharjah, United Arab Emirates*
[164]*Department of Physics and Astronomy, University of Uppsala, Uppsala, Sweden*
[165]*Department of Physics, University of Illinois, Urbana, Illinois, USA*
[166]*Instituto de Física Corpuscular (IFIC), Centro Mixto Universidad de Valencia - CSIC, Valencia, Spain*
[167]*Department of Physics, University of British Columbia, Vancouver, British Columbia, Canada*
[168]*Department of Physics and Astronomy, University of Victoria, Victoria, British Columbia, Canada*
[169]*Fakultät für Physik und Astronomie, Julius-Maximilians-Universität Würzburg, Würzburg, Germany*
[170]*Department of Physics, University of Warwick, Coventry, United Kingdom*
[171]*Waseda University, Tokyo, Japan*
[172]*Department of Particle Physics and Astrophysics, Weizmann Institute of Science, Rehovot, Israel*
[173]*Department of Physics, University of Wisconsin, Madison, Wisconsin, USA*
[174]*Fakultät für Mathematik und Naturwissenschaften, Fachgruppe Physik, Bergische Universität Wuppertal, Wuppertal, Germany*
[175]*Department of Physics, Yale University, New Haven, Connecticut, USA*

[a]Deceased.
[b]Also at Department of Physics, King's College London, London, United Kingdom.
[c]Also at Institute of Physics, Azerbaijan Academy of Sciences, Baku, Azerbaijan.
[d]Also at TRIUMF, Vancouver, British Columbia, Canada.

[e]Also at Department of Physics, University of Thessaly, Greece.
[f]Also at An-Najah National University, Nablus, Palestine.
[g]Also at Department of Physics, University of Fribourg, Fribourg, Switzerland.
[h]Also at Department of Physics, Westmont College, Santa Barbara, USA.
[i]Also at Departament de Fisica de la Universitat Autonoma de Barcelona, Barcelona, Spain.
[j]Also at Affiliated with an institute covered by a cooperation agreement with CERN.
[k]Also at The Collaborative Innovation Center of Quantum Matter (CICQM), Beijing, China.
[l]Also at Faculty of Physics, Sofia University, 'St. Kliment Ohridski', Sofia, Bulgaria.
[m]Also at Università di Napoli Parthenope, Napoli, Italy.
[n]Also at Institute of Particle Physics (IPP), Canada.
[o]Also at University of Colorado Boulder, Department of Physics, Colorado, USA.
[p]Also at Borough of Manhattan Community College, City University of New York, New York, New York, USA.
[q]Also at National Institute of Physics, University of the Philippines Diliman (Philippines), Philippines.
[r]Also at Department of Financial and Management Engineering, University of the Aegean, Chios, Greece.
[s]Also at Centro Studi e Ricerche Enrico Fermi, Italy.
[t]Also at Institucio Catalana de Recerca i Estudis Avancats, ICREA, Barcelona, Spain.
[u]Also at Technical University of Munich, Munich, Germany.
[v]Also at CMD-AC UNEC Research Center, Azerbaijan State University of Economics (UNEC), Azerbaijan.
[w]Also at Yeditepe University, Physics Department, Istanbul, Türkiye.
[x]Also at Institute of Theoretical Physics, Ilia State University, Tbilisi, Georgia.
[y]Also at CERN, Geneva, Switzerland.
[z]Also at Center for Interdisciplinary Research and Innovation (CIRI-AUTH), Thessaloniki, Greece.
[aa]Also at Hellenic Open University, Patras, Greece.
[bb]Also at Department of Physics, Stellenbosch University, South Africa.
[cc]Also at Department of Physics, California State University, Sacramento, USA.
[dd]Also at Département de Physique Nucléaire et Corpusculaire, Université de Genève, Genève, Switzerland.
[ee]Also at Institut für Experimentalphysik, Universität Hamburg, Hamburg, Germany.
[ff]Also at Department of Physics, Stanford University, Stanford, California, USA.
[gg]Also at Institute for Nuclear Research and Nuclear Energy (INRNE) of the Bulgarian Academy of Sciences, Sofia, Bulgaria.
[hh]Also at Washington College, Chestertown, Maryland, USA.
[ii]Also at Institute of Applied Physics, Mohammed VI Polytechnic University, Ben Guerir, Morocco.